UNIVERSIDADE FEDERAL DA BAHIA
INSTITUTO DE QUÍMICA
PROGRAMA DE PÓS-GRADUAÇÃO EM QUÍMICA

TÁCILA OLIVEIRA PINTO DE FREITAS

DISTRIBUIÇÃO, FONTES E FRACIONAMENTO DE ELEMENTOS TERRAS RARAS E OUTROS METAIS EM SOLOS DE MANGUEZAIS E SEDIMENTOS ESTUARINOS

Junho / 2020

Salvador - BA

TÁCILA OLIVEIRA PINTO DE FREITAS

DISTRIBUIÇÃO, FONTES E FRACIONAMENTO DE ELEMENTOS TERRAS RARAS E OUTROS METAIS EM SOLOS DE MANGUEZAIS E SEDIMENTOS ESTUARINOS

Dissertação de mestrado apresentada ao Programa de Pós-Graduação em Química, Instituto de Química, Universidade Federal da Bahia, como requisito parcial para obtenção do grau de Mestre em Química, área de concentração em Química Analítica.

Orientadora: Profª Drª Vanessa Hatje

Junho / 2020

Salvador - BA

Ficha catalográfica elaborada pela Biblioteca Universitária de Ciências e Tecnologias Prof. Omar Catunda, SIBI - UFBA.

F866 Freitas, Tácila Oliveira Pinto

Distribuição, fontes e fracionamento de elementos terras raras e outros metais em solos de manguezais e sedimentos estuarinos / Tácila Oliveira Pinto de Freitas. – Salvador, 2020.
122 f.

Orientadora: Profª. Drª Vanessa Hatje.

Dissertação (Mestrado) – Universidade Federal da Bahia. Instituto de Química, 2020.

1. Manguezais. 2. Metais. 3. Solos. 4. Sedimentos Estuarinos. I. Hatje, Vanessa. II. Universidade Federal da Bahia. III. Título.

CDU 550.4

Resumo

Os manguezais são importantes sistemas costeiros que atuam como sumidouros de elementos traço, incluindo os elementos terras raras (REE). No entanto, muitas hipóteses são levantadas sobre fatores que controlam a distribuição de REE em sedimentos estuarinos, visto que é um ambiente com rápidas alterações nas suas propriedades físico-químicas. Por isto, os REE foram medidos em sedimentos estuarinos e em seis testemunhos de solos de mangue do estuário do rio Jaguaripe, Nordeste, Brasil. Nosso objetivo foi avaliar o fracionamento, distribuição e possíveis fontes desses elementos para este ambiente costeiro. Como resultado, para os sedimentos superficiais estuarinos, o ΣREE variaram entre 202 e 220 mg kg^{-1}, e Y entre 12 e 15 mg kg^{-1}. As abundâncias normalizadas do *Post Archean Australian Shale* (PAAS) mostraram enriquecimento dos REE leves (LREE) sobre os pesados (HREE). Dentre os REE, apenas os LREE mostraram correlação significativa com Al (r= 0,85) e Fe (r= 0,96). A média do ΣREE para solos de mangue ao longo do gradiente de salinidade variou de 161 ± 18 mg kg^{-1} (baixo estuário) a 183 ± 16 mg kg^{-1} (alto estuário), resultado esperado considerando as condições do local de estudo e a característica geral de estuários em remover em maior escala os REE dissolvidos nas regiões de baixa salinidade. As concentrações de ΣREE foram constantes ao longo dos perfis verticais, o que indica mínima alteração diagenética ao longo do tempo. A ausência de correlação dos REE entre Fe e Mn nos solos sugere que estes elementos químicos podem estar co-precipitando como sulfetos metálicos nos solos anóxicos do manguezal. Todavia, a química de sedimentos em estuários e manguezais envolve uma série de processos estuarinos, e para uma melhor compreensão dos resultados aqui obtidos, dados de especiação para sedimentos e geoquímica de água intersticial serão necessários para testar as hipóteses apresentadas.

Palavras-chave: Gradiente estuarino; Remoção; Elementos terras raras; Baía de Todos os Santos; Fracionamento; Diagênese.

Apresentação

Os elementos terras raras (REE) são elementos químicos que apresentam de periodicidade, devido à sua configuração eletrônica na Tabela Periódica. Segundo a Comissão de Nomenclatura em Química Inorgânica da União Internacional de Química Pura e Aplicada (IUPAC - *International Union of Pure and Applied Chemistry*), os elementos químicos denominados "terras raras" incluem desde o La (Z= 57) até o Lu (Z= 71), e são chamados de lantanídeos. Os REE apresentam características químicas específicas que os tornam bons traçadores de processos geoquímicos (Henderson, 1984).

Ao longo da série dos lantanídeos, existem pequenas diferenças nas propriedades químicas que resultam em mudanças nas abundâncias relativas do La a Lu, essa mudança é chamada de fracionamento. Por exemplo, o que é esperado da composição de REE na água do mar, após valores normalizados com a composição de REE da crosta, é um enriquecimento dos REE pesados (HREE; que inclui os elementos químico entre Er e Lu) e empobrecimento dos REE leves (LREE; que inclui os elementos químicos entre La para Nd) (Elderfield, 1988). Esse comportamento tem sido devido ao preenchimento de elétrons do nível f, que resulta na contração lantanídica, uma diminuição gradual e sistemática do raio iônico do REE trivalente de La (o REE mais leve) a Lu (o REE mais pesado) (Henderson, 1984; de Baar et al., 1991).

Por outro lado, o efeito Oddo-Harkins mascara esta contração, pois garante que elementos de número atômico par sejam mais abundantes do que os elementos químicos de número atômico ímpar (Moeller, 1975; Lee, 1999). Esse efeito gera um *zig zag* quando as concentrações destes elementos químicos na natureza, i.e., em amostras de sedimentos, águas e solos são plotados.

Para facilitar a visualização do padrão de distribuição destes elementos e permitir a comparabilidade dos dados, em geral é realizada a normalização dos dados, feita usualmente com padrões de referência. Para sedimentos e rochas sedimentares é comum normalizar os

dados a partir das concentrações de folhelhos. Neste trabalho a normalização foi feita com concentrações dos folhelhos australianos (*Post-Archean Australian Shale,* PAAS). Outras vantagens da normalização dos dados é a identificação de anomalias que alguns desses elementos químicos podem apresentar e a comparabilidade de dados com outros estudos.

Os lantanídeos na forma de átomo neutro têm a mesma configuração eletrônica e o preenchimento do nível $4f^n$ (n= 1 – 14) acontece de forma sequencial ao longo da série (La – Lu), exceto para o lantânio que não possui nenhum elétron no nível f (Lee, 1990). Embora o estado trivalente seja o mais estável em termos de termodinâmica química para a maioria dos REE, o Ce e o Eu são elementos que têm sensibilidade às condições redox e podem apresentar número de oxidação (+IV) e (+II), respectivamente (Sholkovitz, 1992). O estado de oxidação (+II) é menos solúvel e facilmente oxidado para (+III), portanto, é incomum que o Eu seja encontrado nessa condição quando está em solução ou formando complexos (Prasad and Ramanathan, 2008; Hannigan et al., 2010; Prajith et al., 2015).

Dentre todos os REE, apenas o Ce apresenta estabilidade quando encontrado com estado de oxidação (+IV) em rios e águas oceânicas. O cério (+IV) é menos solúvel que (+III), podendo ser removido da solução e se agregar nas fases minerais (Goldberg, 1963). Este comportamento diferenciado do Ce diante dos outros REE pode ser explicado pela sua química redox (de Baar et al., 1988; Liu et al., 1988).

Quando os elementos químicos exibem comportamentos diferentes de outros REE trivalentes no ambiente, eles mostram uma tendência a deslocar sua posição em relação a seus vizinhos, o que pode ser observado graficamente quando as abundâncias dos REE de uma determinada amostra são plotadas (Kulaksiz and Bau, 2007). Essa mudança no padrão de comportamento dentro da série dos lantanídeos é definida como anomalia. Cério e Eu são elementos químicos que possuem mais de um estado de oxidação, portanto, são mais propensos a apresentar tal comportamento.

Neste estudo, as anomalias de Ce e Eu foram calculadas da seguinte forma:

$$Ce/Ce^{*} = Ce_{PAAS}/(La_{PAAS} \times Pr_{PAAS})^{0.5}$$ (McLennan, 1989)

$$Eu/Eu^{*} = Eu_{PAAS}/(Sm_{PAAS} \times Gd_{PAAS})^{0.5}$$ (Taylor and McLennan, 1985)

Quando Eu/Eu* ou Ce/Ce* são iguais a 1, significa dizer que os REE envolvidos nos cálculos têm sua composição semelhante aos REE da crosta terrestre, e que não há fracionamento entre seus vizinhos trivalentes (Sappal et al., 2014). Desta forma, valores entre 0 e 1 são denominadas anomalias negativas, enquanto valores maiores do que 1 indicam anomalias positivas.

O uso de REE teve início com o desenvolvimento de camisas de lampiões a gás (Martins e Isolani, 2005). Desde então, as propriedades dos REE foram conhecidas cada vez mais e seu uso em larga escala foi ampliado ao longo dos anos, sendo ultimamente utilizados em baterias recarregáveis, fabricação de lasers, uso como materiais luminescentes, catalisadores, fabricação de lâmpadas fluorescentes, entre outros (Du and Graedel, 2013). A grande diversidade de aplicações de REE causa preocupação com o crescimento de emissões de fontes antrópicas que uma vez lançadas no meio ambiente, atingem sedimentos marinhos e estuarinos.

Considerando o aumento da contribuição antrópica de REE, espera-se que uma fração substancial destes elementos químicos eventualmente entre nas águas superficiais e seja transportada para os sistemas costeiros, como estuários e manguezais, onde eles podem acumular e prejudicar seu uso como rastreadores de processos naturais em áreas afetadas por insumos antropogênicos (Ogata e Terakado, 2006; Johannesson et al., 2017; Kulaksız and Bau, 2013, 2011; Pedreira et al., 2018). Com isto, em breve tem-se ambientes costeiros que ainda preservam suas condições naturais, sendo alterados, por exemplo o que pode acontecer com o estuário do rio Jaguaripe.

O complexo estuarino do rio Jaguaripe é um dos principais tributários da Baía de Todos os Santos (BTS), tendo 2.200 km^2 de bacia hidrográfica, possuindo uma bacia de drenagem relativamente bem preservada, comparado com o rio Paraguaçu e Subaé, e as atividades antrópicas são insipientes (Hatje e Barros, 2012; Krull et al., 2014). Porém, com os demasiados aportes antrópicos e desenvolvimentos da região esperamos que os padrões naturais de distribuição de REE não prevaleçam em sistemas costeiros por muito tempo. Além disso, não há um consenso sobre como os processos diagenéticos afetam a distribuição de REE nos solos (Caetano et al., 2009). Portanto, com o objetivo de avaliar a abundância e o fracionamento do REE, perfis de solos de mangue e também sedimentos estuarinos de um estuário tropical bem preservado foram analisados buscando-se investigar as fontes, distribuições e processos de controle do REE ao longo do gradiente estuarino.

O trabalho realizado durante o período do curso de mestrado em Química é parte do Projeto Multidiscioplinar Baía de Todos os Santos, que se encontra agora na sua terceira etapa. Os resultados obtidos nesta dissertação de mestrado serão apresentados na forma de um manuscrito que será submetido para um periódico internacional e terá como co-autores Rodrigo P. Aguiar e Vanessa Hatje. Os agradecimentos aos financiadores deste projeto se encontram listados no final do manuscrito.

REFERÊNCIAS

Caetano, M., Prego, R., Vale, C., de Pablo, H., Marmolejo-Rodríguez, J., 2009. Record of diagenesis of rare earth elements and other metals in a transitional sedimentary environment. Marine Chemistry. 116, n. 1–4, 36–46.

Connelly, N.G., Damhus, T., Hartshorn, R.M., Hutton, A.T. Nomenclature of Inorganic Chemistry - IUPAC Recommendations 2005, RSC Publishing: Cambridge, 2005.

De Baar, H. J. W., German, C. R., Elderfield, H., Van Gaans, P., 1988. Rare earth element distributions in anoxic waters of the Cariaco Trench. Geochim. Cosmochim. Acta. 52, 1203-1219.

De Baar H. J. W., Schijf J., Byrne R. H., 1991. Solution chemistry of the rare earth elements in seawater. Euro. Journal Solid State Inorg. Chem. 28, 357-373.

Du, X., Graedel, T. E., 2013. Uncovering the end uses of the rare earth elements. Science of the Total Environment. 461–462, p. 781–784.

Elderfield, H., Whitfield, M., Burton, J. D., Bacon, M. P., Liss, P. S., 1988. The oceanic chemistry of the rare-earth elements. Philosophical Transactions of the Royal Society of London. Series A, Mathematical and Physical Sciences. 325, n. 1583, 105–126.

Goldberg, E. D., Koide, M., Schmitt, R. A., Smith, R. H., 1963. Rare-Earth distributions in the marine environment. Journal of Geophysical Research. 68, n. 14, 4209–4217.

Hannigan, R., Dorval, E., Jones, C., 2010. The rare earth element chemistry of estuarine surface sediments in the Chesapeake Bay. Chemical Geology. 272, n. 1–4, 20–30.

Hatje, V.; Barros, F., 2012. Overview of the 20th century impact of trace metal contamination in the estuaries of Todos os Santos Bay: Past, present and future scenarios. Marine Pollution Bulletin. 64, n. 11, 2603–2614.

Henderson, P., 1984. General geochemical properties and abundances of the rare earth elements. Rare Earth Element Geochemistry, 1–32.

Johannesson, K. H. Palmore, C. D., Fackrell, J., Prouty, N. G., Swarzenski, P. W., Chevis, D. A., Telfeyan, K., White, C. D., Burdige, D. J., 2017. Rare earth element behavior during groundwater–seawater mixing along the Kona Coast of Hawaii. Geochimica et Cosmochimica Acta. 198, 229–258.

Kulaksiz, S.; Bau, M., 2007. Contrasting behaviour of anthropogenic gadolinium and natural rare earth elements in estuaries and the gadolinium input into the North Sea. Earth and Planetary Science Letters. 260, n. 1–2, 361–371.

Kulaksiz, S., Bau, M., 2011. Rare earth elements in the Rhine River, Germany: First case of anthropogenic lanthanum as a dissolved microcontaminant in the hydrosphere. Environment International. 37, n. 5, 973–979.

Kulaksiz, S., Bau, M., 2013. Anthropogenic dissolved and colloid/nanoparticle-bound samarium, lanthanum and gadolinium in the Rhine River and the impending destruction of the natural rare earth element distribution in rivers. Earth and Planetary Science Letters. 362, 43–50.

Krull, M., Abessa, D. M.S., Hatje, V., Barros, F., 2014. Integrated assessment of metal contamination in sediments from two tropical estuaries. Ecotoxicology and Environmental Safety. 106, 195–203.

Lee, J. D., 1999. Química Inorgânica não tão concisa. Tradução: Toma, H. E.; Rocha, R. C.; Edgard Blücher Ltda.: São Paulo, cap. 29.

Liu, Y. G., Miah, M. R. U., Schmitt, R. A., 1988. Cerium: A chemical tracer for paleo-oceanic redox conditions. Geochimica et Cosmochimica Acta. 52, n. 6, 1361–1371.

Martins, T. S., Isolani, P. C., 2005. Terras raras: Aplicações industriais e biológicas. Química Nova. 28, n. 1, 111–117.

Moeller, T., 1975. The Chemistry of the Lanthanides, Pergamon Texts in Comprehensive Inorganic Chemistry; Pergamon Press: New York, vol. 26.

McLennan, S.M. 1989. Rare earth elements in sedimentary rocks: influence of provenance and sedimentary processes. Reviews in Mineralogy and Geochemistry. 21, 169–200.

Pedreira, R. M. A., Pahnke, K., Böning, P., Hatje, V., 2018. Tracking hospital effluent-derived gadolinium in Atlantic coastal waters off Brazil. Water Research. 145, 62–72.

Prasad, M. B. K.; Ramanathan, A., 2008. Distribution of Rare Earth Elements in the Pichavaram Mangrove Sediments of the Southeast Coast of India. Journal of Coastal Research. 1, 126–134.

Prajith, A.; Rao, V. P.; Kessarkar, P. M., 2015. Controls on the distribution and fractionation of yttrium and rare earth elements in core sediments from the Mandovi estuary, western India. Continental Shelf Research. 92, 59–71.

Ogata, T.; Terakado, Y., 2006. Rare earth element abundances in some seawaters and related river waters from the Osaka Bay area, Japan: Significance of anthropogenic Gd. Geochemical Journal. 40, n. 5, 463–474.

Sappal, S. M., Ramanathan, A., Ranjan, R. K., Singh, G., Kumar, A., 2014. Rare Earth Elements as Biogeochemical Indicators in Mangrove Ecosystems (Pichavaram, Tamilnadu, India). Journal of Sedimentary Research. 84, n. 9, 781–791.

Sholkovitz, E. R., 1992. Chemical evolution of rare earth elements: fractionation between colloidal and solution phases of filtered river water. Earth and Planetary Science Letters. 114, n. 1, 77–84.

Taylor, S.R. and McLennan, S.M., 1985. The Continental Crust: Its Composition and Evolution. Blackwell, Oxford, 1-312.

ÍNDICE

Distribution and fractionation of rare earth elements in sediments and mangrove soil profiles across an estuarine gradient

Inst. de Química & Centro Interdisciplinar de Energia e Ambiente, CIENAM, Universidade Federal da Bahia, Ondina, Salvador, Bahia, 40170-115, Brazil

This manuscript will be submitted be to Marine Chemistry
May 2020

Abstract

Mangroves are important coastal systems that act as sinks for sediments and trace elements. However, many hypotheses are raised about factors that control the distribution of REE in estuarine sediments, since it is an environment with rapid changes in its physicochemical properties. For this reason, REE were measured in estuarine sediments and in six mangrove soils cores from the Jaguaripe estuary, Brazil. The aim of this study was to evaluate the fractionation, distribution and possible sources of these elements for this coastal environment. As a result, for surficial estuarine sediments, the ΣREE and Y ranged from 202 to 220 mg kg^{-1} and 12 to 15 mg kg^{-1}, respectively. The normalized abundances to the Post Archean Australian Shale (PAAS) showed that the LREE had consistently enriched over the HREE. Among REE, only LREE showed significant correlation with Al (r= 0.85) and Fe (r= 0.96), indicating that Al and Fe-oxy-hydroxides are the main host phases of the LREE. The average ΣREE for mangrove soils along the salinity gradient ranged from 161 ± 18 mg kg^{-1} (lower estuary) to 183 ± 16 mg kg^{-1} (upper estuary), an expected result considering the conditions of the study site and the general characteristic of estuaries of remove on a larger scale the REEY dissolved in low salinity regions. The concentrations of ΣREE were constant through the vertical profiles, which indicate a minimum diagenetic change over time after deposition in the sediments. Our assumption about REE not showing correlations with Fe or Mn in mangrove soils is that they may be co-precipitating as metal sulphides in the reducing soil environment. However, sediment chemistry in estuaries and mangroves envelop a series of estuarine processes, and for a better understanding of the results obtained here, speciation data for sediments and porewater geochemistry will be necessary to test the hypotheses presented.

Keywords: estuarine gradient; scavenging; rare earth elements; Todos os Santos Bay; fractionation; diagenesis.

HIGHLIGHTS

- Normalized rare earth elements (REE) patterns showed light REE (LREE) enrichment;
- The positive Eu anomalies are a consistent feature in mangrove soils;
- La/Yb ratios are higher at the upper than at the lower estuary;
- Fractionation is more important in estuarine sediments than in mangrove soils;
- Co-precipitation with metal sulphides may be an important burial mechanism.

INTRODUCTION

The rare earth elements (REE) are a group of chemically similar elements that includes the lightest La to the heaviest Lu. They are generally trivalent elements, with the exceptions of Ce and Eu, which can exist as Ce (IV) and Eu (II). Although Y does not have 4f electrons, it has the same ionic radii and similar geochemical behavior to Ho (Kawabe et al., 1991). Due to their coherent and predictable behavior, the REE provides insight into complex geochemical processes that single proxies cannot readily discriminate (Johannesson et al., 2005). The geochemical evolution of the continental crust, chemical weathering (Delgado et al., 2012; Liu et al., 2013), and sedimentary provenance in river, estuarine and marine environments (Elderfield et al., 1990; Sholkovitz, 1993; Caetano et al., 2009, Prego et al., 2009; Piper and Bau, 2013; Mandal et al., 2019) have been largely evaluated by the REE fractionation. The REE and Y (REEY) are also useful for understanding removal and fractionation processes during estuarine mixing (Elderfield et al., 1990; Sholkovitz, 1992, 1993; Sholkovitz and Szymczak, 2000; Rousseau et al., 2015; Andrade et al., 2020). In fact, estuarine REEY removal has been recognized early on as an important mechanism balancing marine REE budgets (Goldstein and Jacobsen, 1987).

Mangroves are important intertidal coastal systems that provide a myriad of ecological services. Together with estuaries, mangroves regulate the exchange of materials at the interfaces between the land, atmosphere, and ocean ecosystems (Sholkovitz, 1976, Hoyle et al., 1984; Ramesh et al., 1999, Censi et al., 2007, Prasad and Ramathan, 2008). The mangrove forest root structure favors the accumulation of fine sediments in soils that can act as sinks and sources of trace and major elements (Furukawa and Wolanski, 1996; Furukawa et al., 1997). That reflects the dynamic nature of mangrove ecosystems that are subject to rapid changes in sediment physicochemical properties such as water content, texture, pH, redox conditions, and salinity due to tidal flushing and the associated soil flooding. The flooding episodes may

develop redox cycles in soils, with alternating periods of oxidizing and reducing conditions. These cycles could, therefore, result in the solubilization of various Fe (III) solid phases, organic matter, and colloids that are strong adsorbents of metallic cations (Davranche et al., 2011).

Fine, C rich sediments in mangrove soils can act as sinks for REEY (Wasserman et al., 2001; Censi et al., 2007; Mandal et al., 2019; Silva-Filho et al., 2011). Interactions between dissolved and particulate phases, dissolution/diffusion, complex formation, and the chemistry of Fe and Mn at varied redox levels may control the distribution of REEY in sedimentary profiles (Kuss et al., 2001, Lawrence and Kamber, 2006). Hence, REEY mobilization from soils through the above-mentioned reactions may lead to the development of specific REEY spatial distribution patterns (Davranche et al., 2011). However, there is a lack of studies providing comprehensive assessments of the spatial distribution of REEY and their sources, and that explore the factors driving the patterns within the complex estuarine-mangrove systems.

Although advances have been made towards understanding REEY geochemistry in surficial mangrove soils, considerably fewer studies have focused on the sedimentary historical records. Mandal et al. (2019) showed that the light REE (LREE) were more abundant than the heavy REE (HREE) in the sediments of the Indian Sundarban, located at the estuarine part of the Ganges River and at the land-ocean boundary of the Bay of Bengal, which also presented a weak positive europium anomaly. Prasad and Ramanathan (2008) found similar results for mangrove soils in Pichavaram. Sappal et al. (2014) observed a convex shale-like pattern of REE and strong positive Eu anomalies in soil profiles from the Pichavaram mangroves, reflecting the natural weathering of the source material. Censi et al. (2005) investigated the dissolved phase, suspended particulate matter, and sediments of the western coast of the Gulf of Thailand and observed Eu and Gd positive anomalies explained by the extensive rock-water

interaction processes occurring in the basin of the Mae Klong and Phetchaburi rivers. Wasserman et al. (2001) compared the La, Ce, Sm, Eu, Yb, and Lu concentrations of cores in mangrove forests and mudflats in Sepetiba Bay, Brazil. Later, Silva-Filho et al. (2011) used the fractionation patterns of REE in mangroves of the same area as tracers of sedimentary processes. Caetano et al. (2009) studied the vertical distribution of trace elements and REE in a sediment core from the Vigo Ria indicating preferential retention of LREE over the HREE in a transitional sedimentary layer where oxyhydroxides were generated. Brito et al. (2018) reported significant correlations between REE, grain-size, Al, Fe, Mg, and Mn, suggesting a preferential association of REE to aluminosilicates, Al hydroxides and Fe oxyhydroxides. Finally, Zhang et al. (2013) examined the influence of mangroves on the distribution of REE in estuarine sediments and core sediments from mangrove forests, forest fringe, and adjacent mudflat in the Zhangjiang estuary. Their results showed that LREE were more enriched than HREE, with a relatively weak negative Eu anomaly, and also indicated that weathered continental materials as the main source for REE.

In this context, we expect that the natural distribution patterns of REE do not prevail in coastal systems such as mangroves and estuaries worldwide, already largely impacted by anthropogenic activities. Besides, there has not been a consensus on how early diagenetic processes affects REEY distribution in soils (Caetano et al., 2009). For these reasons, the main focus of this work is to study the REEY abundance and fractionation in profiles of mangrove soils and also in estuarine sediments of a well-preserved tropical estuary dominated by mangrove forests. This system, identified as the Jaguaripe estuary, is located in the Northeast of Brazil and has insipient anthropogenic activities, which allowed us to study REEY under rare nearly natural conditions, offering the opportunity to evaluate REEY sources, distributions, and controlling processes in sediments and mangrove soils along an estuarine gradient and hence to achieve an improved understanding of the mangrove REE cycle.

MATERIAL AND METHODS

STUDY AREA AND SAMPLING DESIGN

The study area and sampling details have already been presented elsewhere (Hatje et al., 2020, submitted) and is summarized below. The Jaguaripe estuarine complex (Fig. 1) is located in the Todos os Santos Bay (BTS; 12º50'S, 38º38'W), the second largest bay (1,112 km^2) of Brazil. The climate at the bay is tropical humid, with annual mean temperature, precipitation and evaporation of 25ºC, 2,100 mm, and 1,000 mm, respectively (INMET, 1992). The hydrographic basin has 2,200 km^2, the tidal regime is semidiurnal, with maximum tidal range of < 2.5 m, and average discharges are 13 $m^3 s^{-1}$ and 28 $m^3 s^{-1}$ during summer and winter, respectively (Cirano and Lessa, 2007). Mangrove forests in the Jaguaripe present large structural development than the other mangroves forests in the BTS (Costa et al., 2015). The region is considered well-preserved and anthropogenic activities in the basin are insipient (Hatje and Barros, 2012; Krull et al., 2014). Local economy is based on seafood harvesting, a small shrimp farm and small-scale agriculture and artisanal pottery.

In order to cover the estuarine gradient, surficial sediments were collected using a Van Veen grab at 5 stations (J1, J3, J5, J8 and J10, Fig. 1) that have been used for a long-term monitoring study (Hatje and Barros, 2012). Six cores were collected in mangroves along the estuarine gradient (Fig. 1). For each estuarine section, hereafter called upper (cores T5 and T6), middle (cores T3 and T4) and lower estuary (cores T1 and T2), 2 cores were collected using a stainless-steel open-faced auger. Cores were sliced at 1 cm-thick layers throughout the first 10 cm, at 2 cm sections for the 20-50 cm interval and at 3 cm-thick layers for bottom sections. Estuarine sediments were wet sieved to separate the fraction smaller than 63 μm, freeze-dried, homogenized and comminuted in a ball mill. Grain size, elemental composition and metals

(for estuarine samples only) have been previously presented (Hatje and Barros, 2012; Hatje et al, 2020, submitted).

CHEMICAL ANALYZES

All the material used during field and laboratory work were previously soaked in detergent (Extran® 2%, Merck, Germany), followed by immersion in a nitric acid (6N) bath for at least 48h and then rinsed 3 times with ultra-pure water (18.2 MΩ cm^2) (MilliQ, Millipore, Germany).

Approximately 100 mg of sediments and soils were digested using 1 mL of HF (40%, Merck Suprapur®), 5 mL of HNO_3 (65%, Merck Suprapur®) and 2 mL of HCl (30%, Merck Suprapur®) in a microwave oven (Multiwave PRO, Anton Paar, Austria). After digestion, a complexation run was performed after adding 6 mL of saturated boric acid (H_3BO_3) solution to each vial. All samples were digested in duplicates. Reference materials and blanks were run in each digestion batch.

Determination of REEY and trace elements were performed by ICP-MS (iCAP RQ, Thermo Scientific, Germany). Details are presented in the supplementary material (Table S1). The isotopes selected for the quantification of REE were ^{89}Y, ^{139}La, ^{140}Ce, ^{141}Pr, ^{146}Nd, ^{147}Sm, ^{153}Eu, ^{157}Gd, ^{159}Tb, ^{163}Dy, ^{165}Ho, ^{166}Er, ^{169}Tm, ^{172}Yb and ^{175}Lu and we also determined ^{59}Co and ^{207}Pb. Polyatomic and isobaric interferences were monitored. Solutions of Tb and Gd, and La, Ce, Pr, Nd, Sm, and Ba, both at 1 μg kg^{-1}, were run every 20 samples. The concentrations for REE were not corrected for oxide formations because there were considered negligible. Calibration curves of 0.005 to 12 μg kg^{-1} and 0.05 to 35 μg kg^{-1} were used for the quantification of REEY and trace elements, respectively. Indium was used as the internal standard (1 μg kg^{-1}, final concentration).

Aluminium, Fe, Mn, and Si analyses were performed by ICP OES (Shimadzu, ICPE-9820, Japan). Experimental conditions are presented in Table S1. Calibration curves of 0.001 to 2.5 mg kg^{-1} for Mn and 0.5 to 55 mg kg^{-1} for Al, Fe and Si were used for quantification of the major elements. Procedural blanks (HNO_3 2%) were negligible compared with measured concentrations. The accuracy of the analytical procedures was monitored using the certified materials Estuarine Sediment - BCR 667 and MESS-3/NRCC (Tables S2 and Table S3).

RESULTS AND DISCUSSION

SURFICIAL ESTUARINE SEDIMENT COMPOSITION AND REE ABUNDANCES

Surface samples along the estuarine gradient were composed mostly of coarse-grained material. Sand content ranged from 77% to 93%, for J1 and J5 respectively (Table S4), reason that made us to work with the fine fraction of sediments to minimize the effects of grain-size variability and to allow comparability with the mangrove data.

Aluminium contents were fairly constant along the estuary (7.89 to 9.19%), whereas Fe (4.61 to 7.66%) and Si (15.9 to 21%) contents decreased seaward (Table S4). No clear pattern was observed for the Co contents that varied between 14.1 and 20.2 mg kg^{-1}. Lead and Mn presented the highest concentration at the estuary mouth, minimum values at the middle estuary and an increase again at the upper estuary. Concentration of Pb in the fine fraction of sediments at the mouth of the estuary (35.7 mg kg^{-1}) was slightly above the lower-threshold value (TEL; Buchman, 2008). However, we do not expect this level to be toxic, once the fine fraction of sediments represents only 23% of the bulk. The levels presented here corroborate with previous studies that suggested this area as a mostly well-preserved system (Hatje et al., 2010; Hatje and Barros, 2012; Krull et al., 2014), although local low-level contamination associated with point

sources has been observed in a few sites for Hg (Hatje et al., 2019) and petrol hydrocarbons (Egres et al., 2019).

The total REE (ΣREE; Fig. 2) contents varied within a small interval (202 to 220 mg kg^{-1}), with highest concentrations observed at the upper estuary. Our values are in the superior range of concentrations reported for coastal systems such as the Tagus estuary (18 - 210 mg kg^{-1}; (Brito et al., 2018)), Mandovi estuary (129 - 227 mg kg^{-1}; (Shynu et al., 2011)), Zuari estuary (175 - 320 mg kg^{-1}; (Shynu et al., 2013)), Galian Rias (3 - 233 mg kg^{-1}; (Prego et al., 2012, 2009)), and the North Australian estuaries (77 - 263 mg kg^{-1}; (Munksgaard et al., 2003)). Light REE (LREE; La, Ce, Pr, and Nd) was the most abundant fraction (90% of the total) in the estuarine sediments (Fig. 2 and Table S5), followed by the medium REE (MREE; Sm, Eu, Gd, Tb, Dy, and Ho) and the HREE (Er, Tm, Yb, and Lu). Similar observations were made for studies elsewhere (Brito et al., 2018; Elderfield et al., 1990). As for Sappal et al., (2014), Prasad and Ramantahan (2008), Ramesh et al., (1999), Rengarajan and Sarin (2004), Shynu et al., (2011) and Consani et al., (2020), Ce was the most abundant element to contribute to the total ΣREE (87.1 - 99.5 mg kg^{-1}).

The Post Archean Australian Shale (PAAS) (Taylor and McLennan, 1985) is widely used as a normalizing agent to evidence the fractionation of REE relative to the source, also allowing ease comparison between studies. The PAAS-normalized abundances (Fig. 3) displayed a consistent enrichment of the LREE over the HREE, with ratios of $(La/Yb)_{PAAS}$ = 2.75 ± 0.48, La/Gd_{PAAS} = 1.31 ± 0.12, and Gd/Yb_{PAAS} = 2.10 ± 0.28. The fractionation was highest at the most upstream station (J10) and decreased seaward (Fig. S1), in keeping with the general understanding of REE particle reactivity. In estuarine environments, dissolved and particulate REE undergoes flocculation and precipitation processes. The removal of dissolved REE during these processes, especially in waters with low salinity (upper estuary, Table S4), reflects induced coagulation by salt from ubiquitous organic and ferromanganese colloids that

remove REE, promoting their fractionation (Hoyle et al., 1984; Goldstein and Jacobsen, 1988; Byrne and Kim, 1990; Sholkovitz, 1992; Sholkovitz, 1993; Schijf, 1995; Sholkovitz and Szymczak, 2000; Chaillou et al., 2006; Rousseau et al., 2015).

Among the REE, the LREE tend to be more reactive than MREE and HREE (Goldstein and Jacobsen, 1988; Sholkovitz and Elderfield, 1988; Elderfield et al., 1990, Sholkovitz, 1993). LREE is preferably associated with the solid phase due to their more pronounced complexation with ligands on the particles and surfaces of the colloids. On the contrary, the depleted HREE in the sediments is the result of their greater tendency to form stable soluble carbonate and organic complexes with dissolved ligands when compared to LREE and MREE (Fleet 1984; Millero 1992; Schijf et al., 1995; Kuss et al. 2001). These processes cause the removal, preferentially of LREE, and fractionation of the REE pattern along the estuarine gradient. A recent study that evaluated the fractionation of dissolved REE along the continuum between the Paraguaçu estuary through Todos os Santos Bay and the adjacent sea, reported that REE were scavenged in the estuarine low salinity region (< 5) following the order LREE> MREE> HREE and that PAAS-normalized patterns varied from relatively flat at the fluvial endmember to the ocean-like HREE enriched pattern at the estuary mouth (Andrade et al., 2020), supporting the results observed here for estuarine sediments.

The LREE and C_{org} showed low correlation ($r = 0.48$, $p < 0.05$; Table S6) in sediments, but positive and significant correlations ($p < 0.05$; Table S6) were observed between the LREE and Al ($r = 0.85$) and Fe ($r = 0.96$). These results indicated that Al and Fe-oxyhydroxides are the main scavenging phases for the LREE, similarly to what was observed by previous works (Sholkovitz et al., 1994; Chaillou et al., 2006; Caccia and Millero, 2007; Marmolejo-Rodríguez et al., 2007; Caetano et al., 2009). The mobility of the LREE in these oxic sediments may be controlled by the precipitation of Fe insoluble forms. MREE and HREE did not show the same affinity for Al or Fe-oxyhydroxides (Table S6). Iron and Mn behave differently in estuarine

environments and their concentrations may also be controlled by distinct processes. Unlike Fe, Mn has slower oxidation kinetics (Benjamin and Honeyman, 1992) and did not show correlation with LREE and HREE. In estuaries, Mn is mainly associated with inorganic complexes (Stumm and Morgan, 1981) and its behavior is controlled by oxidation and scavenging onto suspended material. Strong positive correlation was found between MREE and Mn ($p < 0.05$; $r = 0.94$; Table S6), which connects the removal of MREE to the Mn cycle. This connection nevertheless needs to be further studied to clarify why only the MREE were associated with Mn.

It is usual to calculate the expected shale-normalized concentration of a REE in order to quantify the anomalous concentrations in relation to its neighboring REE. The Eu (Eu/Eu*) anomalies were calculated as follows:

$$Eu/Eu^{*} = Eu_{PAAS}/(Sm_{PAAS} \times Gd_{PAAS})^{1/2}$$ (Taylor and McLennan, 1985).

Eu showed small positive anomalies (1.22 ± 0.06), with slightly higher values at the upper estuary (Table S5). The occurrence of positive Eu anomalies is unusual in estuarine sediments, but they have been previously observed in other estuaries and attributed to feldspar-rich sources (Ramesh et al., 1999; Brito et al., 2018; Consani et al., 2020). In this study, the positive values may also reflect the weathering of granite abundant in the basin source region (Hatje e de Andrade, 2009). Cerium (Table S5) and other REE showed no significant anomalies (Fig. 3).

DOWN-CORE DISTRIBUTIONS

SEDIMENT CHARACTERIZATION AND MAJOR ELEMENTS COMPOSITION

Sediment characterization of these cores has previously been discussed (Hatje et al 2020, submitted). Mangrove soils are mostly composed of fine sediments (Fig. S2; average silt + clay = 98 ± 4) and present relatively high contents of C_{org} (9.0 ± 2.3).

Iron, Al, and Si displayed only minor variation along the sedimentary profiles (Fig. 4), except for the core T3. In the case of Mn, from the bottom of the cores up to around 40 cm for cores T5 and T6 and up to 20 cm for core T4, concentrations remained mostly constant, and then decreased towards the surface. For core T3, Mn followed the same trend as Fe and Al. Contents of Al, Fe, and Mn were slightest higher in the upper estuary cores, whereas Si was highest at the core T3, which presented the largest amount of sand (Table S7). Granulometry is clearly controlling major elements distributions in soils.

DISTRIBUTIONS PATTERNS OF REE

Abundances of REEY are presented in Table S8. The average ΣREE of the mangrove soil profiles along the salinity gradient tended to increase from the lower (161 ± 18 mg kg^{-1}) to the upper estuary (183 ± 16 mg kg^{-1}), following the same trend observed for the estuarine sediments. The highest percentage of sand in cores T3 and T4 influenced the REE abundances similarly to the major elements and caused lower REE retention in mangrove soils. REE are mostly adsorbed on the fine-grained mangrove soils as previously observed for sediments elsewhere (Sinitsyn et al., 2000; Chaillou et al., 2006; Caetano et al., 2013). Recently it has also been shown that REE may also fractionate between fine and bulk sediments, increasing LREE/HREE ratios in the fine fraction (Consani et al., 2020).

LREEs were the major contributors to the ΣREE for all profiles (88–90%), followed by the MREE, varying between 8 and 10% of the total REE, while the HREE accounted for only to 2–3% of the total. Comparing the ΣREE and the fractionation of estuarine sediments and superficial mangrove soils (Fig. 3), we can observe that: i. REE abundances are lower at

mangrove soils; ii. the influence of the salinity gradient, as expected, was more prominent in the estuarine sediments than in the mangrove soils, despite the regular flooding associated to tidal cycles; iii. the shale normalized pattern becomes flatter and more similar to PAAS in mangrove soils along the whole salinity gradient; and that iv. the positive Eu anomalies are also a consistent feature in mangrove soils. These patterns may reflect the numerous phases (e.g., organic matter, sulphides, lithogenic particles, carbonates, and oxi-hydroxides) that control REE scavenging depending on the local physico-chemical conditions (Elderfield, 1990; Davranche et al., 2004; Caccia and Millero, 2007; Caetano et al., 2009; Brito et al., 2018; Marmolejo-Rodríguez et al., 2007; Sholkovitz et al., 1992; Prego et al., 2009; Prasad and Ramanathan, 2008). Despite the potential importance of organic matter on the REE cycling in mangroves, effects of organic matter in REE has been surprisingly overlooked so far (Freslon et al., 2014). Besides the difference in REE contents, organic matter in estuarine sediments and mangrove soils may have distinct contributions of continental and marine sources, that to a certain extent may be translated into distinct scavenging capacities. Moreover, the texture of sediments, redox potential and contents of organic matter may influence early diagenetic processes related to mineralization of organic matter in mangrove soils and also the reduction of Fe-Mn oxyhydroxides.

Sedimentation rates across the estuarine gradient varies over an order of magnitude from 5.1 ± 0.3 mm $year^{-1}$ (core T3) to 31 ± 2 mm $year^{-1}$ (core T1), corresponding to accumulation periods of around 25 to 100 years, respectively (Hatje et al., 2020 submitted). The vertical profiles of ΣREE were substantially more variable at the lower estuary (Fig. 5) that presents the highest sedimentation rate (core T1). The varying depositional accumulation rates and associated post-deposition processes may contribute to the patterns observed in the abundances of the ΣREE and their fractionation between estuaries and mangrove soils. Depth profiles of ΣREE (Fig. 5) showed that abundances increased by up to ~50% from surface to 5

cm in core T1. This pattern was observed for all cores, but it was more pronounced for the lower estuary, which is more hydrodynamic than the sheltered upper estuary. The LREE (~45%) were the largest contributor for the vertical variation observed, followed by the MREE (~25%), whereas the HREE increased only ~6% (core T1, Fig. 6). When sediments are deposited in a high sedimentation regime, rapid burial may limit the exposure time of the dissolved REE with sediment and, hence, restricts its adsorptive capacity (Ruhlin and Owen, 1986), possibly resulting in a lower concentration of ΣREE in sediments. Besides, the organic matter derived from mangroves is expected to be depleted in REE compared to river born material, thus organic matter input in highly productive systems may act as diluting agent lowering REE abundances in soils. Recently, Mandal et al. (2019) showed that total REE concentrations in mangrove species are much lower than in soils, corroborating with our hypothesis.

Below the subsurface peak in the ΣREE (Fig. 5), concentrations showed little changes with depth, indicating that diagenetic alterations after burial are not mobilizing REE substantially, even in scales from decades to a century. The Fe and Mn concentrations (Fig. 4) did not show vertical profiles that indicate a well-established depth sequence of redox conditions. In fact, all cores were visually very homogeneous (i.e., no clear lamination), dark grey, and presented the characteristic odor of H_2S, suggesting the presence of FeS_2 sulphides. It is unfortunate, however, that S and SO^{2-}_4 were not measured. REE in mangrove soils may be co-precipitating with metal sulphides (Schijf et al., 1995 and Chaillou et al., 2006), but his hypothesis, however, needs to be further investigated.

The Ce and Eu profiles (Fig. S3) are expected to be different than other REE due to their redox behavior. However, Ce and Eu profiles followed similar tendencies to that observed on ΣREE profiles, indicating that anoxic condition is prevalent and mostly invariant along cores.

Depth profiles of La, Gd, and Yb concentrations in mangrove soils, representing LREE, MREE, and HREE, respectively, are presented in Fig. 6. In general, the greatest variabilities were observed by La (3% - 43%), between surface and the top 5-15 cm layers. Below the sub-surface maxima, there was no significant variability in concentrations along most cores. Vertical variations were mostly absent for cores T3 and T4. The Fig. 6 shows an increase in the Gd concentrations (9 to 45%) between surface and 5-15 cm for all cores. For the Yb profiles, only the cores T1, T2, and T5 showed some variability (8% - 26%) along cores.

Variations of LREE/HREE ratios in mangrove soils across the estuary ranged from 1.5 ± 0.3 (lower estuary) to 2.0 ± 0.1 (upper estuary) (Fig. 5).The greatest LREE/HREE ratios found in the upper estuary are associated with the enrichment of LREE in the soils caused by the greater reactivity of LREE and adsorption capacity onto clay matter and other insoluble colloidal matters in the region of low salinity, near the fluvial source (Ramesh et al., 1999; Censi et al., 2004; Dubinin, 2004; Prasad and Ramanathan, 2008). The vertical profiles of the LREE/HREE are similar to ΣREE, indicating that the processes involved in the increased of REE abundances also controlling the enrichment of the LREE in mangrove soils.

The PAAS-normalized REE patterns for selected layers of mangrove soils reveal no changes along the cores, but there was some variation in terms of abundances (Fig. 7). For all cores, normalized abundances were minimum at the surface. The layers below surficial soils revealed higher fractionation relative to the shale (Fig. 5 and 7).

The redox-sensitive REE, Ce and Eu may be used to indicate changes in redox conditions in soils (Elderfield, 1990; Hannigan et al, 2010). The positive Eu anomalies (Fig. 7, Table S8) found in soils indicate reduction of Eu^{+3} to Eu^{+2} and incorporation into the soils which may be attributed to (i) the prevailing reducing conditions in the mangrove environment and (ii) the riverine signature of detrital material from the weathering of source rocks that are carried by the Jaguaripe estuary.

The correlation coefficients between LREE and MREE were significant ($r > 0.8$; $p < 0.05$; Table S10) for all cores. MREE showed high correlations with HREE only in the cores T3, T5 and T6 ($r > 0.8$; $p < 0.05$; Table S10). Only for core T2 there was significant correlation with organic carbon, pointing out their poor association in mangrove soils. In the dissolved fraction/porewater, however, we expect that organic matter has a dominant role the in the solubilization of REE during soil reduction.

Correlations between REE, Fe, and Mn were not significant for most cores either (Table S10). This lack of correlations, associated with the reducing characteristics of the mangrove soils suggests that sulphides may be an important burial phase for REE. Co-precipitation of the REE with metal sulphides may be a widespread process under the reducing mangrove soil conditions. This hypothesis, which needs to be tested, has been previously evoked to explain REE behavior in sediments of the Bay of Biscay (Chaillou et al., 2006).

The patterns observed in sediment chemistry in estuaries and mangroves may be explained by the superimposition of a series of processes that includes large scale estuarine mixing, inputs of fluvial REE and colloidal material, autochthonous organic matter production, suspended particulate material inputs and transport across the estuarine and intertidal gradient, local conditions such as submarine groundwater discharge, redox and salinity gradients. The myriad of processes acting together imping a high complexity in the understanding of the REE cycles in mangroves. To better fingerprint the sources and controls of REE accumulation and remobilization in soils, speciation data for sediments and porewater geochemistry will be necessary to test the hypotheses presented here.

CONCLUSIONS

Fractionating along the estuary causes an enrichment in LREE over HREE in estuarine sediments and mangrove soils which is attributed to the preferential removal of the LREE at

the upper estuary. REE abundances are lower in mangrove soils than in estuarine sediments and average ΣREE tended to be highest at the upper estuary. Positive Eu anomalies were found in all cores and may be attributed to the dominant reducing conditions in the mangrove soils and also the riverine detrital signature from the weathering of source rocks. Vertical REEY profiles show that: i. post-deposition processes might contribute to the patterns observed in the abundances of the ΣREE and their fractionation at surface and subsurface mangrove soils; ii. the ΣREE and REE pattern were mostly constant through profiles below 15 cm, indicating that diagenetic alteration after burial is not leading to REE fractionation, as can be observed by the LREE/HREE profiles; and iii. co-precipitation of REE with metal sulphides may be an important burial mechanism. No clear relationship was observed between REE and organic matter in soils. The latter, however, needs to be better explored looking at REE speciation in sediments and REE abundances in mangrove pore waters. The REE abundances observed here corroborate to the characterization of the Jaguaripe estuary as a pristine system that does not display contamination. The REE abundances can be used as background for the region.

ACKNOWLEDGMENTS

We thank FAPESB (PET0034/2012; PAM Nº. 0020/2014), GASBRAS/FINEP and CNPq 441264/2017-4, 407297/2018-9) for financial support. The authors were sponsored by FAPESB (T. Freitas), CAPES (R. Pedreira) and CNPq (V. Hatje, 304823/2018-0). We also thank the volunteers that helped with the sample collection.

REFERENCES

Andrade, R. L. B., Hatje, V., Pedreira, R. M. A., Böning, P., Pahnke, K., 2020. REE fractionation and human Gd footprint along the continuum between Paraguaçu River to coastal South Atlantic waters. Chemical Geology. 532, 119303.

Benjamin, M. M., Honeyman, B.D., 1992. Trace metals. In: Ž. Butcher, S.S., Charlson, R.J., Orians, G.H., Wolfe, G.V. (Eds.). Global Biogeochemical Cycles. Academic Press, London. 317–352.

Buchman, M. F., 2008. NOAA Screening Quick Reference Tables, NOAA OR&R Report 08-1. Seattle WA, Office of Response and Restoriation Division, National Oceanic and Atmospheric Administration, 34 pages.

Brito, P., Prego, R., Mil-Homens, M., Caçador, I., Caetano, M., 2018. Sources and distribution of yttrium and rare earth elements in surface sediments from Tagus estuary, Portugal. Science of the Total Environment. 621, 317–325.

Byrne, R. H., Kim, K. H., 1990. Rare earth element scavenging in seawater. Geochimica et Cosmochimica Acta. 54, n. 10, 2645–2656.

Caccia, V. G., Millero, F. J., 2007. Distribution of yttrium and rare earths in Florida Bay sediments. Marine Chemistry. 104, n. 3–4, 171–185.

Caetano, M., Prego, R., Vale, C., de Pablo, H., Marmolejo-Rodríguez, J., 2009. Record of diagenesis of rare earth elements and other metals in a transitional sedimentary environment. Marine Chemistry. 116, n. 1–4, 36–46.

Caetano, M., Vale, C., Anes, B., Raimundo, J., Drago, T., Schimdt, S., Nogueira, M., Oliveira, A., Prego, R., 2013. The Condor seamount at Mid-Atlantic Ridge as a supplementary source of trace and rare earth elements to the sediments. Deep-Sea Research Part II: Topical Studies in Oceanography. 98, 24–37.

Censi, P., Mazzola, S., Sprovieri, M., Bonanno, A., Patti, B., Punturo, R., Spoto, S. E. Saiano, F., Alonzo, G., 2004. Rare earth elements distribution in seawater and suspended particulate of the Central Mediterranean Sea. Chemistry and Ecology. 20, n. 5, 323–343.

Censi, P., Spoto, S. E., Nardone, G., Saiano, F., Punturo, R., Di Geronimo, S. I., Mazzola, S., Bonanno, A., Patti, B., Sprovieri, M., Ottonello, D., 2005. Rare-earth elements and yttrium distributions in mangrove coastal water systems: The western Gulf of Thailand. Chemistry and Ecology. 21, n. 4, 255–277.

Censi, P., Sprovieri, M., Saiano, F., Di Geronimo, S. I., Larocca, D., Placenti, F., 2007. The behaviour of REEs in Thailand's Mae Klong estuary: Suggestions from the Y/Ho ratios and lanthanide tetrad effects. Estuarine, Coastal and Shelf Science. 71, n. 3–4, 569–579.

Chaillou, G., Anschutz, P., Lavaux, G., Blanc, G., 2006. Rare earth elements in the modern sediments of the Bay of Biscay (France). Marine Chemistry. 100, n. 1–2, 39–52.

Cirano, M., Lessa, G. C., 2007. Oceanographic Characteristics of Baía de Todos os Santos, Brazil. Revista Brasileira de Geofísica. 25, n.4, 363-387.

Consani, S., Cutroneo, L., Carbone, C., Capello, M., 2020. Baseline of distribution and origin of Rare Earth Elements in marine sediment of the coastal area of the Eastern Gulf of Tigullio (Ligurian Sea, North-West Italy). Marine Pollution Bulletin. 155, 111145.

Costa, P., Dórea, A., Mariano-Neto, E., Barros, F., 2015. Are there general spatial patterns of mangrove structure and composition along estuarine salinity gradients in Todos os Santos Bay? Estuarine, Coastal and Shelf Science. 166, 83–91.

Davranche, M., Pourret, O., Gruau, G., Dia, A., 2004. Impact of humate complexation on the adsorption of REE onto Fe oxyhydroxide. Journal of Colloid and Interface Science. 277, n. 2, 271–279.

Davranche, M., Grybos, M., Gruau, G., Pédrot, M., Dia, A., Marsac, R., 2011. Rare earth element patterns: A tool for identifying trace metal sources during wetland soil reduction. Chemical Geology. 284, n. 1–2, 127–137.

Delgado, J., Pérez-López, R., Galván, L., Nieto, J. M., Boski, T., 2012. Enrichment of rare earth elements as environmental tracers of contamination by acid mine drainage in salt marshes: A new perspective. Marine Pollution Bulletin. 64, n. 9, 1799–1808.

Dubinin, A. V., 2004. Geochemistry of rare earth elements in the ocean. Lithology and Mineral Resources. 39, n. 4, 289–307.

Egres, A. G., Hatje, V., Miranda, D. A., Gallucci, F., Barros, F., 2019. Functional response of tropical estuarine benthic assemblages to perturbation by Polycyclic Aromatic Hydrocarbons. Ecological Indicators. 96, 229–240.

Elderfield, H., Upstill-Goddard, R., Sholkovitz, E. R., 1990. The rare earth elements in rivers, estuaries, and coastal seas and their significance to the composition of ocean waters. Geochimica et Cosmochimica Acta. 54, n. 4, 971–991.

Freslon, N., Bayon, G., Toucanne, S., Bermell, S., Bollinger, C. Chéron, S., Etoubleau, J., Germain, Y., Khripounoff, A., Ponzevera, E., Rouget, M. L., 2014. Rare earth elements and neodymium isotopes in sedimentary organic matter. Geochimica et Cosmochimica Acta. 140, 177-198.

Furukawa, K., Wolanski, E., 1996. Sedimentation in Mangrove Forests. Mangroves and Salt Marshes. 1, 3–10.

Fleet, A. J., 1984. Aqueous and sedimentary geochemistry of the rare earth elements. Elsevier B.V. Chapter 10. 2, 343-373.

Furukawa, K., Wolanski, E., Mueller, H., 1997. Currents and sediment transport in mangrove forests. Estuarine, Coastal and Shelf Science. 44, 301–310.

Goldstein, S. J., Jacobsen, S. B., 1987. The Nd and Sr isotopic systematics of river-water dissolved material Implications for the sources of Nd and Sr in seawater. 66, 245–272, 2015.

Goldstein, S. J., Jacobsen, S. B., 1988. Rare earth elements in river waters. Earth and Planetary Science Letters. 89, n. 1, 35–47.

Hannigan, R., Dorval, E., Jones, C., 2010. The rare earth element chemistry of estuarine surface sediments in the Chesapeake Bay. Chemical Geology. 272, n. 1–4, 20–30.

Hatje, V., de Andrade, J.B., 2009. In: Hatje, V., de Andrade, J.B. (Eds.), Baía De Todos Os Santos: Aspectos Oceanográficos. EDUFBA, Salvador, 302.

Hatje, V., Macedo, S. M., de Jesus, R. M., Cotrim, G., Garcia, K. S., de Queiroz, A. F., Ferreira, S. L.C., 2010. Inorganic As speciation and bioavailability in estuarine sediments of Todos os Santos Bay, BA, Brazil. Marine Pollution Bulletin. 60, n. 12, 2225–2232.

Hatje, V.; Barros, F., 2012. Overview of the 20th century impact of trace metal contamination in the estuaries of Todos os Santos Bay: Past, present and future scenarios. Marine Pollution Bulletin. 64, n. 11, 2603–2614.

Hatje, V., Andrade, R. L.B., Jesus, R. M., Masqué, P., Albergaria-Barbosa, A. C.R., de Andrade, J. B., Santos, A. C.S.S., 2019. Historical records of mercury deposition in dated sediment cores reveal the impacts of the legacy and present-day human activities in Todos os Santos Bay, Northeast Brazil. Marine Pollution Bulletin. 145, 396–406.

Hatje, V., Masqué P., Patire, V., Dórea, A., Barros, F. Blue C stocks, accumulation rates, and associated spatial variability in Brazilian mangroves. 2020 submitted.

Hoyle, J., Elderfield, H., Gledhill, A., Greaves, M., 1984. The behaviour of the rare earth elements during mixing of river and sea waters. Geochimica et Cosmochimica Acta. 48, n. 1, 143–149.

Johannesson, K. H., Cortés, A., Alfredo, J., Leal, R., Ramírez, A. G., Durazo, J., 2005. Geochemistry of rare earth elements in groundwaters from a rhyolite aquifer, central México. Chapter 8. 187–222.

Kawabe, I., Kitahara, Y., Naito, K., 1991. Non-chondritic yttrium/holmium ratio and lanthanide tetrad effect observed in pre-Cenozoic limestones. Geochemical Journal. 25, n. 1, 31–44.

Kuss, J., Garbe-Schönberg, C. D., Kremling, K., 2001. Rare earth elements in suspended particulate material of North Atlantic surface waters. Geochimica et Cosmochimica Acta. 65, n. 2, 187–199.

Krull, M., Abessa, D. M.S., Hatje, V., Barros, F., 2014. Integrated assessment of metal contamination in sediments from two tropical estuaries. Ecotoxicology and Environmental Safety. 106, 195–203.

Lawrence, M. G., Kamber, B. S., 2006. The behaviour of the rare earth elements during estuarine mixing-revisited. Marine Chemistry. 100, n. 1–2, 147–161.

Liu, J., Xiang, R., Chen, Z., Chen, M., Yan, W., Zhang, L., Chen, H., 2013. Sources, transport and deposition of surface sediments from the South China Sea. Deep-Sea Research Part I: Oceanographic Research Papers. 71, 92–102.

Mandal, S. K., Ray, R., González, A. G., Mavromatis, V., Pokrovsky, O. S., Jana, T. K., 2019. State of rare earth elements in the sediment and their bioaccumulation by mangroves: a case study in pristine islands of Indian Sundarban. Environmental Science and Pollution Research. 26, n. 9, 9146–9160.

Marmolejo-Rodríguez, A. J., Prego, R., Meyer-Willerer, A., Shumilin, E., Sapozhnikov, D., 2007. Rare earth elements in iron oxy-hydroxide rich sediments from the Marabasco River-Estuary System (pacific coast of Mexico). REE affinity with iron and aluminium. Journal of Geochemical Exploration. 94, n. 1–3, 43–51.

Millero, F. J., 1992. Stability constants for the formation of rare earth-inorganic complexes as a function of ionic strength. Geochimica et Cosmochimica Acta. 56, n. 8, 3123–3132.

Munksgaard, N. C.; Lim, K.; Parry, D. L., 2003. Rare earth elements as provenance indicators in North Australian estuarine and coastal marine sediments. Estuarine, Coastal and Shelf Science. 57, n. 3, 399–409.

Pedreira, R. M. A., Pahnke, K., Böning, P., Hatje, V., 2018. Tracking hospital effluent-derived gadolinium in Atlantic coastal waters off Brazil. Water Research. 145, 62–72.

Piper, D. Z.; Bau, M., 2013. Normalized Rare Earth Elements in Water, Sediments, and Wine: Identifying Sources and Environmental Redox Conditions. American Journal of Analytical Chemistry. 04, n. 10, 69–83.

Prasad, M. B. K.; Ramanathan, A., 2008. Distribution of Rare Earth Elements in the Pichavaram Mangrove Sediments of the Southeast Coast of India. Journal of Coastal Research. 1, 126–134.

Prego, R., Caetano, M., Vale, C., Marmolejo-Rodríguez, J., 2009. Rare earth elements in sediments of the Vigo Ria, NW Iberian Peninsula. Continental Shelf Research. 29, n. 7, 896–902.

Prego, R., Caetano, M., Bernárdez, P., Brito, P., Ospina-Alvarez, N., Vale, C., 2012. Rare earth elements in coastal sediments of the northern Galician shelf: Influence of geological features. Continental Shelf Research. 35, 75–85.

Ramesh, R., Ramanathan, A. L., James, A. R., Subramanian, V., Jacobsen, S. B., Holland, H. D., 1999. Rare earth elements and heavy metal distribution in estuarine sediments of east coast of India. Hydrobiologia. 397, n. 1966, 89–99.

Rengarajan, R., Sarin, M. M., 2004. Distribution of rare earth elements in the Yamuna and the Chambal rivers, India. Geochemical Journal. 38, n. 6, 551–569.

Rousseau, T. C. C., Sonke, J. E., Chmeleff, J., Van B. P., Souhaut, M., Boaventura, G., Seyler, P., Jeandel, C., 2015. Rapid neodymium release to marine waters from lithogenic sediments in the Amazon estuary. Nature Communications, v. 6.

Ruhlin, D. E., Owen, R. M., 1986. The rare earth element geochemistry of hydrothermal sediments from the East Pacific Rise: Examination of a seawater scavenging mechanism. Geochimica et Cosmochimica Acta. 50, n. 3, 393–400.

Sappal, S. M., Ramanathan, A., Ranjan, R. K., Singh, G., Kumar, A., 2014. Rare Earth Elements as Biogeochemical Indicators in Mangrove Ecosystems (Pichavaram, Tamilnadu, India). Journal of Sedimentary Research. 84, n. 9, 781–791.

Schijf, J., De Baar, H. J. W.; Millero, F. J., 1995. Vertical distributions and speciation of dissolved rare earth elements in the anoxic brines of Bannock Basin, eastern Mediterranean Sea. Geochimica et Cosmochimica Acta. 59, n. 16, 3285–3299.

Shynu, R., Rao, V. P., Kessarkar, P. M., Rao, T. G., 2011. Rare earth elements in suspended and bottom sediments of the Mandovi estuary, central west coast of India: Influence of mining. Estuarine, Coastal and Shelf Science. 94, n. 4, 355–368.

Shynu, R., Rao, V. P., Parthiban, G., Balakrishnan, S., Narvekar, T., Kessarkar, P. M., 2013. REE in suspended particulate matter and sediment of the Zuari estuary and adjacent shelf, western India: Influence of mining and estuarine turbidity. Marine Geology. 346, 326–342.

Silva-Filho, E. V., Sanders, C. J., Bernat, M., Figueiredo, A. M. G., Sella, S. M., Wasserman, J., 2011. Origin of rare earth element anomalies in mangrove sediments, Sepetiba Bay, SE Brazil: Used as geochemical tracers of sediment sources. Environmental Earth Sciences. 64, n. 5, 1257–1267.

Sinitsyn, V. A., Aja, S. U., Kulik, D. A., Wood, S. A., 2000. Acid-base surface chemistry and sorption of some lanthanides on K^+-saturated, Marblehead illite: I. Results of an experimental investigation. Geochimica et Cosmochimica Acta. 64, n. 2, 185–194.

Sholkovitz, E. R., 1976. Flocculation of dissolved organic and inorganic matter during the mixing of river water and seawater. Geochimica et Cosmochimica Acta. 40, n. 7, 831–845.

Sholkovitz, E. R., Elderfield, H., 1988. Cycling of dissolved rare earth elements in Chesapeake Bay. Global Biogeochemical Cycles. 2, n. 2, 157-176.

Sholkovitz, E. R., 1992. Chemical evolution of rare earth elements: fractionation between colloidal and solution phases of filtered river water. Earth and Planetary Science Letters. 114, n. 1, 77–84.

Sholkovitz, E. R., 1993. The geochemistry of rare earth elements in the Amazon River estuary. Geochimica et Cosmochimica Acta. 57, n. 10, 2181–2190.

Sholkovitz, E. R., Landing, W. M., Lewis, B. L., 1994. Ocean particle chemistry: The fractionation of rare earth elements between suspended particles and seawater. Geochimica et Cosmochimica Acta. 58, n. 6, 1567–1579.

Sholkovitz, E., Szymczak, R., 2000. The estuarine chemistry of rare earth elements: Comparison of the Amazon, Fly, Sepik and the Gulf of Papua systems. Earth and Planetary Science Letters. 179, n. 2, 299–309.

Stumm, W., Morgan, J.J., 1981. An introduction emphasizing chemical equilibria in natural waters. Aquatic Chemistry. 2nd Ed. Wiley-Interscience, New York, 282–285.

Taylor, S.R. and McLennan, S.M., 1985. The Continental Crust: Its Composition and Evolution. Blackwell, Oxford, 1-312.

Wasserman, J. C., Figueiredo, A. M. G., Pellegatti, F., Silva-Filho, E. V., 2001. Elemental composition of sediment cores from a mangrove environment using neutron activation analysis. Journal of Geochemical Exploration. 72, n. 2, 129–146.

Zhang, R.; Yan, C.; Liu, J., 2013. Effect of Mangroves on the Horizontal and Vertical Distributions of Rare Earth Elements in Sediments of the Zhangjiang Estuary in Fujian Province, Southeastern China. Journal of Coastal Research. 292, n. 6, 1341–1350.

FIGURES

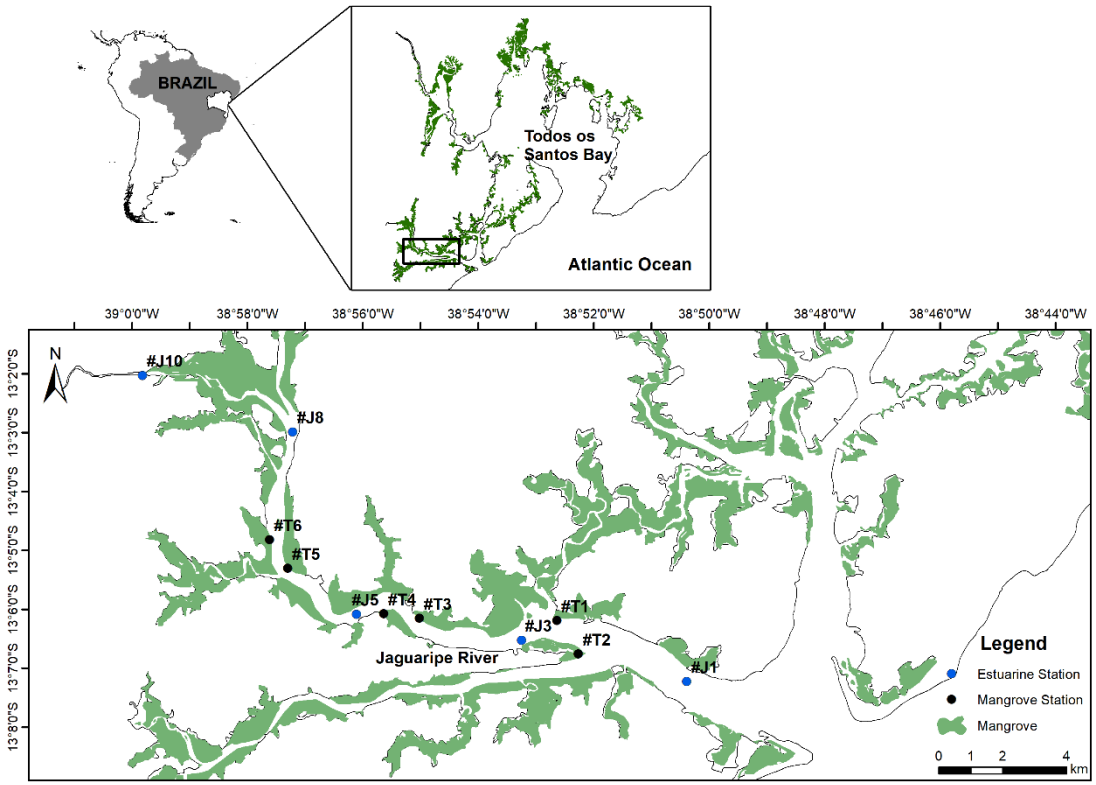

Fig 1. Locations of sampling sites along the Jaguaripe estuary, Bahia, Brazil.

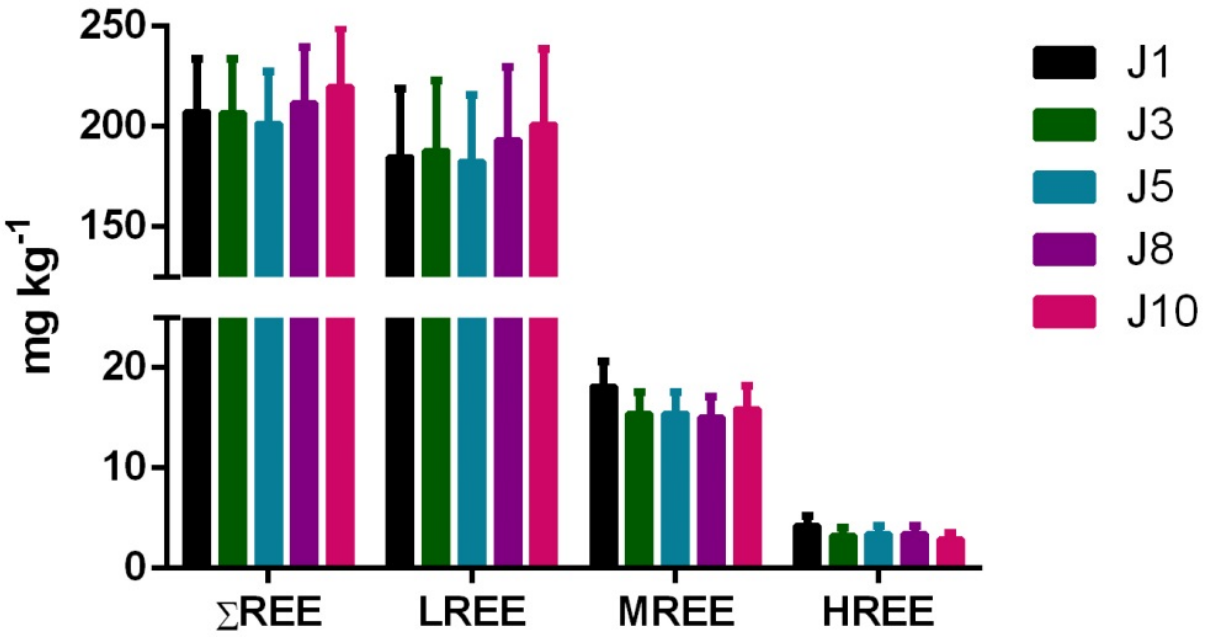

Fig. 2. Total REE (± standard deviation), light (LREE), middle (MREE) and heavy (HREE) REE concentrations for surface sediments of the Jaguaripe estuary.

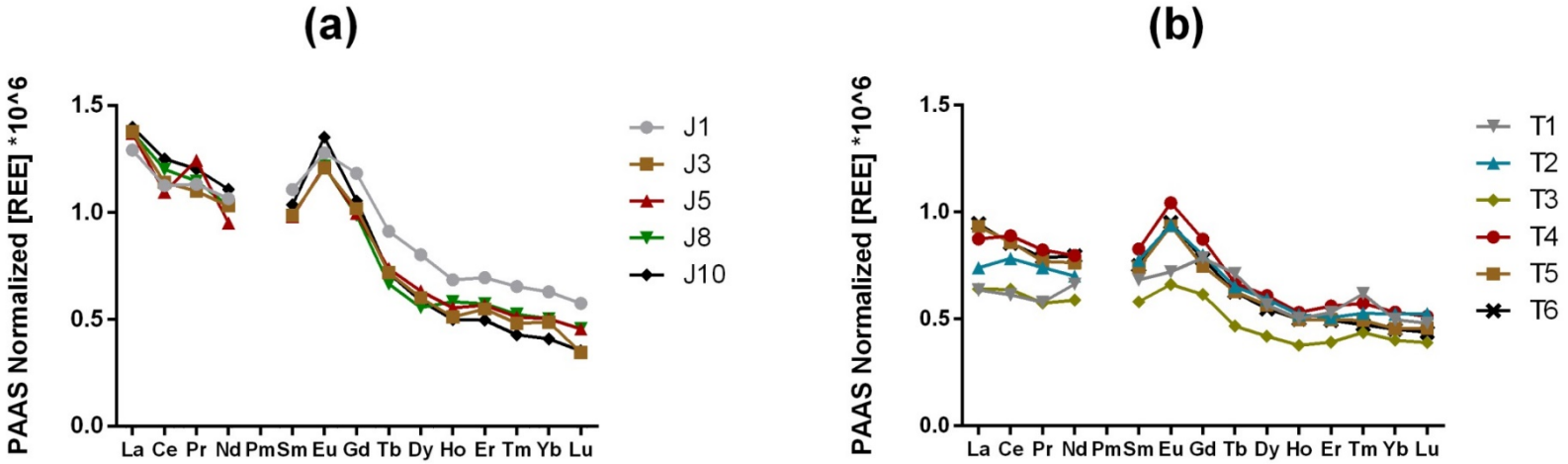

Fig. 3. PAAS-normalized REE patterns in surface sediments across the upper (J10, J8, T5 and T6), middle (J5, J3, T4 and T3), and lower (J1, T1 and T2) Jaguaripe estuary (a) and at surficial mangrove soils (b).

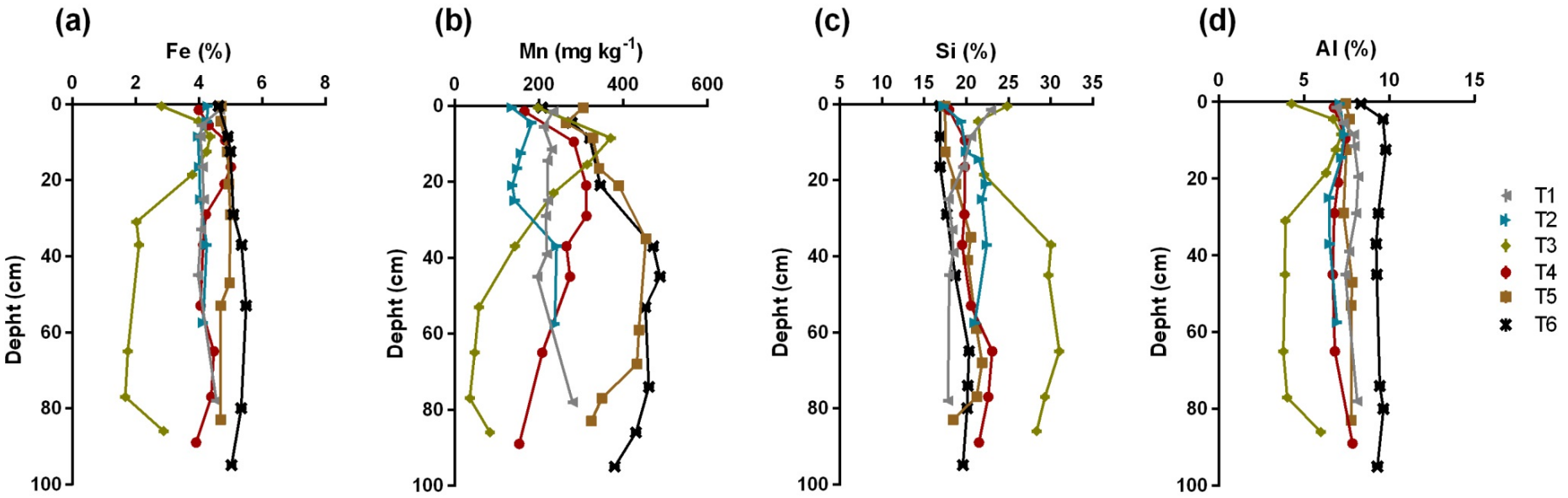

Fig. 4. Depth soil profiles of a) Fe, b) Mn, c) Si and d) Al concentrations in soil profiles (T1- T6) of the Jaguaripe estuary.

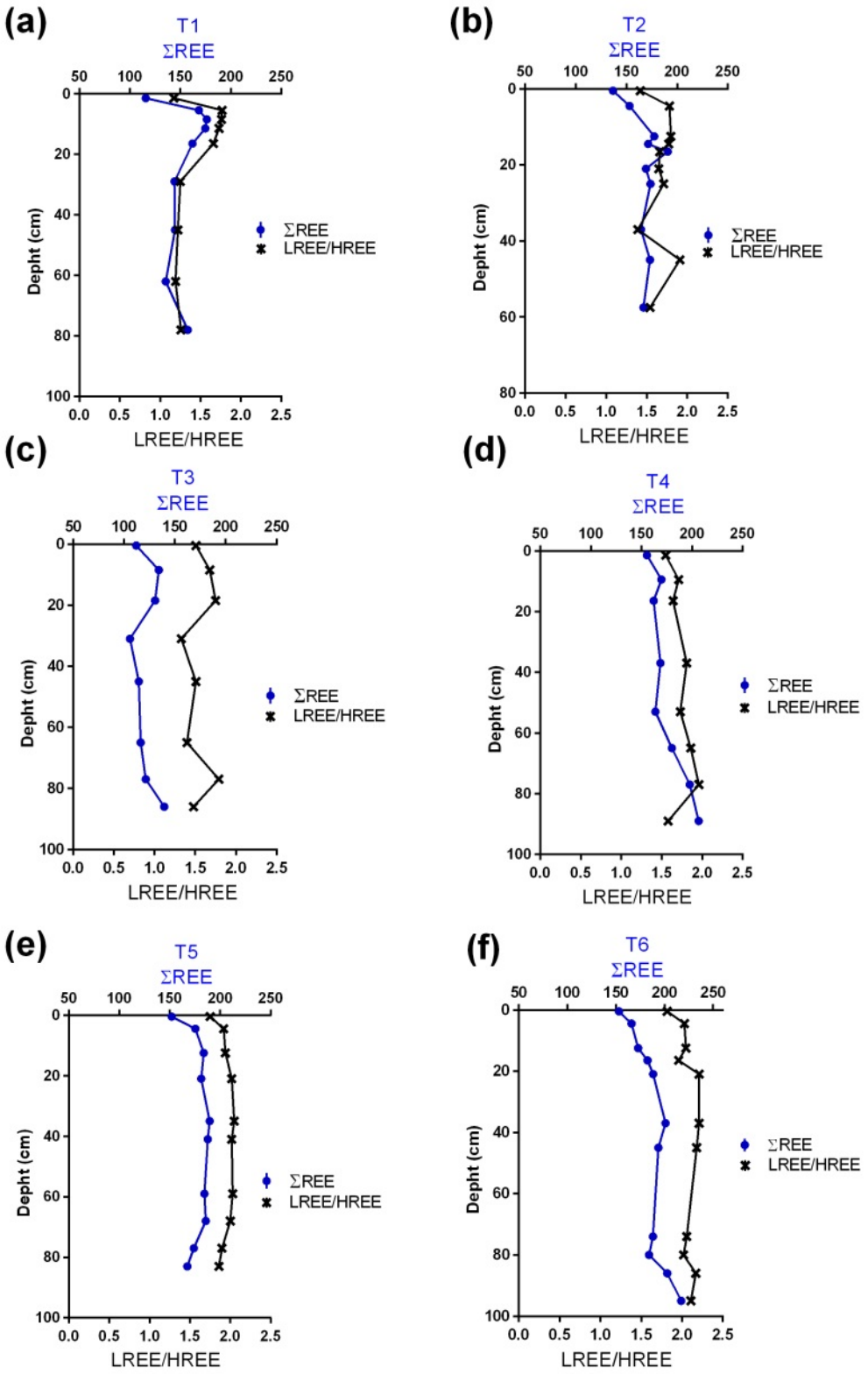

Fig. 5. Deph profiles of ΣREE (mg kg^{-1}) and LREE/HREE ratios in mangrove soils of the Jaguaripe estuary.

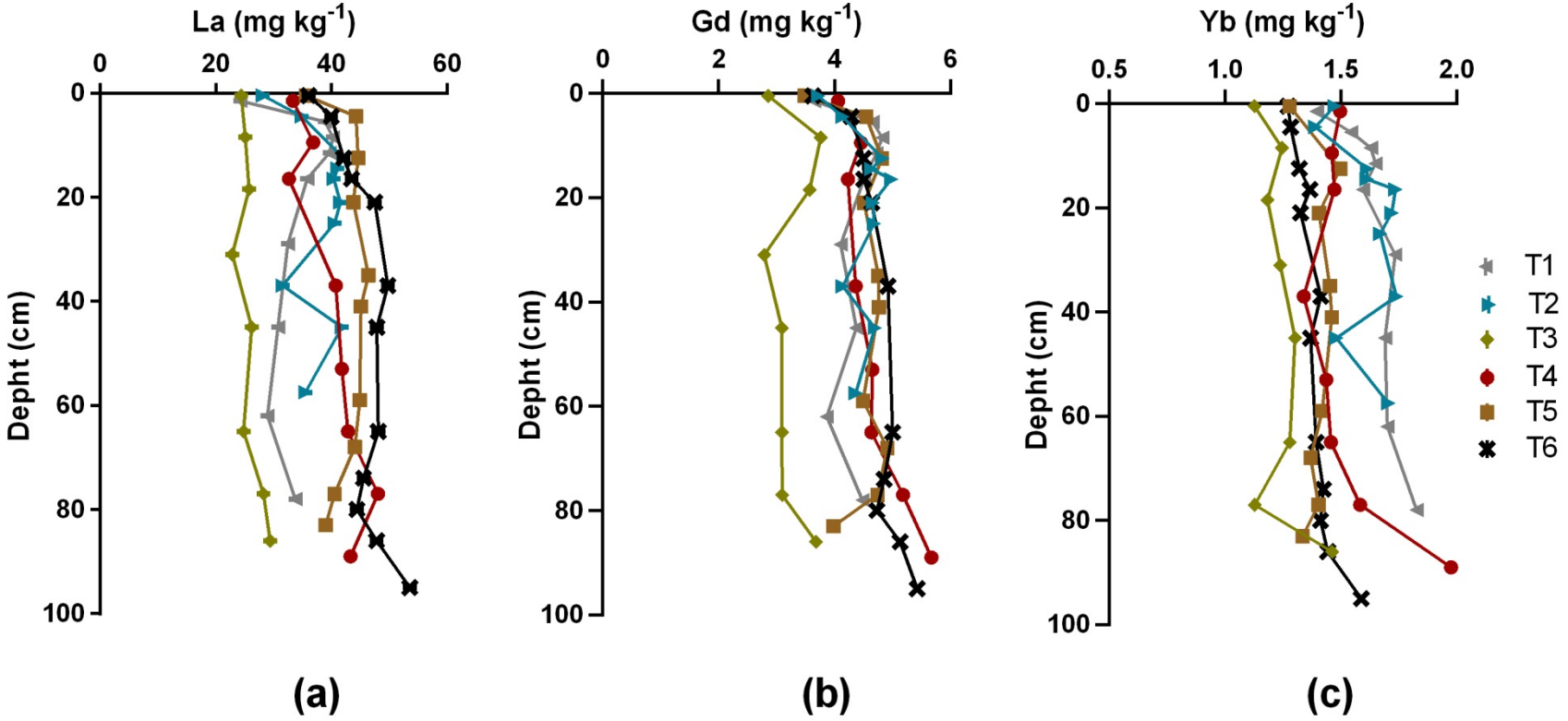

Fig. 6. Deph profiles of (a) La (LREE), (b) Gd (MREE), and (c)Yb (HREE) concentrations in soils profiles (cores 1- 6) of the Jaguaripe estuary.

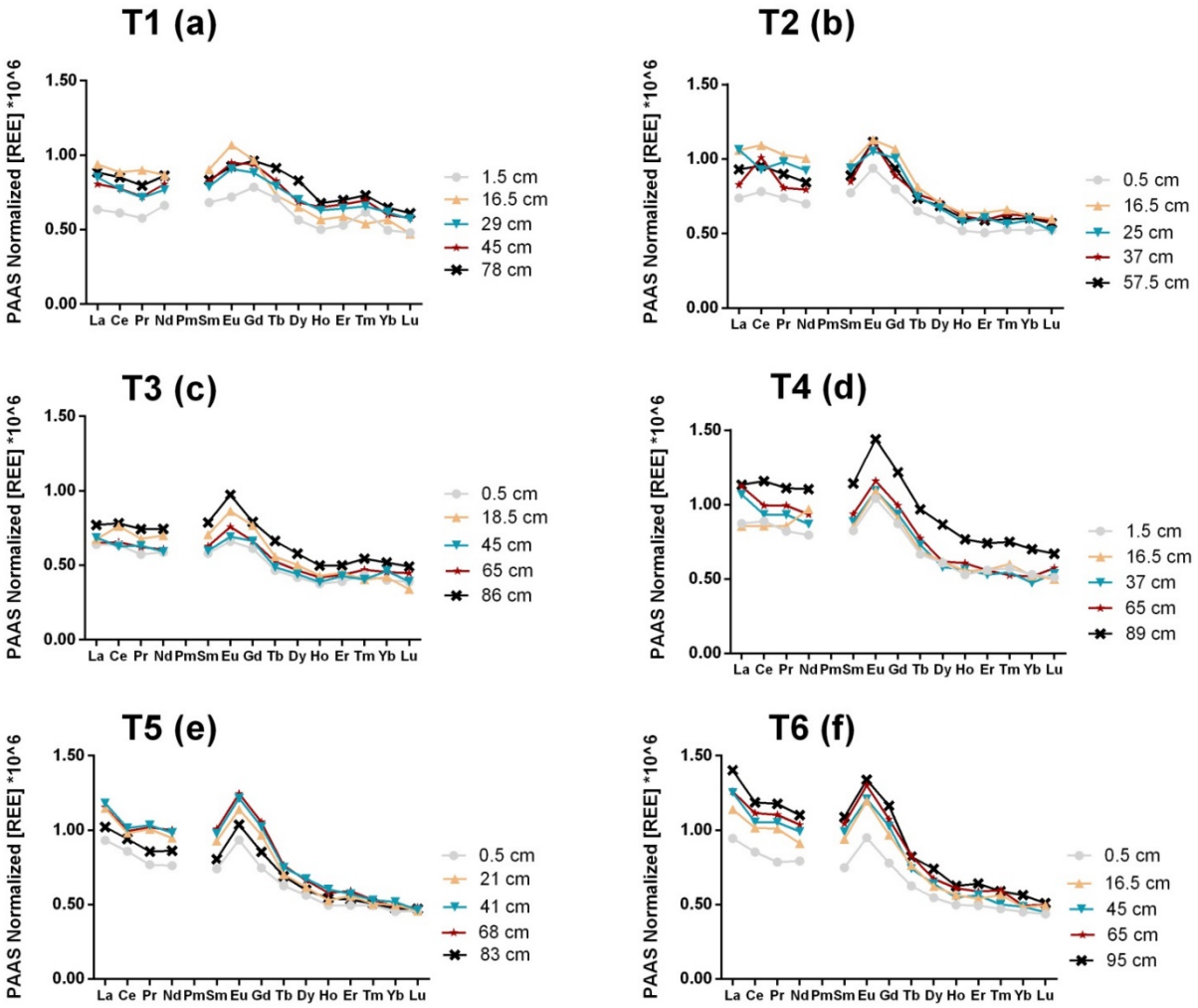

Fig. 7. PAAS-normalized REE distribution in core of mangrove soils (a. T1; b. T2; c. T3; d. T4; e. T5 and f. T6) of Jaguaripe estuary.

SUPLEMENTARY MATERIAL

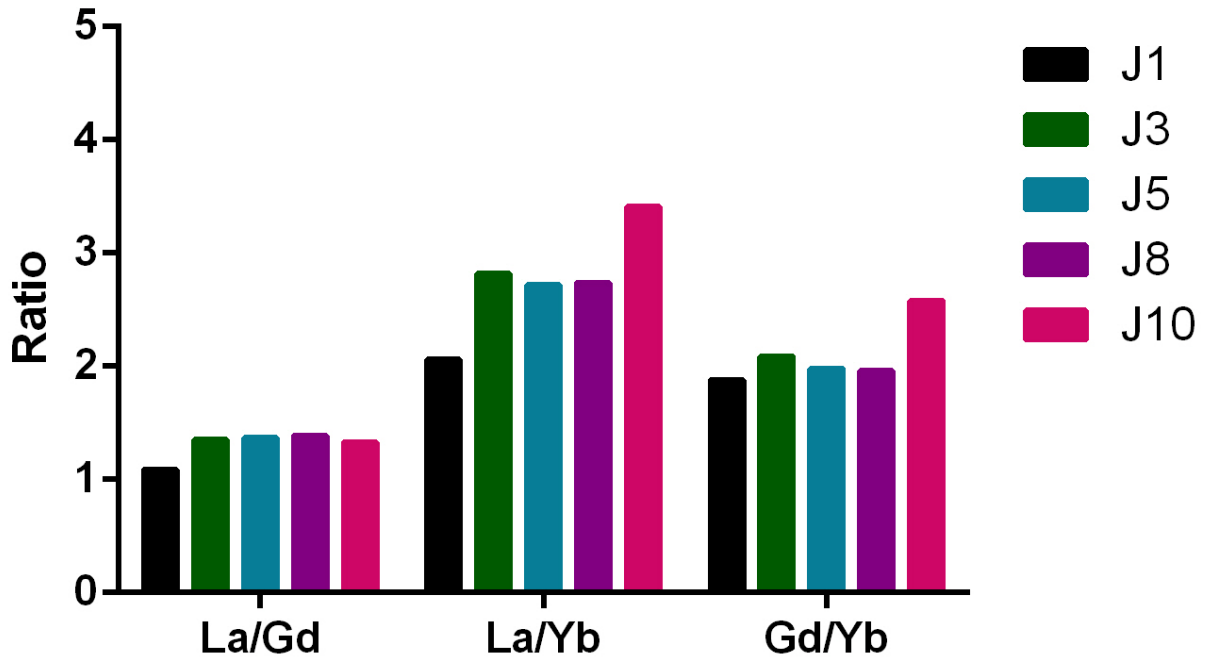

Fig. S1 Ratios $(La/Gd)_{PAAS}$, $(La/Yb)_{PAAS}$ and $(Gd/Yb)_{PAAS}$ in surface sediments from Jaguaripe estuary.

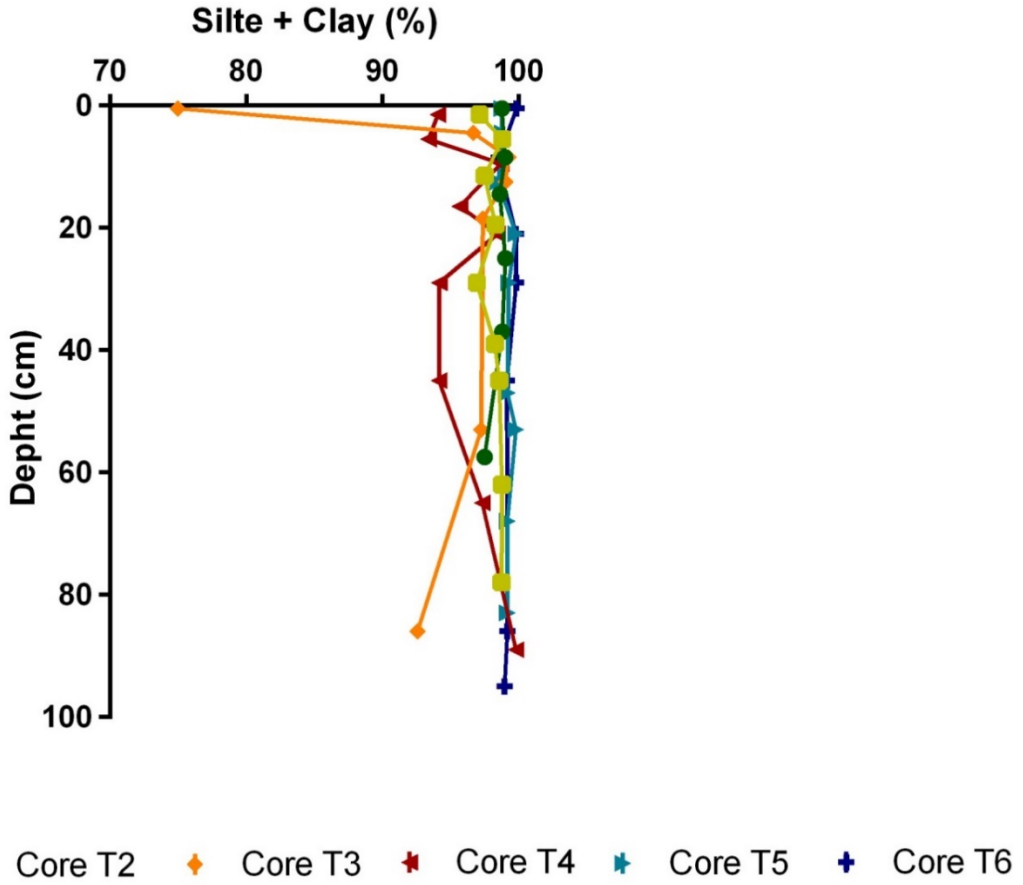

Fig. S2. Content of mud (silte + clay) profiles in mangrove soils (cores T1- T6) of Jaguaripe estuary. Data provided by Hatje et al 2020, submitted.

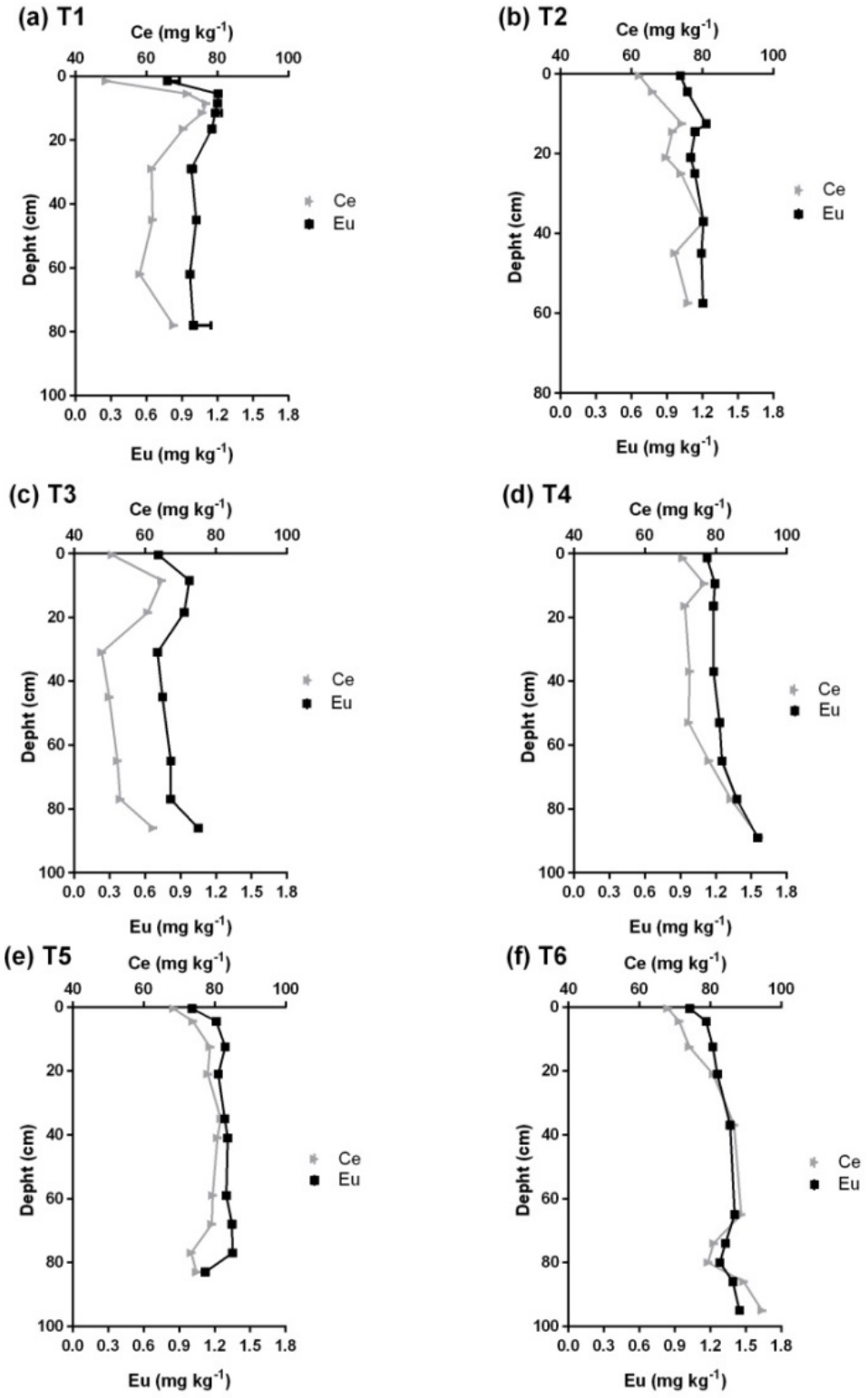

Fig S3. Deph profiles of Ce and Eu concentrations in soil profiles (T1- T6) of the Jaguaripe estuary.

Table S1. Operating conditions of ICP-MS and ICPOES.

Equipament	Parameter	Value
ICP-MS	Forward Power	1550 W
	Ar Flow rate	10 L min^{-1}
	Nebulizer	Micromist
	Flow rate auxiliary	0.8 L min^{-1}
	Dwell time	0.01 s
ICPOES	Forward Power	1300 W
	Nebulizer camera	Cyclonic
	Nebulizer	Concentric
	Flow rate	15 L min^{-1}
	Flow rate auxiliary	0.8 L min^{-1}
	Carrier	0.8 L min^{-1}

Table S2. Certified values and measured concentrations (± standard deviation) of Al, Co, Mn, Pb, Fe and Si for BCR 667 and MESS-3.

CRM		Al	Co	Mn ($mg.kg^{-1}$)	Pb	Fe	Si
BCR 667 N = 2	**Certified**	-	23.0 ±1.30	920 ± 400	31.9 ± 1.10	44800 ± 1.000	-
	Measured	71709 ± 0.04	21.6 ± 0.02	902 ± 0.05	32.0 ± 0.02	47256 ± 0.045	208481 ± 0.04
	Recovery (%)	-	94	98	100	103	-
MESS-3 N = 2	**Certified**	85900 ± 2.300	14.4 ± 2.00	324 ± 12	21.1 ± 0.70	43400 ± 1.100	270000
	Measured	94039 ± 0.07	13.7 ± 0.07	273 ± 0.1	18.9 ± 0.02	48798 ± 0.05	283865
	Recovery (%)	109	95	84	90	112	105

Table S3. Certified and measured concentrations (± standard deviation) of yttrium and REE for the BCR 667 certified material.

	Y	**La**	**Ce**	**Pr**	**Nd**	**Sm**	**Eu**	**Gd**	**Tb**	**Dy**	**Ho**	**Er**	**Tm**	**Yb**	**Lu**
								($mg.kg^{-1}$)							
Certified	16.7-25.3	27.8±1.0	56.7±2.5	6.10±0.50	25.0±1.4	4.66±0.20	1.00±0.05	4.41±0.12	0.628±0.017	4.01±0.14	0.80±0.06	2.35±0.15	0.326±0.025	2.20±0.09	0.325±0.020
Measured	19.7	27.3±0.02	56.1±0.02	6.26±0.03	25.2±0.01	4.75±0.04	1.00±0.01	4.63±0.04	0.675±0.016	3.90±0.28	0.77±0.02	2.32±0.04	0.323±0.035	2.17±0.03	0.317±0.037
Recovery (%)	94	98	99	103	101	102	100	105	99	97	97	99	99	99	98

Table S4. Concentrations of Co, Pb, Mn ($mg.kg^{-1}$) and Al, Fe, Si (%), grain size, C_{org} (%) and salinity zone, in superficial sediment from the Jaguaripe estuary.

Stations	**Co**	**Pb**	**Mn**	**Al**	**Fe**	**Si**	**Grain size[a]**		**C_{org}[a]**	**Average Salinity[b]**
							Sand	Silt + Clay		
		($mg.kg^{-1}$)					(%)			
J1	20.0 ± 0.2	35.7 ± 0.1	1226.4 ± 0.1	8.7	4.6	15.9	76.7	23	3.34	21.5 ± 10
J3	14.1 ± 0.1	23.5 ± 0.1	207.0 ± 0.1	8.7	5.1	17.1	78.4	21.6	4.64	24.7 ± 8.3
J5	22.3 ± 0.1	20.7 ± 0.1	232.0 ± 0.1	7.9	5.0	17.7	92.9	7.1	3.96	17.6 ± 8.9
J8	18.9 ± 0.1	26.9 ± 0.1	313.2	9.1	6.6	17.3	89.5	9.1	5.71	16.2 ± 8.7
J10	20.2 ± 0.1	29.3 ± 0.1	712.8 ± 0.1	9.2	7.7	21.0	86.9	0.8	4.40	6.8 ± 6.0

[a]Krull et al., 2014.
[b]Salinity calculated using published (Hatje et al., 2006; Barros et al. 2008; Barros et. 2012; Barros et al., 2014; Krull et al., 2014; Costa et al., 2015).

Table S5. Concentrations of yttrium and rare earth elements ($mg.kg^{-1}$) in superficial sediment from the Jaguaripe estuary.

Elements	J1	J3	J5	J8	J10
Y	15.00 ± 0.22	13.31 ± 0.10	13.11 ± 0.19	12.37 ± 0.24	11.75 ± 0.06
La	49.37 ± 0.13	52.63 ± 0.02	52.34 ± 0.09	52.54 ± 0.01	53.39 ± 0.03
Ce	89.59 ± 0.20	90.83 ± 0.03	87.09 ± 0.12	95.67 ± 0.06	99.54 ± 0.02
Pr	10.00 ± 0.18	9.70 ± 0.05	10.98 ± 0.12	10.13 ± 0.06	10.63 ± 0.01
Nd	36.10 ± 0.17	34.94 ± 0.04	32.26 ± 0.15	34.97 ± 0.07	37.57 ± 0.02
Sm	6.14 ± 0.19	5.48 ± 0.03	5.44 ± 0.11	5.45 ± 0.08	5.75 ± 0.01
Eu	1.38 ± 0.21	1.30 ± 0.04	1.31 ± 0.13	1.31 ± 0.10	1.46 ± 0.01
Gd	5.52 ± 0.19	4.75 ± 0.06	4.64 ± 0.15	4.60 ± 0.10	4.91 ± 0.01
Tb	0.71 ± 0.17	0.56 ± 0.06	0.57 ± 0.11	0.52 ± 0.15	0.55 ± 0.01
Dy	3.75 ± 0.17	2.82 ± 0.09	2.96 ± 0.12	2.60 ± 0.16	2.74 ± 0.01
Ho	0.68 ± 0.20	0.51 ± 0.07	0.55 ± 0.11	0.58 ± 0.15	0.49 ± 0.01
Er	1.98 ± 0.18	1.56 ± 0.08	1.61 ± 0.11	1.63 ± 0.15	1.41 ± 0.01
Tm	0.27 ± 0.19	0.19 ± 0.07	0.21 ± 0.08	0.21	0.17 ± 0.01
Yb	1.77 ± 0.18	1.38 ± 0.13	1.42 ± 0.07	1.42 ± 0.20	1.15 ± 0.02
Lu	0.25 ± 0.18	0.15	0.20 ± 0.07	0.20	0.15 ± 0.01
Eu/Eu*	1.12	1.20	1.23	1.24	1.29
Ce/Ce*[1]	0.93	0.93	0.84	0.96	0.96
ΣREE	207.5	206.8	201.6	211.8	219.9
LREE	185.1	188.1	182.7	193.3	201.1
MREE	18.2	15.4	15.5	15.0	15.9
HREE	4.27	3.28	3.44	3.46	2.90
LREE/HREE	43.4	57.3	53.1	55.9	69.5

[1] $Ce/Ce^* = Ce_{PAAS}/(La_{PAAS} \times Pr_{PAAS})^{0.5}$ (McLennan, 1989)

Table S6. Correlations of LREE, MREE and HREE with Al, Mn, Fe, Si and C_{org} in surface sediments from the Jaguripe estuary. Concentrations with * indicates significance at $p < 0.05$.

	Al	**Mn**	**Fe**	**Si**	**C_{org}**
LREE	0.85*	0.05	0.96*	0.81*	0.48
MREE	- 0.04	0.94*	- 0.43	- 0.35	-0.79
HREE	- 0.28	0.60	- 0.74	- 0.83	-0.51

Table S7. Grain-size composition, salinity and contents of Al, Mn, Fe, Si and C_{org}.

	Station	Depth	Salinity[a]	Sand[b]	Silt + clay[b]	Al (%)	Fe	Si	C_{org}[b]	Mn (mg kg^{-1})
Lower estuary	Core T1	1.5	21.5 ± 10.1	2.86	97.14	7.53	4.66	22.93	9.44	234
		5.5		1.20	98.80	7.30	4.08	19.39	9.18	211
		11.5		2.48	97.52	8.56	4.31	22.36	10.62	231
		19.5		1.69	98.31	8.18	4.97	20.28	10.95	188
		29		3.05	96.95	8.06	4.68	20.25	11.32	216
		39		1.73	98.27	7.65	4.15	18.46	9.87	219
		45		1.42	98.58	7.07	3.97	17.98	11.33	196
		62		1.22	98.78	9.96	5.31	20.80	5.35	306
		78		1.25	98.75	8.64	4.55	17.83	5.43	251
	Core T2	0.5	24.7 ± 8.3	1.22	98.78	7.10	4.28	17.34	12.29	135
		8.5		1.00	99.00	7.36	3.97	16.83	10.2	111
		14.5		1.36	98.64	6.88	4.51	20.00	7.89	157
		25		0.97	99.03	6.47	3.42	22.37	6.27	137
		37		1.20	98.80	6.51	4.25	22.43	6.03	242
		57.5		2.48	97.52	6.93	4.13	21.01	8.06	238
Middle estuary	Core T3	0.5	17.6 ± 8.9	25.03	74.97	4.52	2.82	24.84	8.41	197
		4.5		3.32	96.68	6.70	3.99	21.42	9.81	157
		8.5		0.75	99.25	7.19	4.35	18.32	10.97	347
		12.5		0.97	99.03	7.22	4.25	14.92	11.52	291
		18.5		2.61	97.39	6.31	3.79	22.12	8.48	242
		53		2.73	97.27	5.52	2.48	25.31	7.06	58
		86		7.82	92.60	5.98	2.88	28.36	6.91	84
	Core T4	1.5	16.2 ± 8.7	5.92	94.08	6.76	4.00	17.96	9.44	165
		5.5		6.62	93.38	5.94	4.31	17.06	10.24	107
		9.5		1.28	98.72	7.43	4.83	19.84	10.80	397
		16.5		4.32	95.68	8.06	5.01	19.83	7.63	418
		21		1.53	98.47	6.99	4.81	18.73	8.87	312

	Station	Depth	Salinity[a]	Sand[b]	Silt + clay[b]	Al	Fe	Si	C_{org}[b]	Mn
						(%)				(mg kg^{-1})
		29		5.82	94.18	6.77	4.21	19.79	5.98	313
		45		5.83	94.17	7.20	4.42	22.55	5.99	254
		65		8.58	97.34	6.81	4.47	23.09	6.84	208
		89		0.19	99.81	8.82	3.91	21.51	11.05	153
Upper estuary	Core T5	0.5	6.8 ± 6.0	1.22	98.78	7.45	4.72	17.49	14.21	305
		4.5		1.20	98.80	7.67	4.70	17.15	14.13	264
		12.5		1.48	98.52	7.48	4.89	17.54	12.39	266
		21		0.19	99.81	7.73	4.95	18.77	12.10	389
		29		0.72	99.28	7.32	4.99	18.40	11.92	325
		47		0.82	99.18	7.83	4.97	17.84	7.65	362
		53		0.18	99.82	8.53	4.68	19.11	7.42	324
		68		0.81	99.19	10.05	5.35	21.88	6.58	458
		83		0.80	99.20	7.77	4.68	18.45	6.99	324
	Core T6	0.5	9.9 ± 7.6	0.13	99.87	8.33	4.62	16.89	9.57	207
		8.5		1.45	98.55	8.00	4.92	16.92	8.49	321
		12.5		1.14	98.86	8.95	4.99	19.11	8.35	258
		21		0.20	99.80	9.89	5.43	19.71	7.11	373
		29		0.16	99.84	9.37	5.09	17.68	6.73	360
		45		0.85	99.15	10.28	5.60	18.69	7.40	441
		86		0.82	99.18	9.93	5.54	20.67	8.15	430
		95		1.01	98.99	8.71	5.03	19.62	7.74	380

[a]Salinity (mean ± sd) calculated using published (Hatje et al., 2006; Barros et al. 2008; Barros et. 2012; Barros et al., 2014; Krull et al., 2014; Costa et al., 2015).
[b]Hatje et al., 2020, submitted.

Table S8. Concentrations of Y and REE (mg kg^{-1}) in profiles of mangrove soils of the Jaguaripe estuary.

	Station	Depth cm	Y	La	Ce	Pr	Nd	Sm	Eu	Gd	Tb	Dy	Ho	Er	Tm	Yb	Lu	Eu/Eu*	Ce/Ce*	ΣREE	LREE	MREE	HREE	L/H
Lower estuary	Core T1	1.5	15.74	24.22	48.73	5.09	22.46	3.78	0.78	3.65	0.55	2.64	0.50	1.51	0.25	1.40	0.21	0.98	1.01	116	101	11.9	3.4	29.9
		5.5	13.79	38.87	71.58	8.42	30.74	5.20	1.21	4.66	0.57	3.06	0.56	1.66	0.22	1.54	0.20	1.15	0.91	168	150	15.3	3.6	41.2
		8.5	14.09	40.25	76.83	8.67	31.16	5.13	1.20	4.82	0.59	3.19	0.57	1.73	0.23	1.63	0.21	1.14	0.95	176	157	15.5	3.8	41.4
		11.5	14.12	39.70	75.76	8.53	31.43	5.22	1.18	4.72	0.59	3.21	0.60	1.74	0.23	1.65	0.21	1.12	0.95	175	155	15.5	3.8	40.6
		16.5	12.86	35.82	70.44	7.94	29.37	5.02	1.15	4.51	0.57	3.05	0.56	1.68	0.22	1.60	0.20	1.14	0.96	162	144	14.9	3.7	38.9
		29	16.82	32.47	61.46	6.32	26.02	4.38	0.98	4.11	0.61	3.28	0.62	1.83	0.27	1.73	0.25	1.09	0.99	144	127	14.0	4.1	31.0
		45	17.47	30.79	61.78	6.38	27.31	4.56	1.02	4.38	0.64	3.20	0.64	1.91	0.28	1.69	0.25	1.08	1.02	145	126	14.4	4.1	30.6
		62	15.22	29.00	58.14	6.03	24.82	4.30	0.97	3.87	0.60	3.22	0.62	1.75	0.26	1.70	0.25	1.12	1.01	136	118	13.6	4.0	29.8
		78	17.73	33.77	67.66	7.02	29.20	4.63	1.00	4.48	0.71	3.87	0.67	1.99	0.30	1.83	0.26	1.03	1.01	157	138	15.4	4.4	31.4
		Average	**15.31**	**33.88**	**65.82**	**7.15**	**28.06**	**4.69**	**1.05**	**4.36**	**0.60**	**3.19**	**0.59**	**1.76**	**0.25**	**1.64**	**0.23**	**1.10**	**0.98**	**153**	**135**	**14.5**	**3.9**	**35.0**
		SD	**1.74**	**5.38**	**9.11**	**1.29**	**3.12**	**0.49**	**0.14**	**0.40**	**0.05**	**0.32**	**0.05**	**0.14**	**0.03**	**0.12**	**0.02**	**0.06**	**0.04**	**20.0**	**18.8**	**1.2**	**0.3**	**5.3**
	Core T2	0.5	11.43	28.17	62.21	6.53	23.70	4.29	1.01	3.72	0.50	2.77	0.52	1.44	0.21	1.47	0.23	1.19	1.06	137	121	12.8	3.3	36.0
		4.5	12.86	34.91	65.95	7.60	27.64	4.65	1.07	4.14	0.52	2.77	0.51	1.51	0.20	1.39	0.18	1.15	0.93	153	136	13.7	3.3	41.6
		12.5	14.19	42.14	74.18	9.00	32.46	5.40	1.23	4.83	0.60	3.14	0.58	1.73	0.23	1.61	0.21	1.13	0.88	177	158	15.8	3.8	41.8
		14.5	13.81	41.09	71.55	8.71	31.27	5.16	1.14	4.63	0.57	3.04	0.56	1.67	0.22	1.61	0.21	1.10	0.87	171	153	15.1	3.7	41.1
		16.5	13.12	40.45	87.00	9.08	34.05	5.38	1.22	4.98	0.63	3.30	0.63	1.82	0.27	1.74	0.26	1.11	1.05	191	171	16.1	4.1	41.7
		21	13.10	41.57	69.74	8.35	30.64	5.12	1.10	4.66	0.56	3.02	0.56	1.71	0.23	1.72	0.23	1.06	0.86	169	150	15.0	3.9	38.7
		25	13.34	40.59	73.96	8.65	31.31	5.21	1.14	4.68	0.58	3.14	0.57	1.73	0.23	1.67	0.23	1.08	0.91	174	154	15.3	3.8	40.1
		37	10.44	31.59	80.30	7.12	26.92	4.70	1.21	4.14	0.59	3.34	0.61	1.68	0.26	1.74	0.25	1.29	1.14	164	146	14.6	3.9	37.1
		45	13.83	41.82	72.21	8.71	31.66	5.25	1.19	4.70	0.57	3.04	0.56	1.66	0.20	1.48	0.19	1.13	0.87	173	154	15.3	3.5	43.6
		57.5	11.80	35.55	75.93	7.95	28.58	4.94	1.20	4.37	0.57	3.20	0.60	1.67	0.24	1.70	0.25	1.22	1.04	167	148	14.9	3.9	38.3

	Station	Depth cm	Y	La	Ce	Pr	Nd	Sm	Eu	Gd	Tb	Dy	Ho	Er	Tm	Yb	Lu	Eu/Eu*	Ce/Ce*	ΣREE	LREE	MREE	HREE	L/H
		Average	**12.79**	**37.79**	**72.68**	**8.17**	**29.82**	**5.01**	**1.15**	**4.48**	**0.57**	**3.08**	**0.57**	**1.66**	**0.23**	**1.61**	**0.22**	**1.15**	**0.96**	**168**	**149**	**14.9**	**3.7**	**39.8**
		SD	**1.20**	**4.94**	**6.55**	**0.85**	**3.08**	**0.36**	**0.07**	**0.39**	**0.04**	**0.19**	**0.04**	**0.11**	**0.02**	**0.13**	**0.03**	**0.07**	**0.10**	**14.8**	**13.6**	**1.0**	**0.3**	**2.7**
Middle estuary	**Core T3**	0.5	8.61	24.41	50.70	5.06	19.90	3.21	0.71	2.86	0.36	1.96	0.37	1.11	0.18	1.13	0.17	1.11	1.05	112	100	9.5	2.6	38.7
		8.5	9.26	25.13	64.71	6.14	23.22	3.94	0.98	3.76	0.45	2.48	0.45	1.34	0.17	1.25	0.16	1.19	1.20	134	119	12.1	2.9	40.8
		18.5	9.69	25.78	60.77	5.99	23.72	3.92	0.93	3.57	0.43	2.35	0.42	1.28	0.16	1.18	0.15	1.17	1.13	131	116	11.6	2.8	41.9
		31	7.94	22.86	47.85	4.95	18.09	3.15	0.71	2.79	0.37	2.02	0.38	1.15	0.18	1.24	0.19	1.12	1.04	106	94	9.4	2.8	34.0
		45	9.35	26.20	49.90	5.58	20.08	3.31	0.75	3.09	0.38	2.06	0.38	1.22	0.16	1.30	0.17	1.10	0.95	114	102	10.0	2.8	35.7
		65	8.74	24.80	52.21	5.49	20.55	3.48	0.82	3.09	0.41	2.18	0.41	1.24	0.19	1.28	0.19	1.17	1.03	116	103	10.4	2.9	35.5
		77	9.55	28.26	53.04	5.94	21.32	3.55	0.82	3.10	0.38	2.02	0.39	1.18	0.15	1.13	0.14	1.16	0.94	121	108	10.2	2.6	41.8
		86	11.82	29.43	62.25	6.57	25.24	4.37	1.05	3.68	0.51	2.70	0.49	1.42	0.22	1.46	0.21	1.23	1.03	140	123	12.8	3.3	37.2
		Average	**9.37**	**25.86**	**55.18**	**5.72**	**21.51**	**3.62**	**0.85**	**3.24**	**0.41**	**2.22**	**0.41**	**1.24**	**0.18**	**1.25**	**0.17**	**1.16**	**1.05**	**122**	**108**	**10.7**	**2.8**	**38.2**
		SD	**1.15**	**2.12**	**6.40**	**0.55**	**2.36**	**0.42**	**0.13**	**0.38**	**0.05**	**0.27**	**0.04**	**0.10**	**0.02**	**0.11**	**0.02**	**0.05**	**0.09**	**11.8**	**10.4**	**1.3**	**0.2**	**3.07**
	Core T4	1.5	10.99	33.37	70.69	7.26	26.95	4.58	1.13	4.06	0.52	2.84	0.53	1.60	0.23	1.50	0.22	1.23	0.97	155	138	13.7	3.6	39.0
		9.5	11.21	36.85	76.73	7.95	30.17	4.79	1.19	4.46	0.57	2.93	0.57	1.62	0.24	1.46	0.21	1.22	0.97	170	152	14.5	3.5	42.9
		16.5	11.99	32.69	71.31	7.57	32.89	4.73	1.18	4.23	0.53	2.88	0.55	1.60	0.24	1.47	0.22	1.24	1.00	162	144	14.1	3.5	40.9
		37	11.77	40.79	72.64	8.24	29.49	4.92	1.18	4.37	0.57	2.71	0.56	1.51	0.22	1.34	0.23	1.20	0.94	169	151	14.3	3.3	45.8
		53	12.63	41.85	72.35	8.64	31.21	5.16	1.23	4.65	0.60	2.89	0.59	1.59	0.26	1.44	0.24	1.18	0.88	164	145	15.1	3.5	41.1
		65	12.91	42.90	78.05	8.78	31.68	5.20	1.25	4.64	0.60	2.90	0.60	1.59	0.21	1.46	0.25	1.20	0.94	180	16	15.2	3.5	46.0
		77	14.54	48.10	84.25	9.58	35.10	5.78	1.38	5.19	0.62	3.30	0.61	1.78	0.23	1.58	0.22	1.19	0.93	198	177	16.9	3.8	46.5
		89	13.53	43.32	92.23	9.81	37.43	6.34	1.55	5.67	0.75	4.06	0.76	2.11	0.30	1.98	0.29	1.22	0.99	207	183	19.1	4.7	39.1
		Average	**12.44**	**39.98**	**77.28**	**8.48**	**31.86**	**5.19**	**1.26**	**4.66**	**0.59**	**3.06**	**0.60**	**1.67**	**0.24**	**1.53**	**0.23**	**1.21**	**0.95**	**175**	**156**	**15.4**	**3.7**	**42.7**
		SD	**1.20**	**5.30**	**7.54**	**0.91**	**3.28**	**0.60**	**0.14**	**0.53**	**0.07**	**0.44**	**0.07**	**0.19**	**0.03**	**0.19**	**0.03**	**0.02**	**0.04**	**18.0**	**16.0**	**1.8**	**0.4**	**3.1**

	Station	Depth cm	Y	La	Ce	Pr	Nd	Sm	Eu	Gd	Tb	Dy	Ho	Er	Tm	Yb	Lu	Eu/Eu*	Ce/Ce*	ΣREE	LREE	MREE	HREE	L/H
Up per estuary	Core T5	0.5	12.24	35.61	68.35	6.78	25.81	4.11	1.01	3.48	0.49	2.63	0.49	1.41	0.20	1.28	0.20	1.26	1.02	1512	137	12.2	3.1	44.2
		4.5	12.55	44.27	73.90	8.38	30.36	5.31	1.21	4.55	0.55	2.91	0.54	1.60	0.21	1.43	0.20	1.16	0.89	175	157	15.1	3.4	45.7
		12.5	13.18	44.62	78.69	8.83	32.49	5.34	1.29	4.82	0.55	3.05	0.57	1.66	0.21	1.50	0.21	1.20	0.91	184	165	15.6	3.6	46.0
		21	11.69	43.83	78.09	8.89	32.12	5.15	1.23	4.51	0.54	2.89	0.52	1.60	0.20	1.41	0.20	1.20	0.91	181	163	14.9	3.4	47.9
		35	12.94	46.45	81.71	9.20	33.05	5.39	1.29	4.76	0.57	3.02	0.56	1.66	0.21	1.45	0.20	1.20	0.91	189	170	15.6	3.5	48.4
		41	12.01	45.14	80.79	9.12	33.33	5.42	1.31	4.77	0.58	3.15	0.60	1.63	0.21	1.46	0.20	1.21	0.92	188	168	15.8	3.5	48.0
		59	13.03	44.94	79.43	8.95	32.53	5.36	1.30	4.49	0.57	2.92	0.54	1.60	0.21	1.42	0.20	1.25	0.91	184	166	15.2	3.4	48.4
		68	13.68	44.07	79.18	8.99	33.94	5.59	1.35	4.91	0.59	3.10	0.57	1.68	0.22	1.37	0.21	1.21	0.92	186	166	16.1	3.5	47.8
		77	13.26	40.56	73.37	8.27	32.63	5.46	1.35	4.74	0.56	2.90	0.56	1.63	0.21	1.40	0.20	1.25	0.92	174	155	15.6	3.4	45.0
		83	13.04	39.04	74.89	7.57	29.23	4.47	1.12	3.98	0.53	2.80	0.54	1.52	0.21	1.33	0.20	1.25	1.01	167	151	13.4	3.3	46.2
		Average	**12.76**	**42.85**	**76.84**	**8.50**	**31.55**	**5.16**	**1.25**	**4.50**	**0.55**	**2.94**	**0.55**	**1.60**	**0.21**	**1.40**	**0.20**	**1.22**	**0.93**	**178**	**160**	**14.9**	**3.4**	**46.7**
		SD	**0.62**	**3.37**	**4.12**	**0.78**	**2.45**	**0.48**	**0.11**	**0.44**	**0.03**	**0.15**	**0.03**	**0.08**	**0.01**	**0.06**	**0.01**	**0.03**	**0.04**	**11.5**	**10.3**	**1.2**	**0.1**	**1.5**
	Core T6	0.5	11.76	36.06	67.95	6.94	26.88	4.15	1.03	3.63	0.48	2.56	0.49	1.41	0.19	1.27	0.19	1.24	0.99	153	138	12.3	3.1	45.1
		4.5	11.37	39.95	71.25	8.20	29.45	4.84	1.16	4.29	0.52	2.74	0.50	1.48	0.19	1.28	0.17	1.20	0.91	166	149	14.1	3.1	47.6
		12.5	11.75	42.11	74.07	8.39	30.68	5.00	1.22	4.50	0.53	2.78	0.51	1.51	0.19	1.32	0.18	1.21	0.91	173	155	14.6	3.2	48.5
		16.5	14.29	43.51	80.80	8.91	30.90	5.22	1.29	4.51	0.59	2.91	0.56	1.54	0.23	1.37	0.21	1.25	0.95	182	164	15.1	3.3	49.0
		21	11.82	47.51	80.78	9.01	32.60	5.24	1.26	4.64	0.55	2.88	0.53	1.55	0.20	1.33	0.18	1.20	0.90	188	170	15.1	3.2	52.2
		37	12.99	49.79	86.69	9.72	35.20	5.75	1.37	4.92	0.61	3.08	0.58	1.65	0.22	1.41	0.19	1.21	0.91	201	181	16.3	3.5	52.4
		45	12.79	47.85	83.92	9.29	33.56	5.50	1.31	4.78	0.57	2.99	0.54	1.60	0.20	1.37	0.19	1.20	0.92	194	175	15.7	3.4	51.9
		65	14.68	48.11	88.67	9.74	35.15	5.80	1.40	5.00	0.64	3.15	0.61	1.68	0.24	1.39	0.22	1.23	0.95	202	182	16.6	3.5	51.5
		74	12.06	45.59	80.91	9.14	33.22	5.48	1.33	4.86	0.59	3.02	0.56	1.62	0.21	1.42	0.19	1.21	0.91	188	169	15.8	3.4	48.9
		80	12.05	44.41	79.30	8.89	32.54	5.33	1,28	4.73	0.57	3.04	0.56	1.63	0.21	1.41	0.19	1.20	0.92	184	165	15.5	3.4	47.9
		86	14.38	47.80	89.38	9.81	35.71	5.76	1,39	5.13	0.61	3.16	0.57	1.66	0.22	1.44	0.20	1.20	0.95	203	183	16.6	3.5	51.9
		95	15.05	53.56	94.51	10.39	37.29	6.04	1,45	5.43	0.64	3.47	0.62	1.83	0.24	1.59	0.22	1.19	0.92	217	196	17.6	3.9	50.5
		Average	**12.92**	**45.52**	**81.52**	**9.04**	**32.77**	**5.34**	**1.29**	**4.70**	**0.58**	**2.98**	**0.55**	**1.60**	**0.21**	**1.38**	**0.20**	**1.21**	**0.93**	**188**	**169**	**15.4**	**3.4**	**49.8**
		SD	**1.33**	**4.69**	**7.78**	**0.91**	**2.94**	**0.51**	**0.12**	**0.46**	**0.05**	**0.23**	**0.04**	**0.11**	**0.02**	**0.08**	**0.01**	**0.02**	**0.03**	**17.7**	**16.1**	**1.4**	**0.2**	**2.3**

Table S9. Correlation of content mud (silte + clay) and Mn (mg kg^{-1}), Al (%), Fe (%) and Si (%) from Jaguaripe mangrove. Concentrations with * indicates significance at $p < 0.05$.

Station	Mn	Al	Fe	Si
T1	0.18	0.16	- 0.06	- 0.65
T2	-0.66	-0.07	-0.29	-0.20
T3	0.18	0.84*	0.53	-0.46
T4	0.22	0.64	0.20	0.35
T5	0.52	0.27	0.07	0.43
T6	-0.13	0.29	-0.02	-0.09

Table S10 (a). Spearman correlation for LREE, MREE, HREE (mg kg^{-1}), Fe, Al, Mn and C_{org} (%) in mangrove soil ($p < 0.05$) for core T1.

	LREE	**MREE**	**HREE**	**Fe**	**Al**	**Mn**	**C_{org}**
LREE	1.00						
MREE	0.92	1.00					
HREE	-0.12	0.13	1.00				
Fe	-0.08	-0.03	-0.17	1.00			
Al	0.17	0.25	0.28	0.70	1.00		
Mn	-0.45	-0.43	0.10	0.35	0.62	1.00	
C_{org}	0.28	0.25	-0.02	-0.27	-0.48	-0.75	1.00

Table S10 (b). Spearman correlation for LREE, MREE, HREE (mg kg^{-1}), Fe, Al, Mn and C_{org} (%) in mangrove soil ($p < 0.05$) for core T2.

	LREE	**MREE**	**HREE**	**Fe**	**Al**	**Mn**	**C_{org}**
LREE	1.00						
MREE	0.99	1.00					
HREE	0.43	0.43	1.00				
Fe	-0.26	-0.26	-0.03	1.00			
Al	-0.77	-0.77	-0.71	0.14	1.00		
Mn	0.37	0.37	0.94	0.26	-0.60	1.00	
C_{org}	-0.66	-0.66	-0.77	0.14	0.89	-0.71	1.00

Table S10 (c). Spearman correlation for LREE, MREE, HREE (mg kg^{-1}), Fe, Al, Mn and C_{org} (%) in mangrove soil ($p < 0.05$) for core T3.

	LREE	**MREE**	**HREE**	**Fe**	**Al**	**Mn**	**C_{org}**
LREE	1.00						
MREE	0.99	1.00					
HREE	0.90	0.90	1.00				
Fe	0.50	0.50	0.30	1.00			
Al	0.70	0.70	0.40	0.90	1.00		
Mn	0.20	0.20	-0.10	0.90	0.80	1.00	
C_{org}	0.40	0.40	0.00	0.80	0.90	0.90	1.00

Table S10 (d). Spearman correlation for LREE, MREE, HREE (mg kg^{-1}), Fe, Al, Mn and C_{org} (%) in mangrove soil ($p < 0.05$) for core T4.

	LREE	**MREE**	**HREE**	**Fe**	**Al**	**Mn**	**C_{org}**
LREE	1.00						
MREE	0.96	1.00					
HREE	0.32	0.36	1.00				
Fe	-0.36	-0.43	-0.64	1.00			
Al	0.39	0.32	0.11	0.25	1.00		
Mn	-0.46	-0.43	-0.43	0.89	0.14	1.00	
C_{org}	0.07	-0.04	0.32	-0.25	0.50	-0.39	1.00

Table S10 (e). Spearman correlation for LREE, MREE, HREE (mg kg^{-1}), Fe, Al, Mn and C_{org} (%) in mangrove soil ($p < 0.05$) for core T5.

	LREE	**MREE**	**HREE**	**Fe**	**Al**	**Mn**	**C_{org}**
LREE	1.00						
MREE	0.82	1.00					
HREE	0.81	0.90	1.00				
Fe	0.03	-0.12	-0.39	1.00			
Al	0.50	0.34	0.29	-0.36	1.00		
Mn	0.17	-0.25	-0.40	0.67	0.25	1.00	
C_{org}	-0.37	-0.22	-0.03	-0.15	-0.77	-0.65	1.00

Table S10 (f). Spearman correlation for LREE, MREE, HREE (mg kg^{-1}), Fe, Al, Mn and C_{org} (%) in mangrove soil ($p < 0.05$) for core T6.

	LREE	**MREE**	**HREE**	**Fe**	**Al**	**Mn**	**C_{org}**
LREE	1.00						
MREE	1.00	1.00					
HREE	1.00	1.00	1.00				
Fe	0.60	0.60	0.60	1.00			
Al	0.37	0.37	0.37	0.94	1.00		
Mn	0.77	0.77	0.77	0.94	0.83	1.00	
C_{org}	-0.49	-0.49	-0.49	-0.71	-0.60	-0.60	1.00

REFERÊNCIAS

Barros, F., Hatje, V., Figueiredo, M. B., Magalhães, W. F., Dórea, H. S., Emídio, E. Soares., 2008. The structure of the benthic macrofaunal assemblages and sediments characteristics of the Paraguaçu estuarine system, NE, Brazil. Estuarine, Coastal and Shelf Science. 78, n. 4, 753–762.

Barros, F. et al., Costa, P. C., Cruz, I., Mariano, D. L.S., Miranda, R. J., 2012. Benthic habitats in Todos os Santos Bay. Rev. Virtual de Quimica. 4, n. 5, 551–565.

Barros, F., Blanchet, H., Hammerstrom, K., Sauriau, P. G., Oliver, J., 2014. A framework for investigating general patterns of benthic β-diversity along estuaries. Estuarine, Coastal and Shelf Science. 149, 223–231.

Costa, P., Dórea, A., Mariano-Neto, E., Barros, F., 2015. Are there general spatial patterns of mangrove structure and composition along estuarine salinity gradients in Todos os Santos Bay? Estuarine, Coastal and Shelf Science. 166, 83–91.

Hatje, V., Barros. F., Figueiredo, D.G., Santos, V. L. C. S., Peso-Aguiar, M.C., 2006. Trace metal contamination and benthic assemblages in Subaé estuarine system, Brazil. Marine Pollution Bulletin. 52, p. 969 – 987.

Hatje, V., Masqué P., Patire, V., Dórea, A., Barros, F. Blue C stocks, accumulation rates, and associated spatial variability in Brazilian mangroves. 2020 submitted.

Krull, M., Abessa, D. M.S., Hatje, V., Barros, F., 2014. Integrated assessment of metal contamination in sediments from two tropical estuaries. Ecotoxicology and Environmental Safety. 106, 195–203.

McLennan, S.M., 1989. Rare earth elements in sedimentary rocks: influence of provenance and sedimentary processes. Reviews in Mineralogy and Geochemistry. 21, 169–200.

VERSÃO DO ARTIGO SUBMETIDO

Distribution and fractionation of rare earth elements in sediments and mangrove soil profiles across an estuarine gradient

Tácila O. P. de Freitas; Rodrigo M. A. Pedreira; Vanessa Hatje*

Inst. de Química & Centro Interdisciplinar de Energia e Ambiente, CIENAM, Universidade Federal da Bahia, Ondina, Salvador, Bahia, 40170-115, Brazil.

*Corresponding: vhatje@ufba.br

Abstract

Many hypotheses have been raised about the controls of the distribution and fractionation of the rare earth elements (REE) in coastal ecosystems. Here, REE were measured in estuarine sediments and in six mangrove soil profiles from a tropical estuary. The aim of this study was to evaluate the fractionation, distribution, and possible sources of these elements. The ΣREE and Y in estuarine sediments ranged from 202 to 220 mg kg^{-1} and from 12 to 15 mg kg^{-1}, respectively. The normalized abundances to the Post Archean Australian Shale (PAAS) showed that LREE were consistently enriched over HREE. Among the REE, only LREE showed significant correlation with Al (r= 0.85) and Fe (r= 0.96) indicating that Al and Fe-oxy-hydroxides are the main host phases of the LREE in estuarine sediments. The average ΣREE for mangrove soils throughout the salinity gradient ranged from 161 ± 18 mg kg^{-1} (lower estuary) to 183 ± 16 mg kg^{-1} (upper estuary). Al-normalized Mn and Fe concentrations showed small peaks down-core, indicating diagenetic remobilization. Vertical REE profiles have shown that post-deposition processes might contribute to the patterns in the abundances of the ΣREE and their fractionation at the surface and subsurface mangrove soils. Below the top 15 cm, diagenetic alteration after burial is not leading to substantial variation in the LREE/HREE profiles. The coincidence of peaks in individual REE/Al down core along with Fe and Mn reflects the participation of the REE in early diagenesis. The REE abundances observed here corroborate to the characterization of the Jaguaripe estuary as a pristine system. The REE abundances can be used as a background for the region.

Keywords: estuarine gradient; scavenging; rare earth elements; Todos os Santos Bay; fractionation; diagenesis.

1. INTRODUCTION

The rare earth elements (REE) comprise 14 lanthanide elements, starting from the lightest La to the heaviest Lu. They are generally trivalent elements, with the exceptions of Ce and Eu, which can exist as Ce (IV) and Eu (II). Although Y does not have 4f electrons, it has the same ionic radii and similar geochemical behavior to Ho and is usually assessed with the REE (Kawabe et al., 1991). Due to their coherent and predictable behavior, the REE provide insight into complex geochemical processes that single proxies cannot readily discriminate (Johannesson et al., 2005). The geochemical evolution of the continental crust, chemical weathering (Delgado et al., 2012; Liu et al., 2013), and sedimentary provenance in river, estuarine and marine environments (Elderfield et al., 1990; Sholkovitz, 1993; Caetano et al., 2009; Piper and Bau, 2013; Mandal et al., 2019) have been largely evaluated by the REE fractionation. The REE and Y (REEY) are also useful for understanding removal and fractionation processes during estuarine mixing (Elderfield et al., 1990; Sholkovitz, 1992, 1993; Sholkovitz and Szymczak, 2000; Rousseau et al., 2015; Andrade et al., 2020). Estuarine REEY removal has been recognized early on as an important mechanism balancing marine REE budgets (Goldstein and Jacobsen, 1987).

Mangroves are important intertidal coastal systems that provide a myriad of ecological services. Together with estuaries, mangroves regulate the exchange of materials at the interfaces between the land, atmosphere, and ocean ecosystems (Sholkovitz, 1976, Hoyle et al., 1984). The mangrove forest root structure favors the accumulation of fine sediments in soils that can act as sinks and sources of trace and major elements. That reflects the dynamic nature of mangrove ecosystems that are subject to rapid changes in soil physicochemical properties such as water content, texture, pH, redox conditions, and salinity due to tidal flushing and the associated soil flooding. The flooding episodes may develop redox cycles in soils, with alternating periods of oxidizing and reducing conditions. These cycles could,

74 therefore, result in the solubilization of various Fe (III) solid phases, organic matter, and
75 colloids that are strong adsorbents of metallic cations (Davranche et al., 2011).
76 Fine, C rich sediments can act as sinks for REEY in estuarine sediments and
77 mangrove soils (Wasserman et al., 2001; Censi et al., 2007; Mandal et al., 2019; Silva-Filho
78 et al., 2011). Interactions between dissolved and particulate phases, dissolution/diffusion,
79 complex formation, and the chemistry of Fe and Mn at varied redox levels may control the
80 distribution of REEY in sedimentary profiles (Kuss et al., 2001, Lawrence and Kamber,
81 2006). Hence, REEY mobilization from soils through the above-mentioned reactions may
82 lead to the development of specific REEY spatial distribution patterns (Davranche et al.,
83 2011). However, there is a lack of studies providing comprehensive assessments of the spatial
84 distribution of REEY and their sources, and that explore the factors driving the patterns
85 within the complex estuarine-mangrove ecosystems.
86 Although advances have been made towards understanding REEY geochemistry in
87 surficial mangrove soils, considerably fewer studies have focused on the sedimentary
88 historical records. Mandal et al. (2019) showed that the light REE (LREE) were more
89 abundant than the heavy REE (HREE) in the sediments of the Indian Sundarban, located at
90 the estuarine part of the Ganges River and at the land-ocean boundary of the Bay of Bengal,
91 which also presented a weak positive europium anomaly. Prasad and Ramanathan (2008)
92 found similar results for mangrove soils in Pichavaram. Sappal et al. (2014) observed a
93 convex shale-like pattern of REE and strong positive Eu anomalies in soil profiles from the
94 Pichavaram mangroves, reflecting the natural weathering of the source material. Censi et al.
95 (2005) investigated the dissolved phase, suspended particulate matter, and sediments of the
96 western coast of the Gulf of Thailand and observed Eu and Gd positive anomalies explained
97 by the extensive rock-water interaction processes occurring in the basin of the Mae Klong
98 and Phetchaburi rivers. Wasserman et al. (2001) compared the La, Ce, Sm, Eu, Yb, and Lu

99 concentrations of cores in mangrove forests and mudflats in Sepetiba Bay, Brazil. Later,
100 Silva-Filho et al. (2011) used the fractionation patterns of REE in mangroves of the same
101 area as tracers of sedimentary processes. Caetano et al. (2009) studied the vertical distribution
102 of trace elements and REE in a sediment core from the Vigo Ria indicating preferential
103 retention of LREE over the HREE in a transitional sedimentary layer where oxyhydroxides
104 were generated. Brito et al. (2018) reported significant correlations between REE, grain-size,
105 Al, Fe, Mg, and Mn, suggesting a preferential association of REE to aluminosilicates, Al
106 hydroxides and Fe oxyhydroxides. Finally, Zhang et al. (2013) examined the influence of
107 mangroves on the distribution of REE in estuarine sediments and soil profiles from mangrove
108 forests, forest fringe, and adjacent mudflat in the Zhangjiang estuary. Their results showed
109 that LREE were enriched over the HREE, with a relatively weak negative Eu anomaly, and
110 also indicated weathered continental materials as the main source for REE.
111 In the past decades, the REE distributions have been used to follow anthropogenic
112 contamination in aquatic systems (e.g., Bau et al., 1996; Hatje et al., 2017; Pedreira, et al.,
113 2018). This reflects the fact that modern technologies increasingly require several REE due to
114 their unique physical and chemical properties. Therefore, we expect that the natural
115 distribution patterns of REE do not prevail in coastal systems such as mangroves and
116 estuaries worldwide, already largely impacted by anthropogenic activities. Besides, there has
117 not been a consensus on how early diagenetic processes affect REEY distribution in soils
118 (Caetano et al., 2009). For these reasons, the main focus of this work is to study the REEY
119 abundance and fractionation in profiles of mangrove soils and also in estuarine sediments of a
120 well-preserved tropical estuary bordered by mangrove forests. This system, identified as the
121 Jaguaripe estuary, is located in the Northeast of Brazil and has insipient anthropogenic
122 activities, which allowed us to study REE under rare, nearly natural conditions. Therefore,
123 offering the opportunity to evaluate REE sources, distributions, and controlling processes in

sediments and mangrove soils along an estuarine gradient and hence to achieve an improved understanding of the REE cycle. Understanding the fate and partitioning of REE in mangrove ecosystems become urgent as the potential impact of REE contamination is expected to increase worldwide, hampering their use as proxies of natural processes.

2. MATERIAL AND METHODS

2.1 STUDY AREA AND SAMPLING DESIGN

The study area and sampling details have already been presented elsewhere (Hatje et al., 2020) and is summarized below. The Jaguaripe estuarine complex (Fig. 1) is located in the Todos os Santos Bay (BTS; 12º50'S, 38º38'W), the second largest bay (1,112 km^2) of Brazil. The climate at the bay is tropical humid, with annual mean temperature, precipitation and evaporation of 25ºC, 2,100 mm, and 1,000 mm, respectively. The hydrographic basin has 2,200 km^2, the tidal regime is semidiurnal, with maximum tidal range of < 2.5 m, and average discharges are 13 $m^3 s^{-1}$ and 28 $m^3 s^{-1}$ during summer and winter, respectively (Cirano and Lessa, 2007). Mangrove forests in the Jaguaripe present larger structural development than the other mangroves forests in the BTS (Costa et al., 2015). The region provides important ecological services (Barros et al., 2012), it is considered well-preserved and anthropogenic activities in the basin are insipient (Hatje and Barros, 2012; Krull et al., 2014). Local economy is based on seafood harvesting, a small shrimp farm, small-scale agriculture and artisanal pottery.

In order to cover the estuarine gradient, surficial sediments were collected using a Van Veen grab at 5 stations (J1, J3, J5, J8 and J10, Fig. 1) that have been used for a long-term monitoring study (Hatje and Barros, 2012). Six cores were collected in mangroves along the estuarine gradient (Fig. 1). For each estuarine section, hereafter called upper (cores T5

and T6), middle (cores T3 and T4) and lower estuary (cores T1 and T2), 2 cores were collected using a stainless-steel open-faced auger. Cores were sliced at 1 cm-thick layers throughout the first 10 cm, at 2 cm sections for the 20-50 cm interval and 3 cm-thick layers for bottom sections. Estuarine sediments were wet sieved to separate the fraction smaller than 63 μm, freeze-dried, homogenized and comminuted in a ball mill. Grain size, elemental composition and metals (for estuarine samples only) have been previously presented (Hatje and Barros, 2012).

2.2 CHEMICAL ANALYZES

All the material used during field and laboratory work were previously soaked in detergent (Extran® 2%, Merck, Germany), followed by immersion in a nitric acid (6 mol L^{-1}) bath for at least 48h and then rinsed 3 times with ultra-pure water (18.2 MΩ cm^2) (MilliQ, Millipore, Germany).

Approximately 100 mg of sediments and soils were digested using 1 mL of HF (40%, Merck Suprapur®, Germany), 5 mL of HNO_3 (65%, Merck Suprapur®, Germany) and 2 mL of HCl (30%, Merck Suprapur®, Germany) in a microwave oven (Multiwave PRO, Anton Paar, Austria). After digestion, a complexation run was performed after adding 6 mL of saturated boric acid (H_3BO_3) solution to each vial. All samples were digested in duplicates. Certified reference materials and blanks were run in each digestion batch.

Determination of REEY and trace elements were performed by ICP-MS (iCAP RQ, Thermo Scientific, Germany). Details are presented in the supplementary material (Table S1). The isotopes selected for the quantification of REE were ^{89}Y, ^{139}La, ^{140}Ce, ^{141}Pr, ^{146}Nd, ^{147}Sm, ^{153}Eu, ^{157}Gd, ^{159}Tb, ^{163}Dy, ^{165}Ho, ^{166}Er, ^{169}Tm, ^{172}Yb and, ^{175}Lu and we also determined ^{59}Co and ^{207}Pb. Polyatomic and isobaric interferences were monitored. Solutions of Tb and Gd, and La, Ce, Pr, Nd, Sm, and Ba, both at 1 μg kg^{-1}, were run every 20 samples.

The concentrations for REE were not corrected for oxide formations because oxides were negligible. Calibration curves of 0.005 to 12 μg kg^{-1} and 0.05 to 35 μg kg^{-1} were used for the quantification of REEY and trace elements, respectively. Indium was used as the internal standard (1 μg kg^{-1}, final concentration).

Aluminium, Fe, Mn, and Si analyses were performed by ICP OES (Shimadzu, ICPE-9820, Japan). Experimental conditions are presented in Table S1. Calibration curves of 0.001 to 2.5 mg kg^{-1} for Mn and 0.5 to 55 mg kg^{-1} for Al, Fe, and Si were used for quantification of the major elements. Procedural blanks (HNO_3 2%) were negligible compared with measured concentrations. The accuracy of the analytical procedures was monitored using the certified reference material Estuarine Sediment - BCR 667 and the MESS-3/NRCC (Tables S2 and Table S3). The recoveries for the analyzed elements agreed well with the certified values (i.e. 84 - 112%).

3. RESULTS AND DISCUSSION

3.1 SURFICIAL ESTUARINE SEDIMENT COMPOSITION AND REE ABUNDANCES

Surface samples along the estuarine gradient were composed mostly of coarse-grained material. Sand content ranged from 77% to 93%, for J1 and J5 respectively (Table S4), the reason that made us work with the fine fraction of sediments to minimize the effects of grain-size variability and to allow comparability with the mangrove data.

Aluminum contents were fairly constant along the estuary (7.89 to 9.19%), whereas Fe (4.61 to 7.66%) and Si (15.9 to 21%) contents decreased seaward (Table S4). No clear pattern was observed for the Co contents that varied between 14.1 and 20.2 mg kg^{-1}. Lead and Mn presented the highest concentrations at the estuary mouth, minimum values at the

middle estuary, and an increase at the upper estuary. The concentration of Pb in the fine fraction of sediments at the mouth of the estuary (35.7 mg kg^{-1}) was slightly above the lower-threshold value (TEL; Buchman, 2008). However, we do not expect this level to be toxic, once the fine fraction of sediments represents only 23% of the bulk. The levels presented here corroborate with previous studies that suggested this area as a well-preserved system (Hatje and Barros, 2012; Krull et al., 2014), although local, low-level contamination associated with point sources has been observed in a few sites for Hg (Hatje et al., 2019) and petroleum hydrocarbons (Egres et al., 2019).

The total REE (ΣREE; Fig. 2) contents in estuarine sediments varied within a small interval (202 to 220 mg kg^{-1}), with the highest concentrations observed at the upper estuary. Our values are in the superior range of concentrations reported for coastal systems such as the Tagus estuary (18 - 210 mg kg^{-1}; Brito et al., 2018), Mandovi estuary (129 - 227 mg kg^{-1}; Shynu et al., 2011), Zuari estuary (175 - 320 mg kg^{-1}; Shynu et al., 2013), Galian Rias (3 - 233 mg kg^{-1}; Prego et al., 2009, 2012), and the North Australian estuaries (77 - 263 mg kg^{-1}; Munksgaard et al., 2003).

Light REE (LREE; La, Ce, Pr, and Nd) corresponded for the most abundant fraction (90% of the total) in the estuarine sediments (Fig. 2 and Table S5), followed by the medium REE (MREE; Sm, Eu, Gd, Tb, Dy, and Ho), and the HREE (Er, Tm, Yb, and Lu). Similar observations were made elsewhere (Elderfield et al., 1990; Brito et al., 2018). As for Shynu et al., (2011), Sappal et al., (2014), Consani et al., (2020), among others, Ce was the most abundant element (87.1 - 99.5 mg kg^{-1}) contributing to the total ΣREE.

The Post Archean Australian Shale (PAAS) (Taylor and McLennan, 1985) has been widely used as a normalizing agent in marine sediments to evidence the fractionation of REE relative to the source, also allowing ease comparison between studies. The PAAS-normalized abundances (Fig. 3) displayed a consistent enrichment of the LREE over the HREE, with

224 ratios of $(La/Yb)_{PAAS}$ = 2.75 ± 0.48, $(La/Gd)_{PAAS}$ = 1.31 ± 0.12, and $(Gd/Yb)_{PAAS}$ = 2.10 ±
225 0.28. The fractionation was highest at the most upstream station (J10) and decreased seaward
226 (Fig. S1), in keeping with the general understanding of the REE particle reactivity. In
227 estuarine environments, dissolved and particulate REE undergo flocculation and precipitation
228 processes. The removal of dissolved REE during these processes, especially in waters with
229 low salinity (upper estuary, Table S4), reflects induced coagulation by salt from ubiquitous
230 organic and ferromanganese colloids that remove REE, promoting their fractionation (Hoyle
231 et al., 1984; Goldstein and Jacobsen, 1988; Byrne and Kim, 1990; Schijf et al., 1995;
232 Sholkovitz and Szymczak, 2000; Chaillou et al., 2006; Rousseau et al., 2015).
233 Among the REE, the LREE tend to be more reactive than MREE and HREE
234 (Sholkovitz and Elderfield, 1988; Elderfield et al., 1990, Sholkovitz, 1993). LREE are
235 preferably associated with the solid phase due to their more pronounced complexation with
236 ligands on the particles and surfaces of the colloids. On the contrary, the depleted HREE in
237 the sediments is the result of their greater tendency to form stable soluble carbonate and
238 organic complexes with dissolved ligands when compared to LREE and MREE (Fleet 1984;
239 Millero 1992; Schijf et al., 1995; Kuss et al. 2001). These processes cause the removal,
240 preferentially of LREE, and fractionation of the REE pattern along the estuarine gradient. A
241 recent study that evaluated the fractionation of dissolved REE along the continuum between
242 the Paraguaçu estuary through Todos os Santos Bay and the adjacent sea, reported that REE
243 were scavenged in the estuarine low salinity region (< 5) following the order LREE> MREE>
244 HREE and that PAAS-normalized dissolved REE patterns varied from relatively flat at the
245 fluvial endmember to the ocean-like HREE enriched pattern at the estuary mouth (Andrade et
246 al., 2020), supporting the results observed here for estuarine sediments.
247 Positive and significant correlations ($p < 0.05$) were observed between LREE and Al
248 ($r = 0.85$) and Fe ($r = 0.96$) in sediments. These results indicated that Al and Fe-

oxyhydroxides are the main scavenging phases for LREE, similarly to what was observed in previous works (Chaillou et al., 2006; Caccia and Millero, 2007; Caetano et al., 2009). The mobility of the LREE in these oxic estuarine sediments may be controlled by the precipitation of Fe insoluble forms. MREE and HREE did not show the same affinity for Al or Fe-oxyhydroxides. Iron and Mn behave differently in estuarine environments and their concentrations may also be controlled by distinct processes. Unlike Fe, Mn has slower oxidation kinetics (Benjamin and Honeyman, 1992). In estuaries, Mn is mainly associated with inorganic complexes (Stumm and Morgan, 1981), and its behavior is controlled by oxidation and scavenging onto suspended material. A strong positive correlation was observed between the Mn and MREE ($r = 0.94$; $p < 0.05$), which connects the removal of MREE to the Mn cycle. All the individual MREE were correlated to Mn, but only for Gd, Sm, Tb and Dy the correlations were significant (respectively $r = 0.96$, $r = 0.99$, $r = 0.97$ and $r = 0.95$, $p < 0.05$). Whereas this connection needs to be further studied, using a larger dataset, the removal of REE from estuarine waters by Fe and Mn carrier phases seems to be an important geochemical process for the control of LREE and MREE abundances, respectively, and REE fractionation in sediments.

It is usual to calculate the expected shale-normalized concentration of a REE to quantify anomalous concentrations in relation to its neighboring REE. The Eu anomalies (Eu/Eu*) were calculated as follows:

$Eu/Eu^{*} = Eu_{PAAS}/(Sm_{PAAS} \times Gd_{PAAS})^{1/2}$ (Taylor and McLennan, 1985).

Eu showed small positive anomalies (1.22 ± 0.06), with slightly higher values at the upper estuary (Table S5). The occurrence of positive Eu anomalies is unusual in estuarine sediments, but it has been previously observed in other estuaries and attributed to feldspar-rich sources (Ramesh et al., 1999; Brito et al., 2018; Consani et al., 2020). The positive

values observed in sediments may also reflect the weathering of granite, abundant in the basin source region (Dominguez and Bittencourt, 2009).

For estimating the Ce anomaly, we used:

$Ce/Ce^{*} = Ce_{PAAS}/(La_{PAAS} \times Pr_{PAAS})^{1/2}$ (McLennan, 1989).

Average values for Ce/Ce^{*} were close to one (0.92 ± 0.05; Table S5), indicating that Ce negative anomalies are small. The largest anomaly (0.84) was observed in the middle estuary. Other REE did not display anomalies (Fig. 3 and Table S5).

3.2 DOWN-CORE DISTRIBUTIONS

3.2.1 SEDIMENT CHARACTERIZATION AND MAJOR ELEMENTS COMPOSITION

Sediment physico-chemical characterization of these cores has been previously discussed (Hatje et al., 2020). Mangrove soils are mostly composed of fine sediments (Fig. S2; average silt + clay = 98 ± 4%) and present relatively high contents of C_{org} (9.0 ± 2.3%; Table S6).

Iron, Al, and Si total concentrations displayed low variability down-core (Table S6), except for the core T3. Total contents of Al, Fe, and Mn were slightly higher in the upper estuarine cores, whereas Si was highest at the core T3, which presented the largest amount of sand. Major elements normalized to Al contents are presented in Figure 4. The Fe/Al ratios presented minor variability along the depth profile (i.e., up to 16% in core T3). Small subsurface peaks could be observed for cores T1, T4, and T6. More pronounced, but still relatively minor peaks compared to previous studies (e.g., Caetano et al., 2009), were observed at 45 cm and at 65 cm for cores T3 and T6, respectively. The Mn/Al ratios were more variable than Fe/Al ratios along cores, and maximum variability (up to ~50%) was

observed for core T3. Normalized Mn profiles showed a gradual decrease from the bottom towards the surface of the cores T2 and T6, with peaks at 40 and 65 (T6 only). The core T3 presented small peaks at 9 and 45 cm, similar to Fe, whereas core T4 presented a peak at 13 cm followed by a decrease towards the bottom.

The Si/Al ratios did not present substantial vertical variability (<16%) with the exception of the core T3 (up to ~43%), which is enriched in sand compared to the other cores, as previously mentioned.

3.2.2 DISTRIBUTIONS PATTERNS OF REE

Abundances of REEY are presented in Table S7. The average ΣREE of the mangrove soil profiles along the salinity gradient tended to increase from the lower (161 ± 18 mg kg^{-1}) to the upper estuary (183 ± 16 mg kg^{-1}), following the same trend observed for the estuarine sediments. The higher percentages of sand in cores T3 and T4 influenced the REE abundances similarly to the major elements and caused lower REE retention in mangrove soils. REE are mostly adsorbed on the fine-grained mangrove soils as previously observed elsewhere (Sinitsyn et al., 2000; Chaillou et al., 2006; Caetano et al., 2013). Recently, it has also been shown that REE may also fractionate between fine and bulk sediments, increasing LREE/HREE ratios in the fine fraction (Consani et al., 2020).

The LREE were the major contributors to the ΣREE for all mangrove soil profiles (88–90%), followed by MREE, varying between 8 and 10%, while HREE accounted for only to 2–3% of the total. Comparing the ΣREE and the fractionation of estuarine sediments and in superficial mangrove soils (Fig. 3), we can observe that: i. REE abundances are lower at mangrove soils; ii. the influence of the salinity gradient was more prominent in the estuarine sediments than in the mangrove soils, leading to a higher fractionation in the former, despite the regular flooding associated with tidal cycles; iii. the shale normalized pattern becomes

323 flatter and more similar to PAAS in mangrove soils along the whole salinity gradient; and
324 that iv. the positive Eu anomalies are also a consistent feature in mangrove soils.
325 These patterns reflect various processes that include differences in the hydrodynamics
326 and in the salinity gradient of the mangroves and estuary, besides the geochemistry of the
327 sediments. The numerous phases (e.g., organic matter, sulfides, lithogenic particles,
328 carbonates, and oxi-hydroxides) that control REE scavenging depend on the local physico-
329 chemical conditions (e.g., Elderfield, 1990; Davranche et al., 2004; Caetano et al., 2009;
330 Brito et al., 2018; Marmolejo-Rodríguez et al., 2007; Sholkovitz et al., 1992; Prego et al.,
331 2009; Prasad and Ramanathan, 2008). The highly reactive, low salinity (0-5) zone in the
332 estuary (stations J10 and J8; e.g. Krull et al., 2014) occurs further upstream of the mangrove
333 stations at the upper estuary (cores T5 and T6) and caused a larger fractionation in estuarine
334 sediments than in mangrove soils.
335 Despite the potential importance of organic matter on the REE cycling in mangroves,
336 the effects of organic matter in REE have been surprisingly overlooked so far (Freslon et al.,
337 2014). In addition to the difference in contents, the organic matter in estuarine sediments and
338 mangrove soils may have distinct contributions of continental and marine sources, that to a
339 certain extent may be translated into distinct scavenging capacities. Moreover, the texture of
340 sediments, redox potential, and contents of organic matter may influence early diagenetic
341 processes related to mineralization of organic matter in mangrove soils and also the reduction
342 of Fe-Mn oxyhydroxides compared to estuarine sediments.
343 The vertical profiles of ΣREE were substantially more variable at the lower estuary
344 (Fig. 5), which presents the highest sedimentation rate (core T1). Sedimentation rates across
345 the estuarine gradient vary over an order of magnitude from 5.1 ± 0.3 mm $year^{-1}$ (core T3) to
346 31 ± 2 mm $year^{-1}$ (core T1), corresponding to accumulation periods of around 100 and 25
347 years, respectively (Hatje et al., 2020). Current REE fluxes varied from 0.26 to 1.90 g m^2

348 year^{-1}, respectively for cores T3 and T1. For all cores, expressive changes in fluxes occurred
349 between surface and sub-surface layers. The diverse depositional accumulation rates, flux
350 deposition, and associated post-deposition processes determine the patterns observed in the
351 abundances of the ΣREE and their fractionation down soil profiles.

352 Depth profiles of ΣREE (Fig. 5) showed that abundances increased by up to ~50%
353 from the surface to 5 cm in core T1. This pattern was observed for all cores, but it was more
354 pronounced for the lower estuary, which is more hydrodynamic than the sheltered upper
355 estuary. The LREE (~45%) were the largest contributors for the vertical variation observed,
356 followed by the MREE (~25%), whereas the HREE varied only ~6% (core T1). When
357 sediments are deposited in a high sedimentation regime, rapid burial may limit the exposure
358 time of the dissolved REE with sediments and, hence, restricts its adsorptive capacity (Ruhlin
359 and Owen, 1986), possibly resulting in a lower concentration of ΣREE in sediments.
360 Although some plants can bioaccumulate REE, as they do for other trace elements, the
361 organic matter derived from mangroves is expected to be depleted in REE compared to river-
362 borne material. Therefore, autochthonous organic matter inputs in highly productive systems
363 may act as a diluting agent lowering REE abundances in soils. Recently, Mandal et al. (2019)
364 showed that total REE concentrations in mangrove species are much lower than in soils,
365 corroborating with our hypothesis.

366 Below the subsurface peak in the ΣREE (Fig. 5), total abundance showed little
367 changes with depth, indicating that diagenetic alterations after burial are not mobilizing REE
368 in soils substantially, and the impact on the soil chemistry is undetectable in the ΣREE. While
369 the Fe and Mn normalized concentrations showed relatively small peaks, in general, vertical
370 profiles did not show a clear well-established depth sequence of redox conditions, and no
371 oxic superficial layer was observed in the mangrove soils. All cores were visually very
372 homogeneous (i.e., no clear lamination), dark grey, and presented the characteristic odor of

373 H_2S, suggesting the presence of FeS_2 sulfides, which is expected to be abundant due to the
374 salinity of the mangrove soils. It is unfortunate, however, that S and SO^{2-}_4 were not
375 measured. REE in mangrove soils may be co-precipitating with metal sulfides (Schijf et al.,
376 1995 and Chaillou et al., 2006), but this hypothesis, however, needs to be further investigated
377 coupled with the chemistry of porewaters that seems to be the best tracer for the assessment
378 of REE mobilization in mangrove soils.

379 Depth profiles of La, Gd, and Yb concentrations in mangrove soils, representing the
380 LREE, MREE, and HREE, respectively, are presented in Fig. 6. In general, the greatest
381 variabilities were observed by La (3% - 43%), between surface and the top 5-15 cm layers.
382 Below the sub-surface maxima, there was no significant variability in concentrations along
383 most cores. Vertical variations were mostly absent for cores T3 and T4. The Gd also showed
384 an increase in concentrations (9 to 45%) between the surface and 5-15 cm for all cores. For
385 the Yb profiles, only T1, T2, and T5 showed some variability (8% - 26%) along cores. To
386 better observe the potential effect of diagenesis, the REE were normalized by Al. As an
387 example, Figure 7 shows the ratios of La/Al, Gd/Al, Yb/Al together with Fe/Al and Mn/Al
388 for comparison. It can be observed that the peaks found in normalized REE coincide with the
389 precipitation of Fe-Mn-oxyhydroxides at ~20 cm and also at 60 cm. Similar correspondence
390 in Mn/Al and Fe/Al peaks down-core were also observed for core T1, reflecting the
391 participation of REE in early diagenesis. However, other cores did not show the same trend.
392 Several studies have previously observed the incorporation of REE in Fe-oxyhydroxides in
393 surface sediments (e.g. Elderfield and Sholkovitz, 1987; Caccia and Millero, 2007) but only a
394 few looked at profiles (Caetano et al., 2009).

395 The Ce/Al and Eu/Al profiles (Fig. S3) are expected to be different than other REE
396 due to their redox behavior. However, normalized Ce and Eu profiles followed similar
397 tendencies to that observed for most normalized REE profiles. Peeks in normalized

concentrations were only clearly observed for T1 and T6 at sub-surface, and also at 45 cm and 60 cm for cores T3 and T6, respectively. For the other cores, profiles were mostly invariant, although with some variability.

Variations in the REE fractionation, observed by LREE/HREE ratios in mangrove soils across the estuary, ranged from 1.5 ± 0.3 (lower estuary) to 2.0 ± 0.1 (upper estuary) (Fig. 5). The greatest LREE/HREE ratios found in the upper estuary are associated with the enrichment of LREE in the soils caused by their greater reactivity and adsorption capacity onto clay matter and other insoluble colloidal matters in this region that is higher up in the catchment (Ramesh et al., 1999; Censi et al., 2004; Dubinin, 2004; Prasad and Ramanathan, 2008). The more fluvial environments are usually associated with smaller grain size sediments that can favor the retention of REE in the particulate phase. Along with the position in an estuary, proximity to freshwater inputs also drives removal processes so important in the low salinity zone. The vertical profiles of the LREE/HREE are similar to ΣREE, indicating that the same processes are controlling both the REE abundances and the enrichment of the LREE in mangrove soils.

The PAAS-normalized REE patterns for mangrove soils did not display substantial changes along the cores, indicating little or absence of REE fractionation, but there was some variation in terms of abundances (Fig. 8). For all cores, normalized abundances were minimum at the surface, probably caused by the constant sediment-water changes that occur in this layer that is frequently inundated, by the dilution caused by the autochthonous organic matter productions and also, perhaps, by bioturbation that promotes the oxygenation of sediments. In general, the layers below surficial soils revealed higher fractionation relative to the shale (Fig. 5 and 8).

The redox-sensitive REE, Ce and Eu, may be used to indicate changes in redox conditions in soils (Elderfield, 1990; Hannigan et al, 2010). The positive Eu anomalies (Fig.

8, Table S7) found in soils indicate a reduction of Eu^{+3} to Eu^{+2} and incorporation into the soils which may be attributed to (i) the prevailing reducing conditions in the mangrove environment and (ii) the riverine signature of detrital material from the weathering of source rocks that are carried by the Jaguaripe estuary.

The correlation coefficients between LREE and MREE were high and significant ($r > 0.90$; $p < 0.05$) for all cores. MREE also showed positive correlations with HREE ($r > 0.76$; $p < 0.05$). Only for the core T6, there was a significant negative correlation with organic carbon ($r = - 0.67$, $p < 0.05$), pointing out the poor association of REE and organic matter in mangrove soils. In the dissolved fraction/porewater, however, we expect organic matter to have a more dominant role in the solubilization of REE during soil diagenesis.

Correlations between REE, Fe, and Mn were not significant for most cores either. This lack of correlations, associated with the reducing characteristics of mangrove soils, where sulfate reduction is the dominant biogeochemical process, suggests that sulfides may be an important burial phase for REE. Co-precipitation of the REE with Fe sulfides may be a widespread process under the reducing mangrove soil conditions. This hypothesis, which needs to be tested, has been previously evoked to explain REE behavior in sediments of the Bay of Biscay (Chaillou et al., 2006).

The patterns observed in sediment chemistry in estuaries and mangroves may be explained by the superimposition of a series of processes that includes large scale estuarine mixing, inputs of fluvial REE, colloidal material and fine sediments, autochthonous organic matter dilution, suspended particulate material inputs and transport across the estuarine and intertidal gradient, in addition to local conditions such as submarine groundwater discharge, redox, and salinity gradients. The myriad of processes acting together impose a high complexity in the understanding of the REE cycles in mangroves. To better fingerprint the sources and controls of REE accumulation and remobilization in soils, speciation data for

448 sediments and porewater geochemistry, it will be necessary to test the hypotheses presented
449 here.

450 Background REE concentrations in mangrove soils could be determined using data
451 from profiles. The onset of anthropogenic activities and contamination in Todos os Santos
452 Bay coincides with the establishment of a refinery in the 1950s, followed by the slow
453 industrialization of the north shores of the bay. Multiple dated cores have allowed mapping
454 the chronology of metal contamination for the bay (Andrade et al., 2017; Hatje et al., 2019).
455 Although we consider that mangrove soils are not significantly affected by human activities
456 in the Jaguaripe basin, we used only the base of mangrove cores, which date ~1960 (e.g.,
457 cores T2, T5, and T6) to determine the background concentrations. Consequently, we also
458 excluded the soil layers more prone to post-depositional physical and chemical
459 remobilization. The background concentrations ranged from 0.22 ± 0.02 for Lu and 85.02 ±
460 8.29 for Ce (Table S7).

461

462 **4. CONCLUSIONS**

463 Fractionating along the estuary causes an enrichment in the LREE over the HREE in
464 estuarine sediments and mangrove soils which is attributed to the preferential removal of the
465 LREE at the upper estuary. REE abundances are lower in mangrove soils than in estuarine
466 sediments and the average ΣREE tended to be highest at the upper estuary. Positive Eu
467 anomalies were found in all cores and may be attributed to the dominant reducing conditions
468 in mangrove soils and also to the riverine detrital signature from the weathering of source
469 rocks. Vertical REE profiles show that: i. post-deposition processes might contribute to the
470 patterns observed in the abundances of the ΣREE and their fractionation at the surface and
471 subsurface mangrove soils; ii. the ΣREE and REE patterns were mostly constant through
472 profiles below 15 cm, indicating that diagenetic alteration after burial is not leading to

473 substantial REE fractionation, as can be observed by the LREE/HREE profiles; and iii. co-
474 precipitation of REE with metal sulfides may be an important burial mechanism. No clear
475 relationship was observed between REE and organic matter in soils. The latter, however,
476 needs to be better explored looking at REE speciation in sediments and REE abundances in
477 mangrove pore waters. The REE abundances observed here corroborate to the
478 characterization of the Jaguaripe estuary as a pristine system that does not display
479 contamination. The REE abundances can be used as background values for the region.
480

481 **5. ACKNOWLEDGMENTS**

482 We thank FAPESB (PET0034/2012; PAM 0020/2014), GASBRAS/FINEP, and
483 CNPq 441264/2017-4, 407297/2018-9) for financial support. The authors were sponsored by
484 FAPESB (T. Freitas), CAPES (R. Pedreira), and CNPq (V. Hatje, 304823/2018-0). We also
485 thank the volunteers that helped with the sample collection and discussions with M. Caetano
486 and R. Andrade.
487

488 **6. CREDIT AUTHOR STATEMENT**

489 VH: conceptualization, investigation, supervision, writing-reviewing and editing, funding
490 acquisition; TOPF: chemical analysis, ICP analysis, original draft, formal analysis,
491 investigating; RMAP: ICP analysis, reviewing draft.
492

493 **7. REFERENCES**

494 Andrade, R. L. B., Hatje, V., Masqué, P., Zurbrick, C. M., Boyle, E. A., Santos, W. P. C.,
495 2017. Chronology of anthropogenic impacts reconstructed from sediment records of trace
496 metals and Pb isotopes in Todos os Santos Bay (NE Brazil). Marine Pollution Bulletin.
497 125 (1 – 2), 459 – 471. https://doi.org/10.1016/j.marpolbul.2017.07.053

498 Andrade, R. L. B., Hatje, V., Pedreira, R. M. A., Böning, P., Pahnke, K., 2020. REE
499 fractionation and human Gd footprint along the continuum between Paraguaçu River to
500 coastal South Atlantic waters. Chemical Geology. 532, 119303.
501 https://doi.org/10.1016/j.chemgeo.2019.119303
502 Barros, F., de Carvalho, G.C., Costa, Y., Hatje, V., 2012. Subtidal benthic macroinfaunal
503 assemblages in tropical estuaries: generality amongst highly variable gradients. Marine
504 Environmental Research. 81, 43-52. http://dx.doi.org/10.1016/j.marenvres.2012.08.006
505 Bau, M., 1996. Controls on the fractionation of isovalent trace elements in magmatic and
506 aqueous systems: evidence from Y/Ho, Zr/Hf, and lanthanide tetrad effect. Contributions
507 to Mineralogy and Petrology. 123, 323 – 333. https://doi.org/10.1007/s004100050159
508 Benjamin, M. M., Honeyman, B.D., 1992. Trace metals. In: Ž. Butcher, S.S., Charlson,
509 R.J., Orians, G.H., Wolfe, G.V. (Eds.). Global Biogeochemical Cycles. Academic Press,
510 London, pp. 317–352.
511 Buchman, M., 2008. Screening quick reference tables (SQuiRTs). US National Oceanic
512 and Atmospheric Administration, Office of Response and Restoration Division.
513 Brito, P., Prego, R., Mil-Homens, M., Caçador, I., Caetano, M., 2018. Sources and
514 distribution of yttrium and rare earth elements in surface sediments from Tagus estuary,
515 Portugal. Science of the Total Environment. 621, 317–325.
516 https://doi.org/10.1016/j.scitotenv.2017.11.245
517 Byrne, R. H., Kim, K. H., 1990. Rare earth element scavenging in seawater. Geochimica
518 et Cosmochimica Acta. 54 (10), 2645–2656. https://doi.org/10.1016/0016-
519 7037(90)90002-3
520 Caccia, V. G., Millero, F. J., 2007. Distribution of yttrium and rare earths in Florida Bay
521 sediments. Marine Chemistry. 104 (3–4), 171–185.
522 https://doi.org/10.1016/j.marchem.2006.11.001

523 Caetano, M., Prego, R., Vale, C., de Pablo, H., Marmolejo-Rodríguez, J., 2009. Record of
524 diagenesis of rare earth elements and other metals in a transitional sedimentary
525 environment. Marine Chemistry. 116 (1–4), 36–46.
526 https://doi.org/10.1016/j.marchem.2009.09.003
527 Caetano, M., Vale, C., Anes, B., Raimundo, J., Drago, T., Schimdt, S., Nogueira, M.,
528 Oliveira, A., Prego, R., 2013. The Condor seamount at Mid-Atlantic Ridge as a
529 supplementary source of trace and rare earth elements to the sediments. Deep-Sea
530 Research Part II: Topical Studies in Oceanography. 98, 24–37.
531 https://doi.org/10.1016/j.dsr2.2013.01.009
532 Censi, P., Mazzola, S., Sprovieri, M., Bonanno, A., Patti, B., Punturo, R., Spoto, S. E.
533 Saiano, F., Alonzo, G., 2004. Rare earth elements distribution in seawater and suspended
534 particulate of the Central Mediterranean Sea. Chemistry and Ecology. 20 (5), 323–343.
535 https://doi.org/10.1080/02757540410001727954
536 Censi, P., Spoto, S. E., Nardone, G., Saiano, F., Punturo, R., Di Geronimo, S. I., Mazzola,
537 S., Bonanno, A., Patti, B., Sprovieri, M., Ottonello, D., 2005. Rare-earth elements and
538 yttrium distributions in mangrove coastal water systems: The western Gulf of Thailand.
539 Chemistry and Ecology. 21 (4), 255–277. https://doi.org/10.1080/02757540500213216
540 Censi, P., Sprovieri, M., Saiano, F., Di Geronimo, S. I., Larocca, D., Placenti, F., 2007.
541 The behaviour of REEs in Thailand's Mae Klong estuary: Suggestions from the Y/Ho
542 ratios and lanthanide tetrad effects. Estuarine, Coastal and Shelf Science. 71 (3–4), 569–
543 579. https://doi.org/10.1016/j.ecss.2006.09.003
544 Chaillou, G., Anschutz, P., Lavaux, G., Blanc, G., 2006. Rare earth elements in the
545 modern sediments of the Bay of Biscay (France). Marine Chemistry. 100 (1–2), 39–52.
546 https://doi.org/10.1016/j.marchem.2005.09.007

547 Cirano, M., Lessa, G. C., 2007. Oceanographic Characteristics of Baía de Todos os
548 Santos, Brazil. Revista Brasileira de Geofísica. 25 (4), 363-387.
549 https://doi.org/10.1590/S0102-261X2007000400002
550 Consani, S., Cutroneo, L., Carbone, C., Capello, M., 2020. Baseline of distribution and
551 origin of Rare Earth Elements in marine sediment of the coastal area of the Eastern Gulf
552 of Tigullio (Ligurian Sea, North-West Italy). Marine Pollution Bulletin. 155, 111145.
553 https://doi.org/10.1016/j.marpolbul.2020.111145
554 Costa, P., Dórea, A., Mariano-Neto, E., Barros, F., 2015. Are there general spatial
555 patterns of mangrove structure and composition along estuarine salinity gradients in
556 Todos os Santos Bay? Estuarine, Coastal and Shelf Science. 166, 83–91.
557 https://doi.org/10.1016/j.ecss.2015.08.014
558 Davranche, M., Pourret, O., Gruau, G., Dia, A., 2004. Impact of humate complexation on
559 the adsorption of REE onto Fe oxyhydroxide. Journal of Colloid and Interface Science.
560 277 (2), 271–279. https://doi.org/10.1016/j.jcis.2004.04.007
561 Davranche, M., Grybos, M., Gruau, G., Pédrot, M., Dia, A., Marsac, R., 2011. Rare earth
562 element patterns: A tool for identifying trace metal sources during wetland soil reduction.
563 Chemical Geology. 284 (1–2), 127–137. https://doi.org/10.1016/j.chemgeo.2011.02.014
564 Delgado, J., Pérez-López, R., Galván, L., Nieto, J. M., Boski, T., 2012. Enrichment of
565 rare earth elements as environmental tracers of contamination by acid mine drainage in
566 salt marshes: A new perspective. Marine Pollution Bulletin. 64 (9), 1799–1808.
567 https://doi.org/10.1016/j.marpolbul.2012.06.001
568 Dominguez, J. M. L., Bittencourt, A. C. S. P. Geologia. In: Hatje, V., de Andrade, J.B.
569 Baía De Todos Os Santos: Aspectos Oceanográficos. Salvador: EDUFBA, 2009. Cap. II,
570 27 – 66.

571 Dubinin, A. V., 2004. Geochemistry of rare earth elements in the ocean. Lithology and
572 Mineral Resources. 39 (4), 289–307.
573 https://doi.org/10.1023/B:LIMI.0000033816.14825.a2
574 Egres, A. G., Hatje, V., Miranda, D. A., Gallucci, F., Barros, F., 2019. Functional
575 response of tropical estuarine benthic assemblages to perturbation by Polycyclic
576 Aromatic Hydrocarbons. Ecological Indicators. 96, 229–240.
577 https://doi.org/10.1016/j.ecolind.2018.08.062
578 Elderfield, H., Sholkovitz, E. R., 1987. Rare earth elements in the pore waters of reducing
579 nearshore sediments. Earth and Planetary Science Letters. 82 (3 – 4), 280 – 288.
580 https://doi.org/10.1016/0012-821X(87)90202-0
581 Elderfield, H., Upstill-Goddard, R., Sholkovitz, E. R., 1990. The rare earth elements in
582 rivers, estuaries, and coastal seas and their significance to the composition of ocean
583 waters. Geochimica et Cosmochimica Acta. 54 (4), 971–991.
584 https://doi.org/10.1016/0016-7037(90)90432-K
585 Freslon, N., Bayon, G., Toucanne, S., Bermell, S., Bollinger, C. Chéron, S., Etoubleau, J.,
586 Germain, Y., Khripounoff, A., Ponzevera, E., Rouget, M. L., 2014. Rare earth elements
587 and neodymium isotopes in sedimentary organic matter. Geochimica et Cosmochimica
588 Acta. 140, 177-198. https://doi.org/10.1016/j.gca.2014.05.016
589 Fleet, A. J., 1984. Aqueous and sedimentary geochemistry of the rare earth elements.
590 Elsevier B.V. Chapter 10. 2, 343-373. https://doi.org/10.1016/B978-0-444-42148-
591 7.50015-0
592 Goldstein, S. J., Jacobsen, S. B., 1987. The Nd and Sr isotopic systematics of river-water
593 dissolved material: Implications for the sources of Nd and Sr in seawater. 66 (3 – 4), 245–
594 272. https://doi.org/10.1016/0168-9622(87)90045-5

595 Goldstein, S. J., Jacobsen, S. B., 1988. Rare earth elements in river waters. Earth and
596 Planetary Science Letters. 89 (1), 35–47. https://doi.org/10.1016/0012-821X(88)90031-3
597 Hannigan, R., Dorval, E., Jones, C., 2010. The rare earth element chemistry of estuarine
598 surface sediments in the Chesapeake Bay. Chemical Geology. 272 (1–4), 20–30.
599 https://doi.org/10.1016/j.chemgeo.2010.01.009
600 Hatje, V.; Barros, F., 2012. Overview of the 20th century impact of trace metal
601 contamination in the estuaries of Todos os Santos Bay: Past, present and future scenarios.
602 Marine Pollution Bulletin. 64 (11), 2603–2614.
603 https://doi.org/10.1016/j.marpolbul.2012.07.009
604 Hatje, V., Pedreira, R. M. A., Rezende, C. E., Schettini, C. A. F., Souza, G.C., Marin, D.
605 C., Hackspacher, P. C., 2017. The environmental impacts of one of the largest tailing dam
606 failures worldwide. Scientific Reports. 7, 10706. https://doi.org/10.1038/s41598-017-
607 11143-x
608 Hatje, V., Andrade, R. L.B., Jesus, R. M., Masqué, P., Albergaria-Barbosa, A. C.R., de
609 Andrade, J. B., Santos, A. C.S.S., 2019. Historical records of mercury deposition in dated
610 sediment cores reveal the impacts of the legacy and present-day human activities in
611 Todos os Santos Bay, Northeast Brazil. Marine Pollution Bulletin. 145, 396–406.
612 https://doi.org/10.1016/j.marpolbul.2019.06.041
613 Hatje, V., Masqué P., Patire, V., Dórea, A., Barros, F. Blue C stocks, accumulation rates,
614 and associated spatial variability in Brazilian mangroves (final review). Limnology and
615 Oceanography.
616 Hoyle, J., Elderfield, H., Gledhill, A., Greaves, M., 1984. The behaviour of the rare earth
617 elements during mixing of river and sea waters. Geochimica et Cosmochimica Acta. 48
618 (1), 143–149. https://doi.org/10.1016/0016-7037(84)90356-9

619 Johannesson K.H., Cortés A., Ramos Leal J.A., Ramírez A.G., Durazo J., 2005.
620 Geochemistry of Rare Earth Elements in Groundwaters from a Rhyolite Aquifer,
621 Central México. In: Johannesson K.H. (Eds.), Rare Earth Elements in Groundwater
622 Flow Systems. Water Science and Technology Library, 51. Springer, Dordrecht, pp.
623 187 – 222.
624 Kawabe, I., Kitahara, Y., Naito, K., 1991. Non-chondritic yttrium/holmium ratio and
625 lanthanide tetrad effect observed in pre-Cenozoic limestones. Geochemical Journal. 25
626 (1), 31–44. https://doi.org/10.2343/geochemj.25.31
627 Kuss, J., Garbe-Schönberg, C. D., Kremling, K., 2001. Rare earth elements in suspended
628 particulate material of North Atlantic surface waters. Geochimica et Cosmochimica Acta.
629 65 (2), 187–199. https://doi.org/10.1016/S0016-7037(00)00518-4
630 Krull, M., Abessa, D. M.S., Hatje, V., Barros, F., 2014. Integrated assessment of metal
631 contamination in sediments from two tropical estuaries. Ecotoxicology and
632 Environmental Safety. 106, 195–203. https://doi.org/10.1016/j.ecoenv.2014.04.038
633 Lawrence, M. G., Kamber, B. S., 2006. The behaviour of the rare earth elements during
634 estuarine mixing-revisited. Marine Chemistry. 100 (1–2), 147–161.
635 https://doi.org/10.1016/j.marchem.2005.11.007
636 Liu, J., Xiang, R., Chen, Z., Chen, M., Yan, W., Zhang, L., Chen, H., 2013. Sources,
637 transport and deposition of surface sediments from the South China Sea. Deep-Sea
638 Research Part I: Oceanographic Research Papers. 71, 92–102.
639 https://doi.org/10.1016/j.dsr.2012.09.006
640 Mandal, S. K., Ray, R., González, A. G., Mavromatis, V., Pokrovsky, O. S., Jana, T. K.,
641 2019. State of rare earth elements in the sediment and their bioaccumulation by
642 mangroves: a case study in pristine islands of Indian Sundarban. Environmental Science
643 and Pollution Research. 26 (9), 9146–9160. https://doi.org/10.1007/s11356-019-04222-1

644 Marmolejo-Rodríguez, A. J., Prego, R., Meyer-Willerer, A., Shumilin, E., Sapozhnikov,
645 D., 2007. Rare earth elements in iron oxy-hydroxide rich sediments from the Marabasco
646 River-Estuary System (pacific coast of Mexico). REE affinity with iron and aluminium.
647 Journal of Geochemical Exploration. 94 (1–3), 43–51.
648 https://doi.org/10.1016/j.gexplo.2007.05.003
649 McLennan, S. M., 1989. Rare Earth Elements in Sedimentary Rocks: Influence of
650 Provenance and Sedimentary Processes. In: Lipin, B. R. and McKay, G. A., (Eds.),
651 Reviews in Mineralogy and Geochemistry. 21, 169–200.
652 Millero, F. J., 1992. Stability constants for the formation of rare earth-inorganic
653 complexes as a function of ionic strength. Geochimica et Cosmochimica Acta. 56 (8),
654 3123–3132. https://doi.org/10.1016/0016-7037(92)90293-R
655 Munksgaard, N. C., Lim, K., Parry, D. L., 2003. Rare earth elements as provenance
656 indicators in North Australian estuarine and coastal marine sediments. Estuarine, Coastal
657 and Shelf Science. 57 (3), 399–409. https://doi.org/10.1016/S0272-7714(02)00368-2
658 Pedreira, R. M. A., Pahnke, K., Böning, P., Hatje, V., 2018. Tracking hospital effluent-
659 derived gadolinium in Atlantic coastal waters off Brazil. Water Research. 145, 62–72.
660 https://doi.org/10.1016/j.watres.2018.08.005
661 Piper, D. Z., Bau, M., 2013. Normalized Rare Earth Elements in Water, Sediments, and
662 Wine: Identifying Sources and Environmental Redox Conditions. American Journal of
663 Analytical Chemistry. 04 (10), 69–83. http://dx.doi.org/10.4236/ajac.2013.410A1009
664 Prasad, M. B. K., Ramanathan, A., 2008. Distribution of Rare Earth Elements in the
665 Pichavaram Mangrove Sediments of the Southeast Coast of India. Journal of Coastal
666 Research. 1, 126–134. https://doi.org/10.2112/05-0533.1

667 Prego, R., Caetano, M., Vale, C., Marmolejo-Rodríguez, J., 2009. Rare earth elements in
668 sediments of the Vigo Ria, NW Iberian Peninsula. Continental Shelf Research. 29 (7),
669 896–902. https://doi.org/10.1016/j.csr.2009.01.009
670 Prego, R., Caetano, M., Bernárdez, P., Brito, P., Ospina-Alvarez, N., Vale, C., 2012. Rare
671 earth elements in coastal sediments of the northern Galician shelf: Influence of geological
672 features. Continental Shelf Research. 35, 75–85. https://doi.org/10.1016/j.csr.2011.12.010
673 Ramesh, R., Ramanathan, A. L., James, A. R., Subramanian, V., Jacobsen, S. B.,
674 Holland, H. D., 1999. Rare earth elements and heavy metal distribution in estuarine
675 sediments of east coast of India. Hydrobiologia. 397, 89–99.
676 https://doi.org/10.1023/A:1003646631589
677 Rousseau, T. C. C., Sonke, J. E., Chmeleff, J., Van B. P., Souhaut, M., Boaventura, G.,
678 Seyler, P., Jeandel, C., 2015. Rapid neodymium release to marine waters from lithogenic
679 sediments in the Amazon estuary. Nature Communications. 6, 7592.
680 https://doi.org/10.1038/ncomms8592
681 Ruhlin, D. E., Owen, R. M., 1986. The rare earth element geochemistry of hydrothermal
682 sediments from the East Pacific Rise: Examination of a seawater scavenging mechanism.
683 Geochimica et Cosmochimica Acta. 50 (3), 393–400. https://doi.org/10.1016/0016-
684 7037(86)90192-4
685 Sappal, S. M., Ramanathan, A., Ranjan, R. K., Singh, G., Kumar, A., 2014. Rare Earth
686 Elements as Biogeochemical Indicators in Mangrove Ecosystems (Pichavaram,
687 Tamilnadu, India). Journal of Sedimentary Research. 84 (9), 781–791.
688 https://doi.org/10.2110/jsr.2014.63
689 Schijf, J., De Baar, H. J. W.; Millero, F. J., 1995. Vertical distributions and speciation of
690 dissolved rare earth elements in the anoxic brines of Bannock Basin, eastern

691 Mediterranean Sea. Geochimica et Cosmochimica Acta. 59 (16), 3285–3299.
692 https://doi.org/10.1016/0016-7037(95)00219-P
693 Shynu, R., Rao, V. P., Kessarkar, P. M., Rao, T. G., 2011. Rare earth elements in
694 suspended and bottom sediments of the Mandovi estuary, central west coast of India:
695 Influence of mining. Estuarine, Coastal and Shelf Science. 94 (4), 355–368.
696 https://doi.org/10.1016/j.ecss.2011.07.013
697 Shynu, R., Rao, V. P., Parthiban, G., Balakrishnan, S., Narvekar, T., Kessarkar, P. M.,
698 2013. REE in suspended particulate matter and sediment of the Zuari estuary and adjacent
699 shelf, western India: Influence of mining and estuarine turbidity. Marine Geology. 346,
700 326–342. https://doi.org/10.1016/j.margeo.2013.10.004
701 Silva-Filho, E. V., Sanders, C. J., Bernat, M., Figueiredo, A. M. G., Sella, S. M.,
702 Wasserman, J., 2011. Origin of rare earth element anomalies in mangrove sediments,
703 Sepetiba Bay, SE Brazil: Used as geochemical tracers of sediment sources.
704 Environmental Earth Sciences. 64 (5), 1257–1267. https://doi.org/10.1007/s12665-011-
705 0942-y
706 Sinitsyn, V. A., Aja, S. U., Kulik, D. A., Wood, S. A., 2000. Acid-base surface chemistry
707 and sorption of some lanthanides on K^+-saturated, Marblehead illite: I. Results of an
708 experimental investigation. Geochimica et Cosmochimica Acta. 64 (2), 185–194.
709 https://doi.org/10.1016/S0016-7037(99)00175-1
710 Sholkovitz, E. R., 1976. Flocculation of dissolved organic and inorganic matter during the
711 mixing of river water and seawater. Geochimica et Cosmochimica Acta. 40 (7), 831–845.
712 https://doi.org/10.1016/0016-7037(76)90035-1
713 Sholkovitz, E. R., Elderfield, H., 1988. Cycling of dissolved rare earth elements in
714 Chesapeake Bay. Global Biogeochemical Cycles. 2 (2), 157-176.
715 https://doi.org/10.1029/GB002i002p00157

716 Sholkovitz, E. R., 1992. Chemical evolution of rare earth elements: fractionation between
717 colloidal and solution phases of filtered river water. Earth and Planetary Science Letters.
718 114 (1), 77–84. https://doi.org/10.1016/0012-821X(92)90152-L
719 Sholkovitz, E. R., 1993. The geochemistry of rare earth elements in the Amazon River
720 estuary. Geochimica et Cosmochimica Acta. 57 (10), 2181–2190.
721 https://doi.org/10.1016/0016-7037(93)90559-F
722 Sholkovitz, E., Szymczak, R., 2000. The estuarine chemistry of rare earth elements:
723 Comparison of the Amazon, Fly, Sepik and the Gulf of Papua systems. Earth and
724 Planetary Science Letters. 179 (2), 299–309. https://doi.org/10.1016/S0012-
725 821X(00)00112-6
726 Stumm, W., Morgan, J.J., 1981. An introduction emphasizing chemical equilibria in
727 natural waters. Aquatic Chemistry. 2nd Ed. Wiley-Interscience, New York. 656, 282–
728 285.
729 Taylor, S.R., McLennan, S.M., 1985. The Continental Crust: Its Composition and
730 Evolution. Blackwell, Oxford, 1-312.
731 Wasserman, J. C., Figueiredo, A. M. G., Pellegatti, F., Silva-Filho, E. V., 2001.
732 Elemental composition of sediment cores from a mangrove environment using neutron
733 activation analysis. Journal of Geochemical Exploration. 72, (2), 129–146.
734 https://doi.org/10.1016/S0375-6742(01)00158-3
735 Zhang, R., Yan, C., Liu, J., 2013. Effect of Mangroves on the Horizontal and Vertical
736 Distributions of Rare Earth Elements in Sediments of the Zhangjiang Estuary in Fujian
737 Province, Southeastern China. Journal of Coastal Research. 292, (6), 1341–1350.
738 https://doi.org/10.2112/JCOASTRES-D-11-00215.1

FIGURES

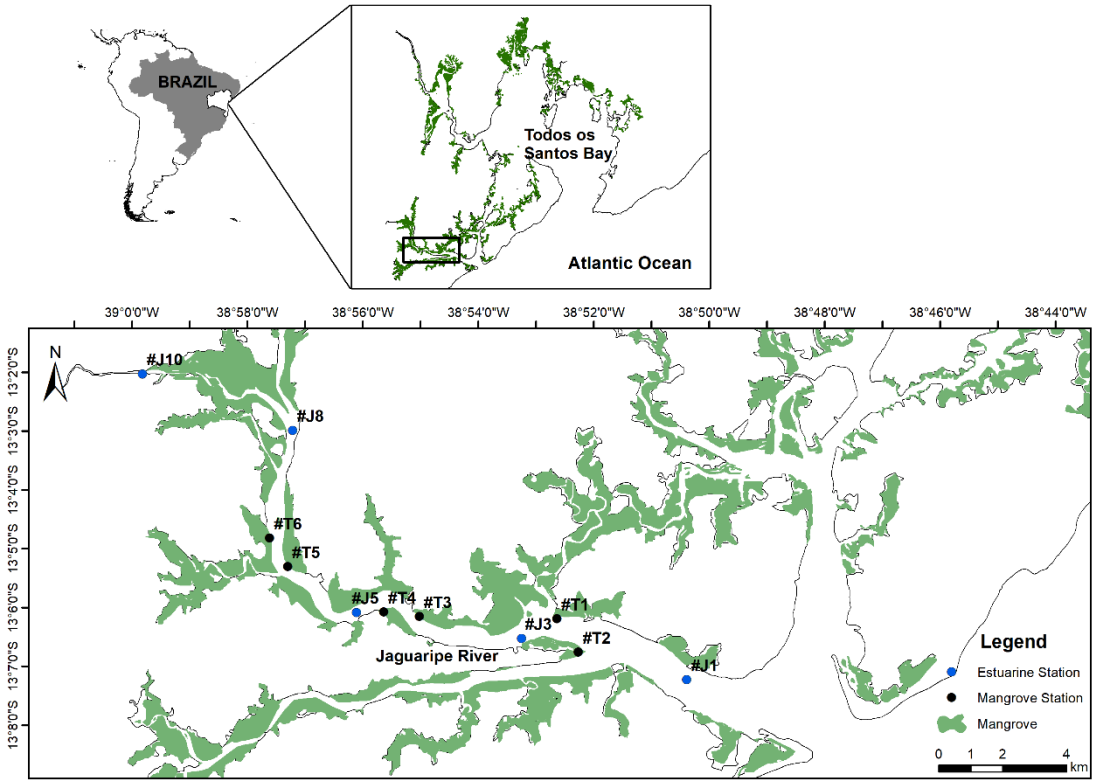

Fig 1. Locations of sampling sites along the Jaguaripe estuary, Bahia, Brazil.

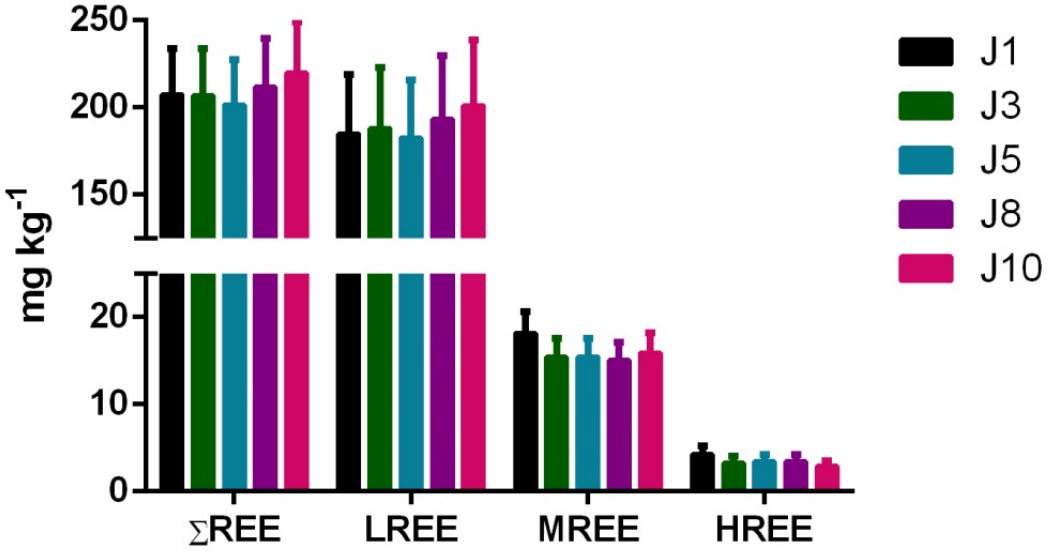

Fig. 2. Total REE (± standard deviation), light (LREE), middle (MREE) and heavy (HREE) REE concentrations for surface sediments of the Jaguaripe estuary.

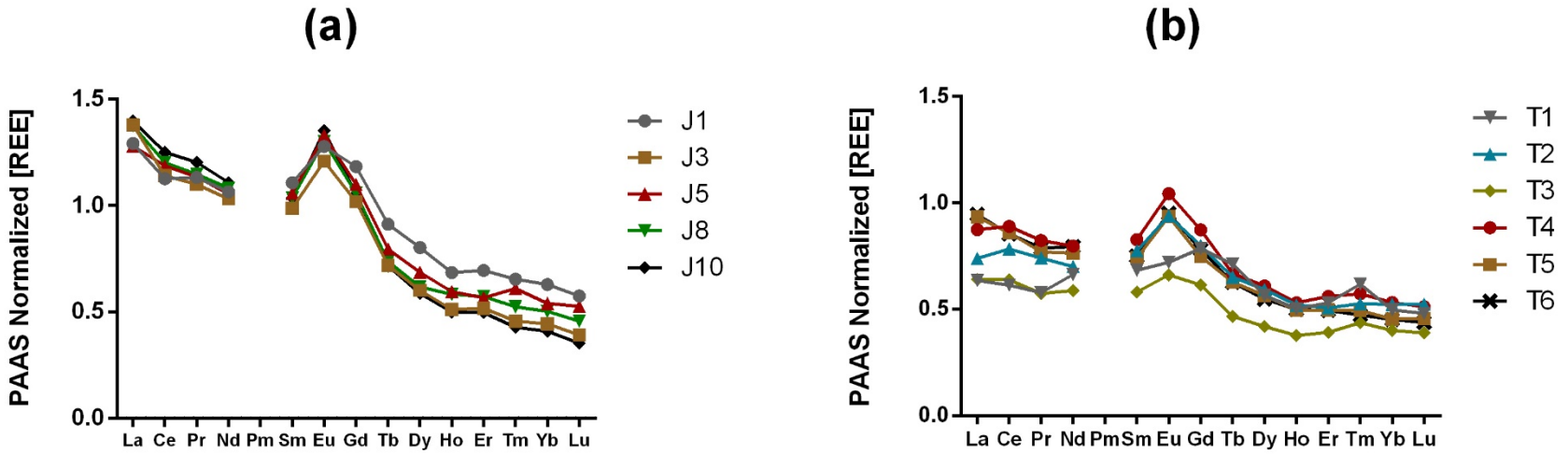

Fig. 3. PAAS-normalized REE patterns in surface sediments across the upper (J10, J8, T5 and T6), middle (J5, J3, T4 and T3), and lower (J1, T1 and T2) Jaguaripe estuary (a) and at surficial mangrove soils (b).

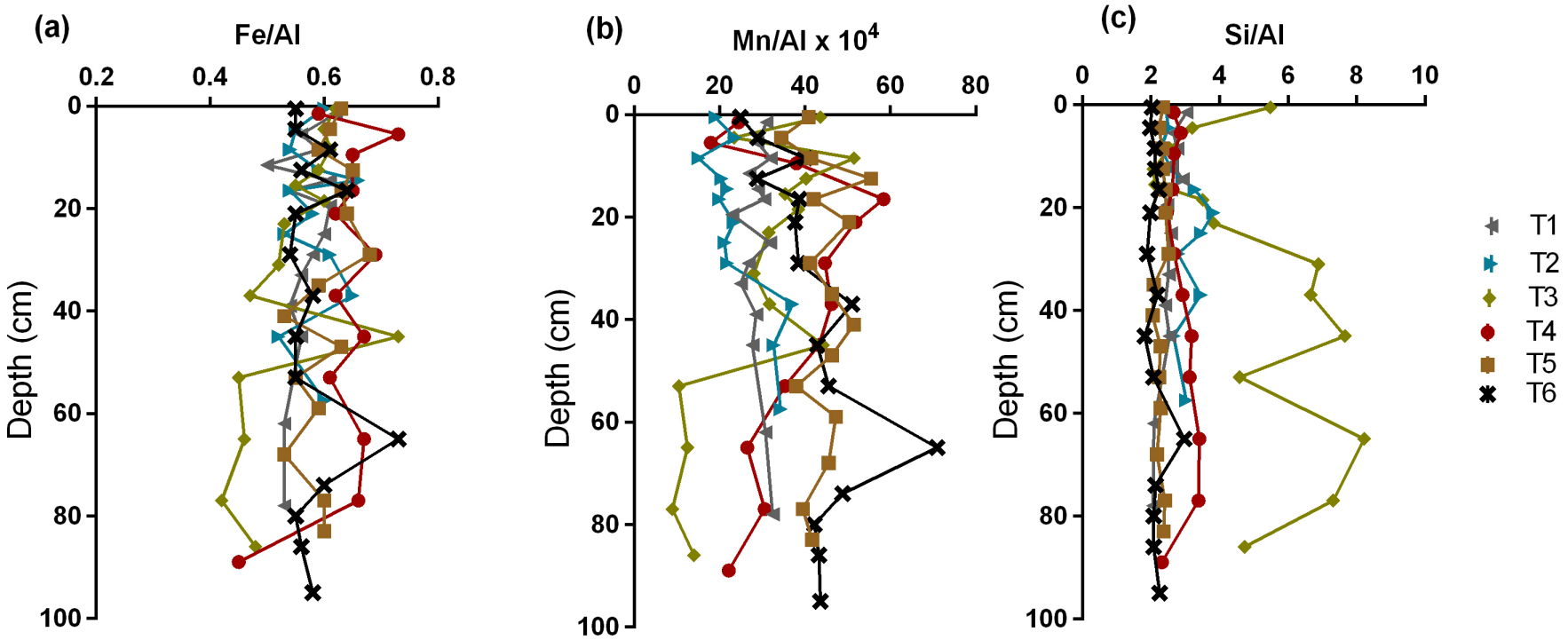

Fig. 4. Depth profiles of normalized concentrations of Fe, Mn and Si by Al in soil profiles (T1- T6) of the Jaguaripe estuary.

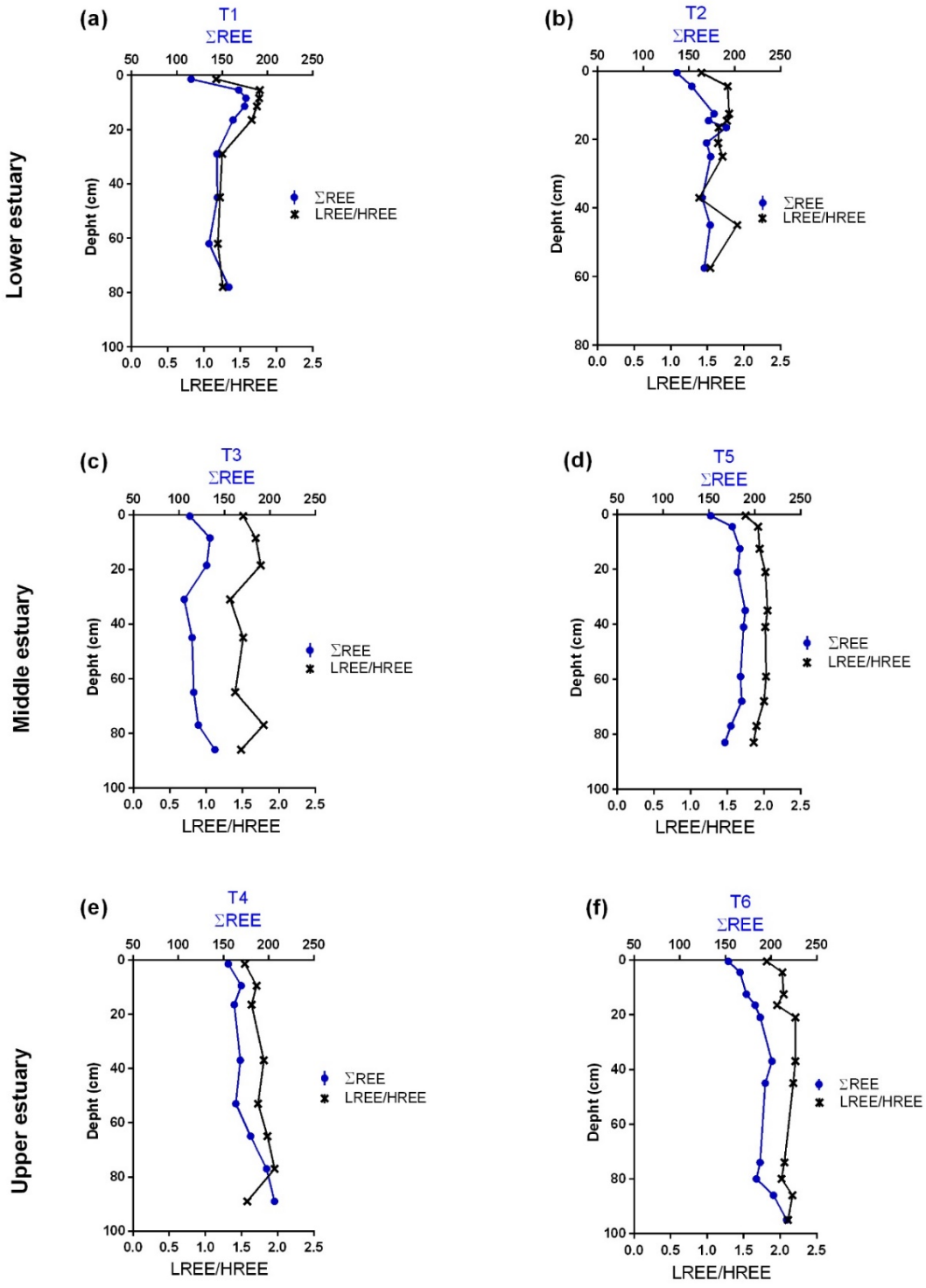

Fig. 5. Depth profiles of ΣREE (mg kg^{-1}) and LREE/HREE ratios in mangrove soils of the Jaguaripe estuary.

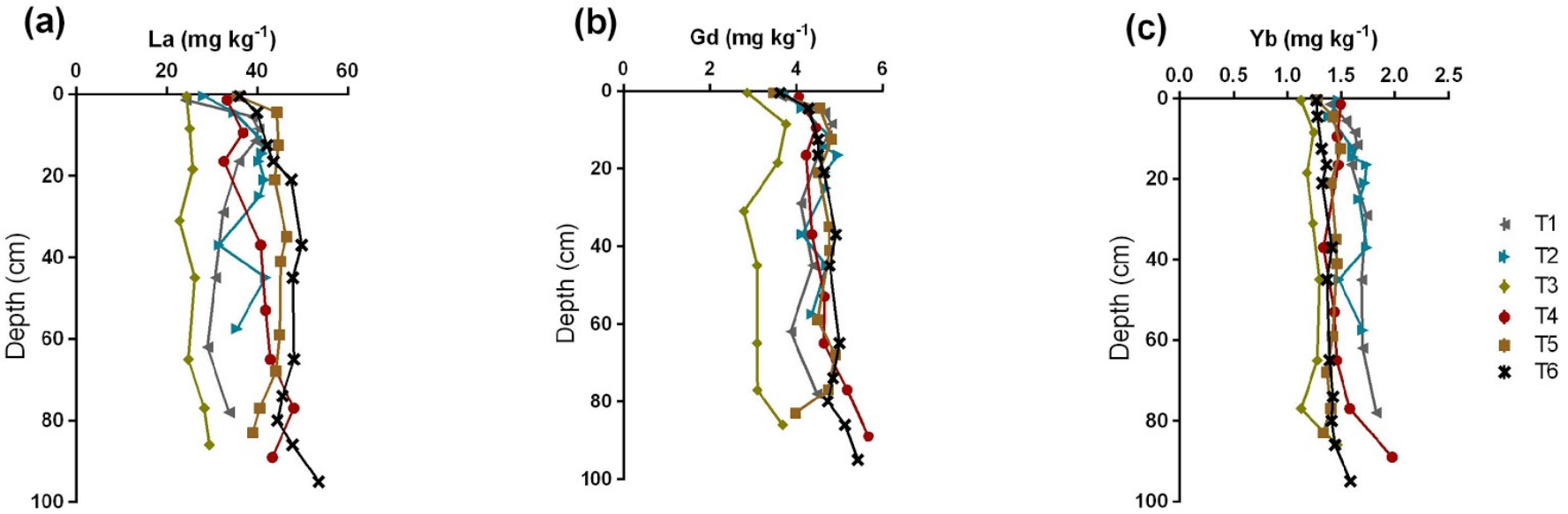

Fig. 6. Depth profiles of (a) La (LREE), (b) Gd (MREE), and (c)Yb (HREE) concentrations in soils (cores 1- 6) of the Jaguaripe estuary.

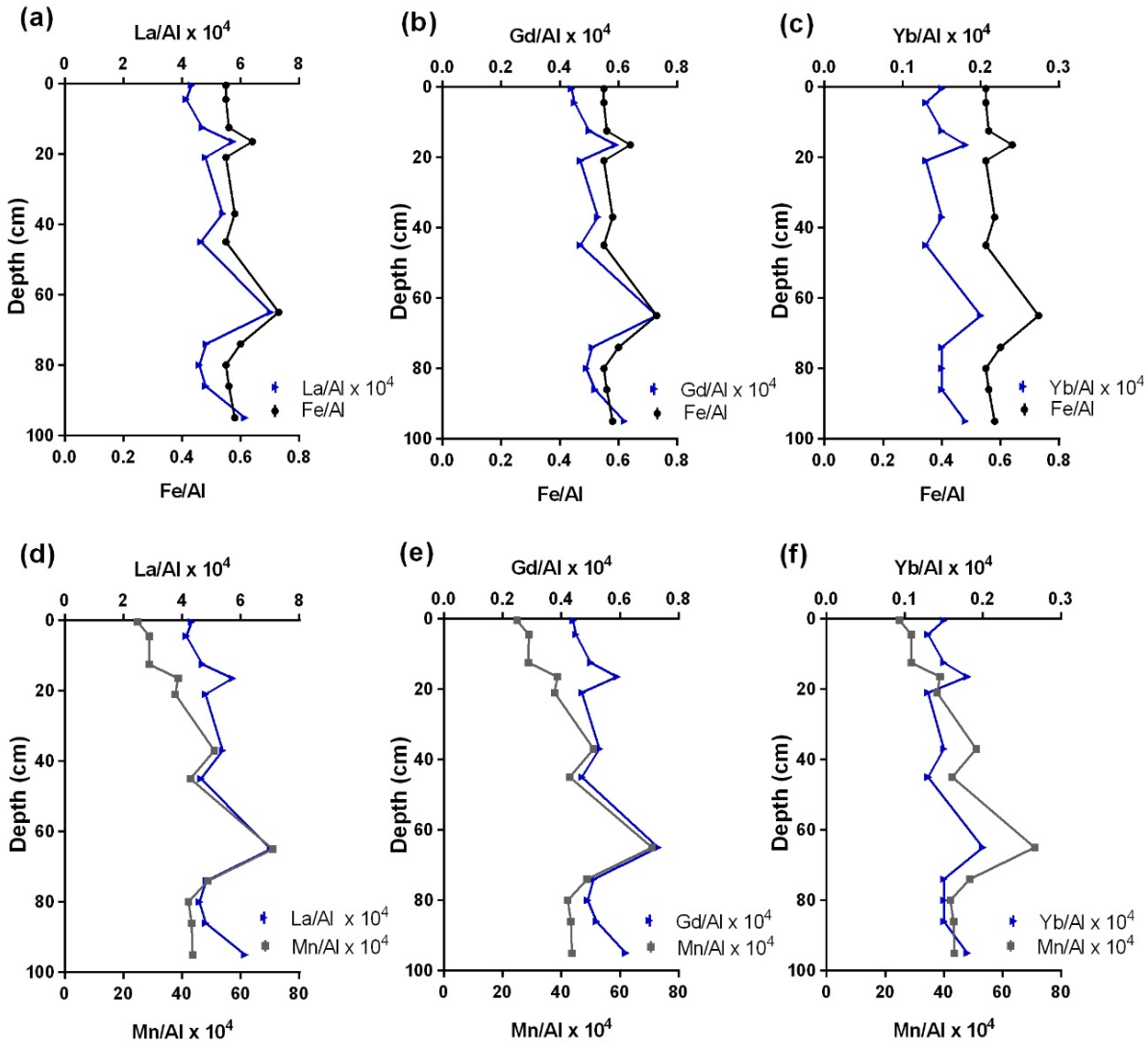

Fig.7. Depth profiles of La, Gd, and Yb concentrations normalized by Al (a, b, c) and Mn (d, e, f) in soil (core T6) of the Jaguaripe estuary.

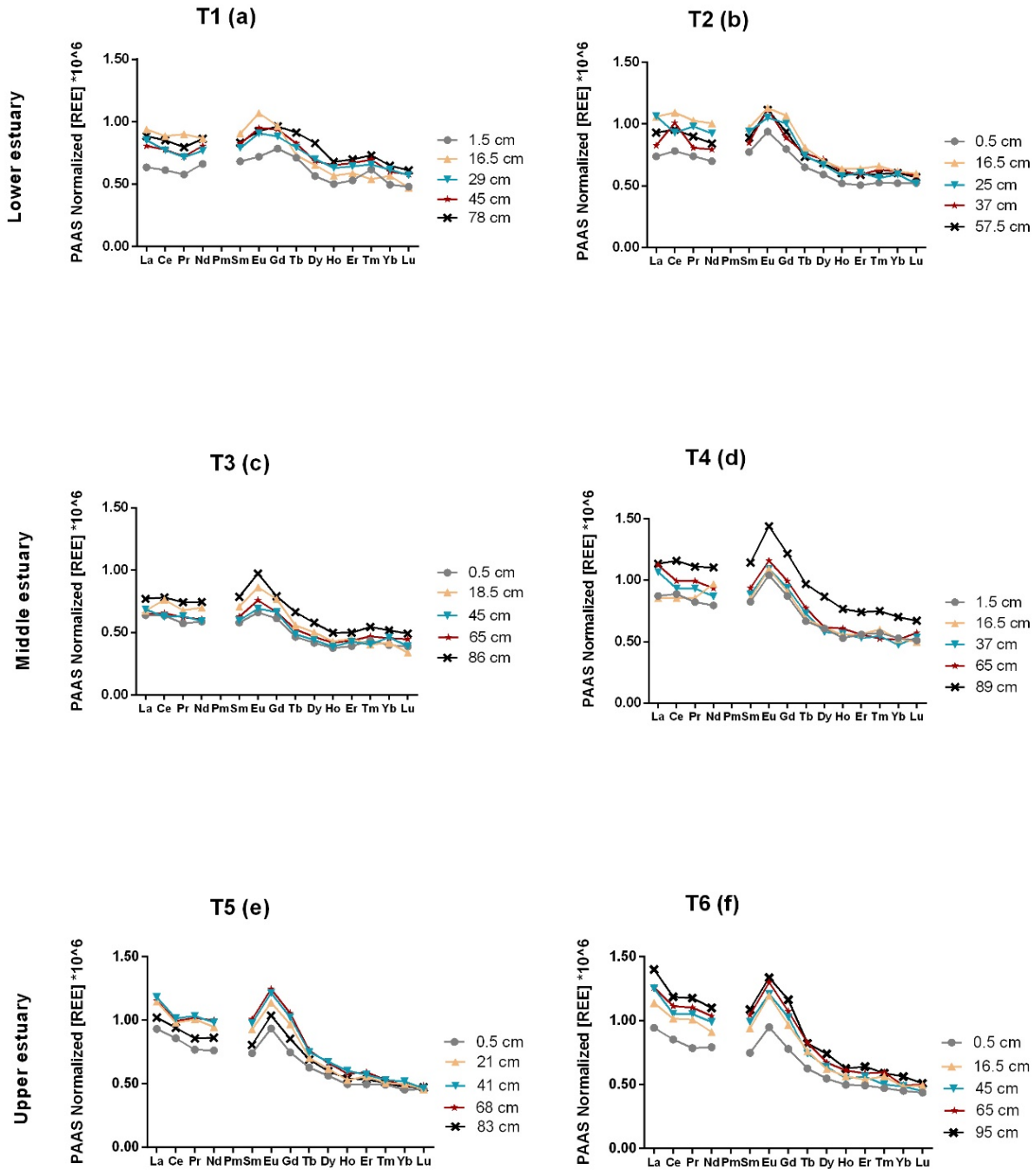

Fig. 8. PAAS-normalized REE distribution in mangrove soil profiles (a. T1; b. T2; c. T3; d. T4; e. T5 and f. T6) of Jaguaripe estuary.

SUPLEMENTARY MATERIAL

Distribution and fractionation of rare earth elements in sediments and mangrove soil profiles across an estuarine gradient

Tácila O. P. de Freitas; Rodrigo M. A. Pedreira; Vanessa Hatje*

Inst. de Química & Centro Interdisciplinar de Energia e Ambiente, CIENAM, Universidade Federal da Bahia, Ondina, Salvador, Bahia, 40170-115, Brazil

*Corresponding: vhatje@ufba.br

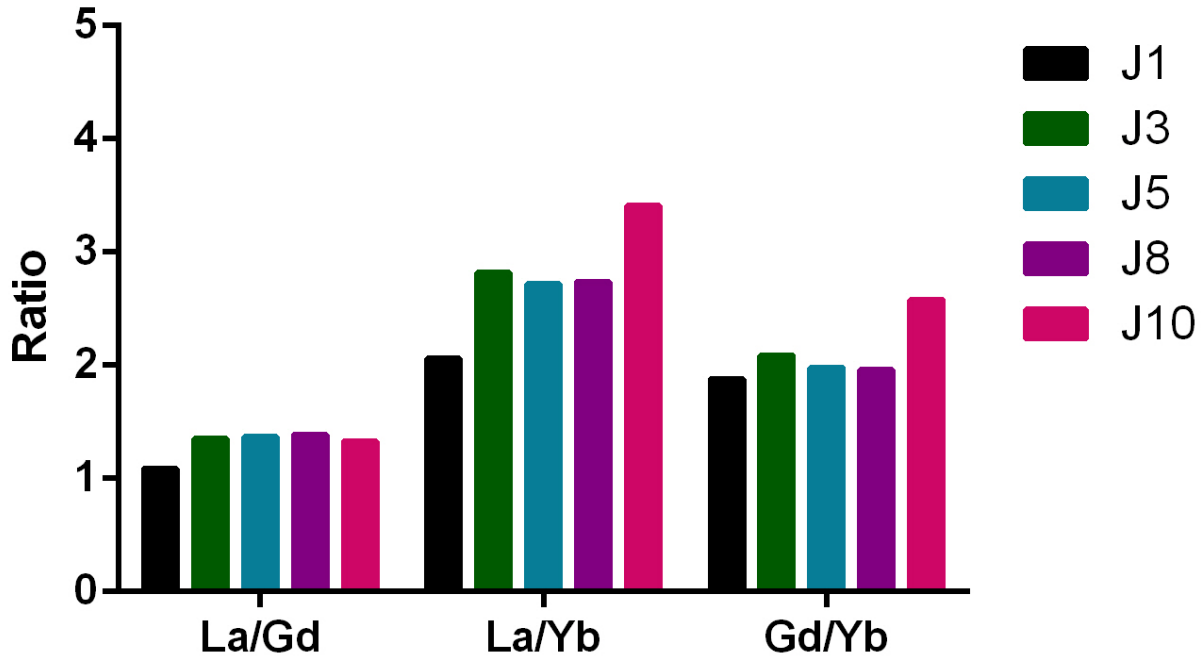

Fig. S1. Ratios of $(La/Gd)_{PAAS}$, $(La/Yb)_{PAAS}$ and $(Gd/Yb)_{PAAS}$ in surface sediments from Jaguaripe estuary.

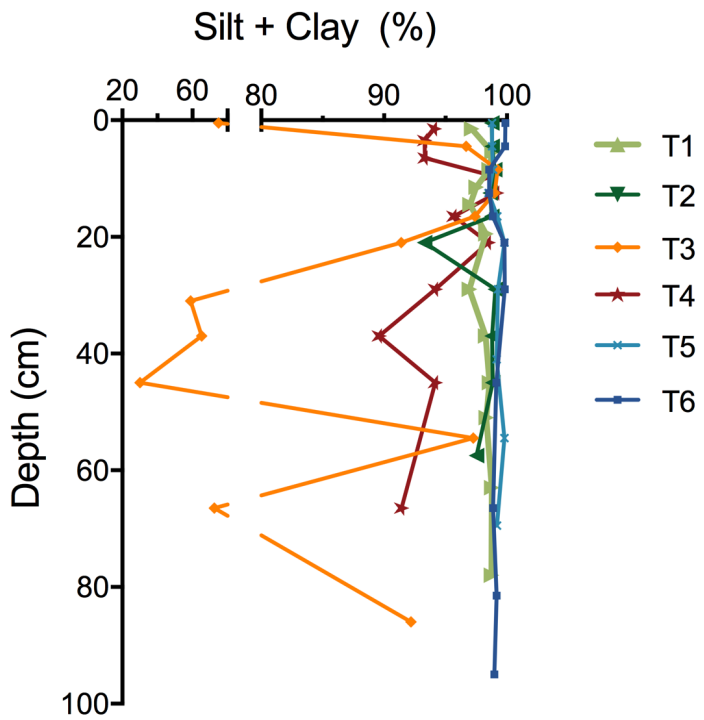

Fig. S2. Content of mud (silt + clay) in mangrove soil profiles (cores T1- T6) of the Jaguaripe estuary. Data provided by Hatje et al. (2020).

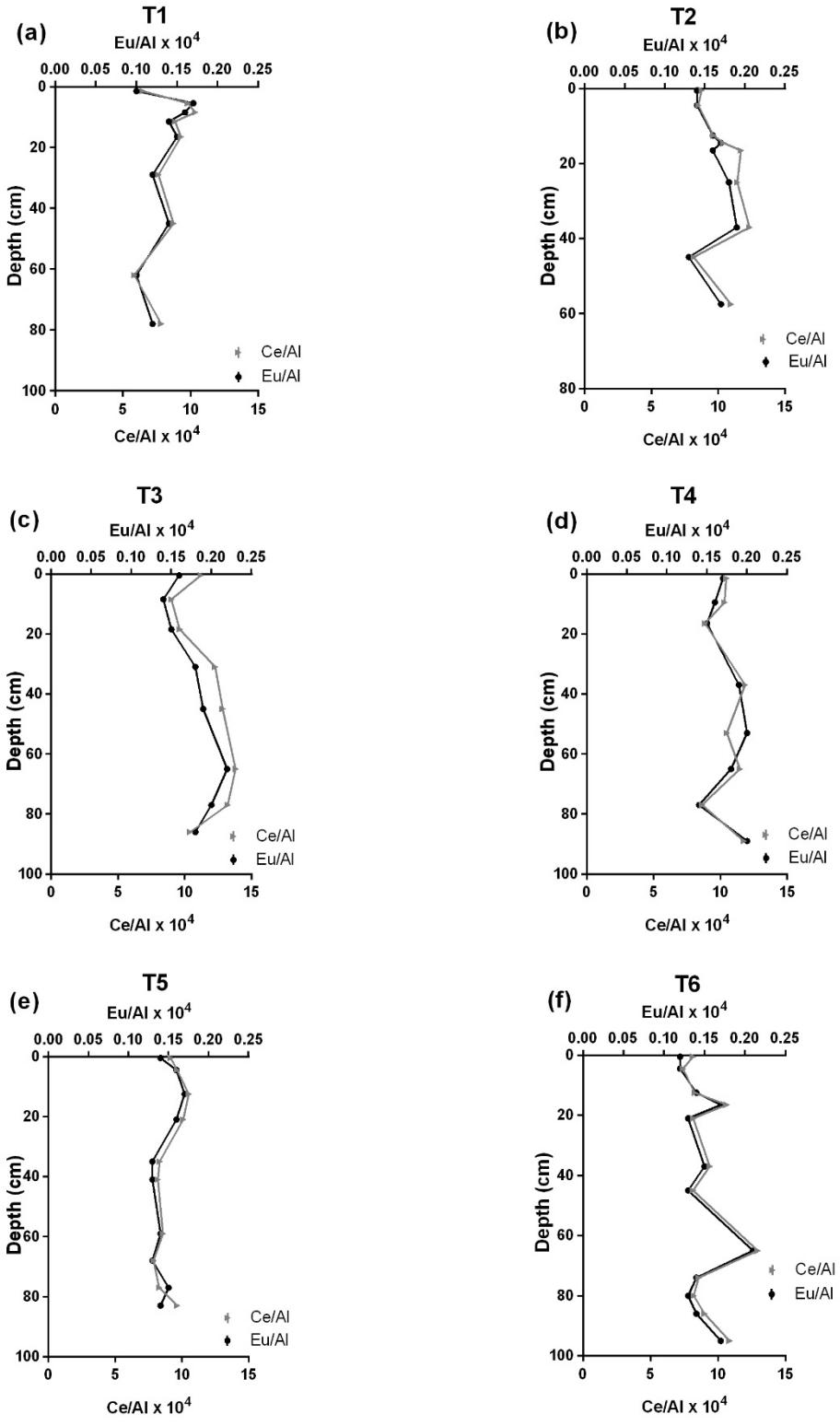

Fig S3. Depth profiles of Ce and Eu by Al concentrations in soil profiles (T1- T6) of the Jaguaripe estuary.

Table S1. Operating conditions of ICP-MS and ICPOES.

Equipment	Parameter	Value
ICP-MS	Forward Power	1550 W
	Ar Flow rate	10 L min^{-1}
	Nebulizer	Micromist
	Flow rate auxiliary	0.8 L min^{-1}
	Dwell time	0.01 s
ICPOES	Forward Power	1300 W
	Nebulizer camera	Cyclonic
	Nebulizer	Concentric
	Flow rate	15 L min^{-1}
	Flow rate auxiliary	0.8 L min^{-1}
	Carrier	0.8 L min^{-1}

Table S2. Certified values and measured concentrations (± standard deviation) of Al, Co, Mn, Pb, Fe and Si for BCR 667 and MESS-3.

CRM		Al	Co	Mn ($mg.kg^{-1}$)	Pb	Fe	Si
BCR 667 n = 2	**Certified value**	-	23.0 ±1.30	920 ± 400	31.9 ± 1.10	44800 ± 1000	-
	Measured value	71709 ± 2550	21.6 ± 0.4	902 ± 49	32.0 ± 0.65	47256 ± 2129	208481 ± 8008
	Recovery (%)	-	94	98	100	103	-
MESS-3 n = 2	**Certified value**	85900 ± 2300	14.4 ± 2.00	324 ± 12	21.1 ± 0.70	43400 ± 1100	270000
	Measured value	94039 ± 6332	13.7 ± 0.96	273 ± 18	18.9 ± 0.38	48798 ± 2368	283865
	Recovery (%)	109	95	84	90	112	105

Table S3. Certified and measured concentrations (± standard deviation) of yttrium and REE for the BCR 667 certified material.

	Y	La	Ce	Pr	Nd	Sm	Eu	Gd	Tb	Dy	Ho	Er	Tm	Yb	Lu
								($mg.kg^{-1}$)							
Certified	16.7-25.3	27.8±1.0	56.7±2.5	6.10±0.50	25.0±1.4	4.66±0.20	1.00±0.05	4.41±0.12	0.628±0.017	4.01±0.14	0.80±0.06	2.35±0.15	0.326±0.025	2.20±0.09	0.325±0.020
Measured	19.7	27.3±0.6	56.1±1.1	6.26±0.18	25.2±0.4	4.75±0.18	1.00±0.01	4.63±0.19	0.675±0.011	3.90±1.08	0.77±0.02	2.32±0.08	0.323±0.011	2.17±0.07	0.317±0.011
Recovery (%)	94	98	99	103	101	102	100	105	99	97	97	99	99	99	98

Table S4. Concentrations of Co, Pb, Mn, Al, Fe, Si, grain size distribution, and C_{org} contents in superficial sediments and salinity the in the Jaguaripe estuary.

Stations	**Co** (mg kg^{-1})	**Pb** (mg kg^{-1})	**Mn** (mg kg^{-1})	**Al** (%)	**Fe** (%)	**Si** (%)	**Grain size**[a] (%)		**C_{org}**[a] (%)	**Average Salinity**[b]
							Sand	Silt + Clay		
J1	20.0 ± 4.0	35.7 ± 5.3	1226 ± 29	8.7	4.6	15.9	76.7	23.0	3.34	21.5 ± 10
J3	14.1 ± 0.4	23.5 ± 1.8	207 ± 9.0	8.7	5.1	17.1	78.4	21.6	4.64	24.7 ± 8.3
J5	22.3 ± 1.1	20.7 ± 0.4	232 ± 18	7.9	5.0	17.7	92.9	7.1	3.96	17.6 ± 8.9
J8	18.9 ± 0.1	26.9 ± 0.2	313	9.1	6.6	17.3	89.5	9.1	5.71	16.2 ± 8.7
J10	20.2 ± 0.5	29.3 ± 0.8	713 ± 92	9.2	7.7	21.0	86.9	0.8	4.40	6.8 ± 6.0

[a]Krull et al., 2014. [b]Annual average salinity for the estuarine waters calculated using published data (Barros et al., 2008; Barros et al., 2012, Barros et al., 2014; Krull et al., 2014; Costa et al., 2015).

Table S5. Concentrations of yttrium and rare earth elements ($mg.kg^{-1}$) in superficial sediments from the Jaguaripe estuary.

Elements	J1	J3	J5	J8	J10
Y	15.0 ± 3.34	13.3 ± 1.28	13.1 ± 2.52	12.4 ± 2.94	11.8 ± 0.73
La	49.4 ± 6.33	52.6 ± 1.02	52.3 ± 4.83	52.5 ± 0.40	53.4 ± 1.62
Ce	89.6 ± 17.65	90.8 ± 3.09	87.1 ± 10.50	95.7 ± 5.42	99.5 ± 2.10
Pr	10.0 ± 1.82	9.70 ± 0.47	11.0 ± 1.36	10.2 ± 0.61	10.6 ± 0.12
Nd	36.1 ± 6.27	34.9 ± 1.30	32.3 ± 4.88	35.0 ± 2.46	37.6 ± 0.77
Sm	6.14 ± 1.19	5.48 ± 0.16	5.44 ± 0.61	5.45 ± 0.42	5.75 ± 0.08
Eu	1.38 ± 0.29	1.30 ± 0.06	1.31 ± 0.17	1.31 ± 0.13	1.46 ± 0.01
Gd	5.52 ± 1.03	4.75 ± 0.27	4.64 ± 0.68	4.60 ± 0.47	4.91 ± 0.01
Tb	0.71 ± 0.12	0.56 ± 0.03	0.57 ± 0.06	0.52 ± 0.08	0.55 ± 0.01
Dy	3.75 ± 0.65	2.82 ± 0.25	2.96 ± 0.35	2.60 ± 0.41	2.74 ± 0.04
Ho	0.68 ± 0.13	0.51 ± 0.04	0.55 ± 0.06	0.58 ± 0.08	0.49 ± 0.01
Er	1.98 ± 0.36	1.56 ± 0.12	1.61 ± 0.18	1.63 ± 0.24	1.41 ± 0.01
Tm	0.27 ± 0.05	0.19 ± 0.01	0.21 ± 0.02	0.21 ± 0.04	0.17 ± 0.01
Yb	1.77 ± 0.32	1.38 ± 0.17	1.42 ± 0.09	1.42 ± 0.29	1.15 ± 0.02
Lu	0.25 ± 0.04	0.15 ± 0.03	0.20 ± 0.01	0.20 ± 0.04	0.15 ± 0.01
Eu/Eu*	1.12	1.20	1.23	1.24	1.29
Ce/Ce*	0.93	0.93	0.84	0.96	0.96
ΣREE	208	207	202	212	220
LREE	185	188	183	193	201
MREE	18.2	15.4	15.5	15.0	15.9
HREE	4.27	3.28	3.44	3.46	2.90
LREE/HREE	43.4	57.3	53.1	55.9	69.5

Table S6. Grain-size composition, salinity and total contents of Al, Mn, Fe, Si and C_{org} in soil profiles of the Jaguaripe estuary.

	Station	Depth (cm)	Salinity[a]	Sand[b]	Silt + clay[b]	Al (%)	Fe	Si	C_{org}[b]	Mn (mg.kg^{-1})
Lower estuary	Core T1	1.5	21.5 ± 10.1	2.86	97.14	7.53	4.66	22.93	9.44	234
		5.5		1.20	98.80	7.30	4.08	19.39	9.18	211
		8.5		1.44	98.56	7.41	4.35	20.57	8.91	237
		11.5		2.48	97.52	8.56	4.31	22.36	10.62	231
		14.5		3.00	97.01	7.57	4.62	22.10	11.52	220
		16.5		-	-	7.59	4.12	19.65	-	232
		19.5		1.69	98.31	8.18	4.97	20.28	10.95	188
		25		-	-	6.95	4.14	17.89	-	221
		29		3.05	96.95	8.06	4.68	20.25	11.32	216
		33		-	-	7.31	4.07	18.34	-	183
		39		1.73	98.27	7.65	4.15	18.46	9.87	219
		45		1.42	98.58	7.07	3.97	17.98	11.33	196
		62		1.22	98.78	9.96	5.31	20.80	5.35	306
		78		1.25	98.75	8.64	4.55	17.83	5.43	251
	Core T2	0.5	24.7 ± 8.3	1.22	98.78	7.10	4.28	17.34	12.29	135
		4.5		1.19	98.81	7.76	4.26	19.39	11.88	183
		8.5		1.00	99.00	7.36	3.97	16.83	10.2	111
		12.5		1.36	98.65	7.69	4.51	20.00	9.47	157
		14.5		-	-	6.88	4.51	20.00	-	150
		16.5		1.23	98.77	7.43	4.01	24.34	7.89	148
		21		6.57	93.31	5.86	3.42	22.37	6.27	137
		25		-	-	6.47	3.42	22.37	-	137
		29		0.97	99.07	7.09	4.36	19.78	7.26	155
		37		1.20	98.80	6.51	4.25	22.43	6.03	242
		45		1.15	98.85	8.85	4.62	23.54	6.51	290
		57.5		2.48	97.52	6.93	4.13	21.01	8.06	238
Mid	Core T3	0.5	17.6 ± 8.9	25.03	74.97	4.52	2.82	24.84	8.41	197
		4.5		3.32	96.68	6.70	3.99	21.42	9.81	157

	Station	Depth (cm)	Salinity[a]	Sand[b]	Silt + clay[b]	Al (%)	Fe	Si	C_{org}[b]	Mn (mg.kg^{-1})
		8.5		0.75	99.25	7.19	4.35	18.32	10.97	347
		12.5		0.97	99.03	7.22	4.25	14.92	11.52	291
		15.5		2.61	97.39	8.88	4.86	18.83	8.48	314
		18.5		-	-	6.31	3.79	22.12	8.48	242
		23		-	-	7.42	3.95	28.47	6.97	234
		31		41.03	58.97	3.89	2.03	26.81	5.29	109
		37		34.66	65.34	4.51	2.10	30.06	4.61	143
		45		69.92	30.08	3.88	2.85	29.76	3.14	172
		53		2.73	97.27	5.52	2.48	25.31	7.06	58
		65		28.53	72.47	3.78	1.75	31.04	3.37	47
		77		-	-	4.01	1.67	29.35	5.20	36
		86		7.82	92.60	5.98	2.88	28.36	6.91	84
		1.5		5.92	94.08	6.76	4.00	17.96	9.44	165
		5.5		6.62	93.38	5.94	4.31	17.06	10.24	107
		9.5		1.28	98.72	7.43	4.83	19.84	10.80	397
		13.5		0.84	99.16	8.11	5.25	21.35	8.55	474
		16.5		4.32	95.68	8.06	5.01	19.83	7.63	418
		21		1.53	98.47	6.99	4.81	18.73	8.87	312
	Core T4	29	16.2 ± 8.7	5.82	94.18	6.77	4.21	19.79	5.98	313
		37		10.39	89.60	6.13	4.13	19.52	5.74	265
		45		5.83	94.17	7.20	4.42	22.55	5.99	254
		53		-	-	6.04	4.05	20.57	-	160
		65		8.58	97.34	6.81	4.47	23.09	6.84	208
		77		-	-	9.76	4.39	22.62	-	216
		89		0.19	99.81	8.82	3.91	21.51	11.05	153
Upper		0.5		1.22	98.78	7.45	4.72	17.49	14.21	305
		4.5		1.20	98.80	7.67	4.70	17.15	14.13	264
		8.5		1.11	98.88	7.92	4.71	18.44	15.12	328
	Core T5	12.5	6.8 ± 6.0	1.48	98.52	7.48	4.89	17.54	12.39	415
		16.5		0.79	99.21	8.16	5.17	19.75	11.72	343
		21		0.19	99.81	7.73	4.95	18.77	12.10	389

Station	Depth (cm)	Salinity[a]	Sand[b]	Silt + clay[b]	Al (%)	Fe	Si	C_{org}[b]	Mn (mg.kg^{-1})
	29		0.72	99.28	7.32	4.99	18.40	11.92	302
	35		-	-	9.81	5.76	20.53	-	454
	41		0.82	99.18	9.84	5.23	20.18	7.65	506
	47		-	-	7.83	4.97	17.84	-	362
	53		0.18	99.82	8.53	4.68	19.11	7.42	324
	59		-	-	9.26	5.49	21.21	-	437
	68		0.81	99.19	10.05	5.35	21.88	6.58	458
	77		-	-	8.85	5.34	21.23	-	349
	83		0.80	99.20	7.77	4.68	18.45	6.99	324
	0.5		0.13	99.87	8.33	4.62	16.89	9.57	207
	4.5		0.14	99.86	9.63	5.31	19.03	10.31	278
	8.5		1.45	98.55	8.00	4.92	16.92	8.49	321
	12.5		1.14	98.86	8.95	4.99	19.11	8.35	258
	16.5		1.15	98.85	7.59	4.86	16.91	8.43	294
	21		0.20	99.80	9.89	5.43	19.71	7.11	373
	29		0.16	99.84	9.37	5.09	17.68	6.73	360
Core T6	37	9.9 ± 7.6	-	-	9.23	5.35	20.25	-	471
	45		0.85	99.15	10.28	5.60	18.69	7.40	441
	53		-	-	9.93	5.49	20.60	-	453
	65		1.11	98.89	6.85	5.03	20.35	8.49	486
	74		-	-	9.44	5.69	20.19	-	461
	80		0.82	99.18	9.66	5.33	20.11	8.15	408
	86		-	-	9.93	5.54	20.67	-	430
	95		1.01	98.99	8.71	5.03	19.62	7.74	380

[a]Annual mean salinity (mean ± sd) calculated using published data (Hatje et al., 2012; Krull et al., 2014; Costa et al., 2015). [b]Hatje et al., 2020.

Table S7. Concentrations of Y and REE (mg kg^{-1}) in profiles of mangrove soils of the Jaguaripe estuary.

	Station	Depth cm	Y	La	Ce	Pr	Nd	Sm	Eu	Gd	Tb	Dy	Ho	Er	Tm	Yb	Lu	Eu/Eu*	Ce/Ce*	ΣREE	LREE	MREE	HREE	L/H
Lower estuary	Core T1	1.5	15.74	24.22	48.73	5.09	22.46	3.78	0.78	3.65	0.55	2.64	0.50	1.51	0.25	1.40	0.21	0.98	1.01	116	101	11.9	3.4	29.9
		5.5	13.79	38.87	71.58	8.42	30.74	5.20	1.21	4.66	0.57	3.06	0.56	1.66	0.22	1.54	0.20	1.15	0.91	168	150	15.3	3.6	41.2
		8.5	14.09	40.25	76.83	8.67	31.16	5.13	1.20	4.82	0.59	3.19	0.57	1.73	0.23	1.63	0.21	1.14	0.95	176	157	15.5	3.8	41.4
		11.5	14.12	39.70	75.76	8.53	31.43	5.22	1.18	4.72	0.59	3.21	0.60	1.74	0.23	1.65	0.21	1.12	0.95	175	155	15.5	3.8	40.6
		16.5	12.86	35.82	70.44	7.94	29.37	5.02	1.15	4.51	0.57	3.05	0.56	1.68	0.22	1.60	0.20	1.14	0.96	162	144	14.9	3.7	38.9
		29	16.82	32.47	61.46	6.32	26.02	4.38	0.98	4.11	0.61	3.28	0.62	1.83	0.27	1.73	0.25	1.09	0.99	144	127	14.0	4.1	31.0
		45	17.47	30.79	61.78	6.38	27.31	4.56	1.02	4.38	0.64	3.20	0.64	1.91	0.28	1.69	0.25	1.08	1.02	145	126	14.4	4.1	30.6
		62	15.22	29.00	58.14	6.03	24.82	4.30	0.97	3.87	0.60	3.22	0.62	1.75	0.26	1.70	0.25	1.12	1.01	136	118	13.6	4.0	29.8
		78	17.73	33.77	67.66	7.02	29.20	4.63	1.00	4.48	0.71	3.87	0.67	1.99	0.30	1.83	0.26	1.03	1.01	157	138	15.4	4.4	31.4
		Average	**15.31**	**33.88**	**65.82**	**7.15**	**28.06**	**4.69**	**1.05**	**4.36**	**0.60**	**3.19**	**0.59**	**1.76**	**0.25**	**1.64**	**0.23**	**1.10**	**0.98**	**153**	**135**	**14.5**	**3.9**	**35.0**
		SD	**1.74**	**5.38**	**9.11**	**1.29**	**3.12**	**0.49**	**0.14**	**0.40**	**0.05**	**0.32**	**0.05**	**0.14**	**0.03**	**0.12**	**0.02**	**0.06**	**0.04**	**20.0**	**18.8**	**1.2**	**0.3**	**5.3**
	Core T2	0.5	11.43	28.17	62.21	6.53	23.70	4.29	1.01	3.72	0.50	2.77	0.52	1.44	0.21	1.47	0.23	1.19	1.06	137	121	12.8	3.3	36.0
		4.5	12.86	34.91	65.95	7.60	27.64	4.65	1.07	4.14	0.52	2.77	0.51	1.51	0.20	1.39	0.18	1.15	0.93	153	136	13.7	3.3	41.6
		12.5	14.19	42.14	74.18	9.00	32.46	5.40	1.23	4.83	0.60	3.14	0.58	1.73	0.23	1.61	0.21	1.13	0.88	177	158	15.8	3.8	41.8
		14.5	13.81	41.09	71.55	8.71	31.27	5.16	1.14	4.63	0.57	3.04	0.56	1.67	0.22	1.61	0.21	1.10	0.87	171	153	15.1	3.7	41.1
		16.5	13.12	40.45	87.00	9.08	34.05	5.38	1.22	4.98	0.63	3.30	0.63	1.82	0.27	1.74	0.26	1.11	1.05	191	171	16.1	4.1	41.7
		21	13.10	41.57	69.74	8.35	30.64	5.12	1.10	4.66	0.56	3.02	0.56	1.71	0.23	1.72	0.23	1.06	0.86	169	150	15.0	3.9	38.7
		25	13.34	40.59	73.96	8.65	31.31	5.21	1.14	4.68	0.58	3.14	0.57	1.73	0.23	1.67	0.23	1.08	0.91	174	154	15.3	3.8	40.1
		37	10.44	31.59	80.30	7.12	26.92	4.70	1.21	4.14	0.59	3.34	0.61	1.68	0.26	1.74	0.25	1.29	1.14	164	146	14.6	3.9	37.1
		45	13.83	41.82	72.21	8.71	31.66	5.25	1.19	4.70	0.57	3.04	0.56	1.66	0.20	1.48	0.19	1.13	0.87	173	154	15.3	3.5	43.6
		57.5	11.80	35.55	75.93	7.95	28.58	4.94	1.20	4.37	0.57	3.20	0.60	1.67	0.24	1.70	0.25	1.22	1.04	167	148	14.9	3.9	38.3
		Average	**12.79**	**37.79**	**72.68**	**8.17**	**29.82**	**5.01**	**1.15**	**4.48**	**0.57**	**3.08**	**0.57**	**1.66**	**0.23**	**1.61**	**0.22**	**1.15**	**0.96**	**168**	**149**	**14.9**	**3.7**	**39.8**
		SD	**1.20**	**4.94**	**6.55**	**0.85**	**3.08**	**0.36**	**0.07**	**0.39**	**0.04**	**0.19**	**0.04**	**0.11**	**0.02**	**0.13**	**0.03**	**0.07**	**0.10**	**14.8**	**13.6**	**1.0**	**0.3**	**2.7**

	Station	Depth cm	Y	La	Ce	Pr	Nd	Sm	Eu	Gd	Tb	Dy	Ho	Er	Tm	Yb	Lu	Eu/Eu*	Ce/Ce*	ΣREE	LREE	MREE	HREE	L/H
Middle estuary	Core T3	0.5	8.61	24.41	50.70	5.06	19.90	3.21	0.71	2.86	0.36	1.96	0.37	1.11	0.18	1.13	0.17	1.11	1.05	112	100	9.5	2.6	38.7
		8.5	9.26	25.13	64.71	6.14	23.22	3.94	0.98	3.76	0.45	2.48	0.45	1.34	0.17	1.25	0.16	1.19	1.20	134	119	12.1	2.9	40.8
		18.5	9.69	25.78	60.77	5.99	23.72	3.92	0.93	3.57	0.43	2.35	0.42	1.28	0.16	1.18	0.15	1.17	1.13	131	116	11.6	2.8	41.9
		31	7.94	22.86	47.85	4.95	18.09	3.15	0.71	2.79	0.37	2.02	0.38	1.15	0.18	1.24	0.19	1.12	1.04	106	94	9.4	2.8	34.0
		45	9.35	26.20	49.90	5.58	20.08	3.31	0.75	3.09	0.38	2.06	0.38	1.22	0.16	1.30	0.17	1.10	0.95	114	102	10.0	2.8	35.7
		65	8.74	24.80	52.21	5.49	20.55	3.48	0.82	3.09	0.41	2.18	0.41	1.24	0.19	1.28	0.19	1.17	1.03	116	103	10.4	2.9	35.5
		77	9.55	28.26	53.04	5.94	21.32	3.55	0.82	3.10	0.38	2.02	0.39	1.18	0.15	1.13	0.14	1.16	0.94	121	108	10.2	2.6	41.8
		86	11.82	29.43	62.25	6.57	25.24	4.37	1.05	3.68	0.51	2.70	0.49	1.42	0.22	1.46	0.21	1.23	1.03	140	123	12.8	3.3	37.2
		Average	**9.37**	**25.86**	**55.18**	**5.72**	**21.51**	**3.62**	**0.85**	**3.24**	**0.41**	**2.22**	**0.41**	**1.24**	**0.18**	**1.25**	**0.17**	**1.16**	**1.05**	**122**	**108**	**10.7**	**2.8**	**38.2**
		SD	**1.15**	**2.12**	**6.40**	**0.55**	**2.36**	**0.42**	**0.13**	**0.38**	**0.05**	**0.27**	**0.04**	**0.10**	**0.02**	**0.11**	**0.02**	**0.05**	**0.09**	**11.8**	**10.4**	**1.3**	**0.2**	**3.07**
	Core T4	1.5	10.99	33.37	70.69	7.26	26.95	4.58	1.13	4.06	0.52	2.84	0.53	1.60	0.23	1.50	0.22	1.23	0.97	155	138	13.7	3.6	39.0
		9.5	11.21	36.85	76.73	7.95	30.17	4.79	1.19	4.46	0.57	2.93	0.57	1.62	0.24	1.46	0.21	1.22	0.97	170	152	14.5	3.5	42.9
		16.5	11.99	32.69	71.31	7.57	32.89	4.73	1.18	4.23	0.53	2.88	0.55	1.60	0.24	1.47	0.22	1.24	1.00	162	144	14.1	3.5	40.9
		37	11.77	40.79	72.64	8.24	29.49	4.92	1.18	4.37	0.57	2.71	0.56	1.51	0.22	1.34	0.23	1.20	0.94	169	151	14.3	3.3	45.8
		53	12.63	41.85	72.35	8.64	31.21	5.16	1.23	4.65	0.60	2.89	0.59	1.59	0.26	1.44	0.24	1.18	0.88	164	145	15.1	3.5	41.1
		65	12.91	42.90	78.05	8.78	31.68	5.20	1.25	4.64	0.60	2.90	0.60	1.59	0.21	1.46	0.25	1.20	0.94	180	16	15.2	3.5	46.0
		77	14.54	48.10	84.25	9.58	35.10	5.78	1.38	5.19	0.62	3.30	0.61	1.78	0.23	1.58	0.22	1.19	0.93	198	177	16.9	3.8	46.5
		89	13.53	43.32	92.23	9.81	37.43	6.34	1.55	5.67	0.75	4.06	0.76	2.11	0.30	1.98	0.29	1.22	0.99	207	183	19.1	4.7	39.1
		Average	**12.44**	**39.98**	**77.28**	**8.48**	**31.86**	**5.19**	**1.26**	**4.66**	**0.59**	**3.06**	**0.60**	**1.67**	**0.24**	**1.53**	**0.23**	**1.21**	**0.95**	**175**	**156**	**15.4**	**3.7**	**42.7**
		SD	**1.20**	**5.30**	**7.54**	**0.91**	**3.28**	**0.60**	**0.14**	**0.53**	**0.07**	**0.44**	**0.07**	**0.19**	**0.03**	**0.19**	**0.03**	**0.02**	**0.04**	**18.0**	**16.0**	**1.8**	**0.4**	**3.1**
Up per estuary	Core T5	0.5	12.24	35.61	68.35	6.78	25.81	4.11	1.01	3.48	0.49	2.63	0.49	1.41	0.20	1.28	0.20	1.26	1.02	152	137	12.2	3.1	44.2
		4.5	12.55	44.27	73.90	8.38	30.36	5.31	1.21	4.55	0.55	2.91	0.54	1.60	0.21	1.43	0.20	1.16	0.89	175	157	15.1	3.4	45.7
		12.5	13.18	44.62	78.69	8.83	32.49	5.34	1.29	4.82	0.55	3.05	0.57	1.66	0.21	1.50	0.21	1.20	0.91	184	165	15.6	3.6	46.0
		21	11.69	43.83	78.09	8.89	32.12	5.15	1.23	4.51	0.54	2.89	0.52	1.60	0.20	1.41	0.20	1.20	0.91	181	163	14.9	3.4	47.9

Station	Depth cm	Y	La	Ce	Pr	Nd	Sm	Eu	Gd	Tb	Dy	Ho	Er	Tm	Yb	Lu	Eu/Eu*	Ce/Ce*	ΣREE	LREE	MREE	HREE	L/H
	35	12.94	46.45	81.71	9.20	33.05	5.39	1.29	4.76	0.57	3.02	0.56	1.66	0.21	1.45	0.20	1.20	0.91	189	170	15.6	3.5	48.4
	41	12.01	45.14	80.79	9.12	33.33	5.42	1.31	4.77	0.58	3.15	0.60	1.63	0.21	1.46	0.20	1.21	0.92	188	168	15.8	3.5	48.0
	59	13.03	44.94	79.43	8.95	32.53	5.36	1.30	4.49	0.57	2.92	0.54	1.60	0.21	1.42	0.20	1.25	0.91	184	166	15.2	3.4	48.4
	68	13.68	44.07	79.18	8.99	33.94	5.59	1.35	4.91	0.59	3.10	0.57	1.68	0.22	1.37	0.21	1.21	0.92	186	166	16.1	3.5	47.8
	77	13.26	40.56	73.37	8.27	32.63	5.46	1.35	4.74	0.56	2.90	0.56	1.63	0.21	1.40	0.20	1.25	0.92	174	155	15.6	3.4	45.0
	83	13.04	39.04	74.89	7.57	29.23	4.47	1.12	3.98	0.53	2.80	0.54	1.52	0.21	1.33	0.20	1.25	1.01	167	151	13.4	3.3	46.2
	Average	**12.76**	**42.85**	**76.84**	**8.50**	**31.55**	**5.16**	**1.25**	**4.50**	**0.55**	**2.94**	**0.55**	**1.60**	**0.21**	**1.40**	**0.20**	**1.22**	**0.93**	**178**	**160**	**14.9**	**3.4**	**46.7**
	SD	**0.62**	**3.37**	**4.12**	**0.78**	**2.45**	**0.48**	**0.11**	**0.44**	**0.03**	**0.15**	**0.03**	**0.08**	**0.01**	**0.06**	**0.01**	**0.03**	**0.04**	**11.5**	**10.3**	**1.2**	**0.1**	**1.5**
	0.5	11.76	36.06	67.95	6.94	26.88	4.15	1.03	3.63	0.48	2.56	0.49	1.41	0.19	1.27	0.19	1.24	0.99	153	138	12.3	3.1	45.1
	4.5	11.37	39.95	71.25	8.20	29.45	4.84	1.16	4.29	0.52	2.74	0.50	1.48	0.19	1.28	0.17	1.20	0.91	166	149	14.1	3.1	47.6
	12.5	11.75	42.11	74.07	8.39	30.68	5.00	1.22	4.50	0.53	2.78	0.51	1.51	0.19	1.32	0.18	1.21	0.91	173	155	14.6	3.2	48.5
	16.5	14.29	43.51	80.80	8.91	30.90	5.22	1.29	4.51	0.59	2.91	0.56	1.54	0.23	1.37	0.21	1.25	0.95	182	164	15.1	3.3	49.0
	21	11.82	47.51	80.78	9.01	32.60	5.24	1.26	4.64	0.55	2.88	0.53	1.55	0.20	1.33	0.18	1.20	0.90	188	170	15.1	3.2	52.2
	37	12.99	49.79	86.69	9.72	35.20	5.75	1.37	4.92	0.61	3.08	0.58	1.65	0.22	1.41	0.19	1.21	0.91	201	181	16.3	3.5	52.4
	45	12.79	47.85	83.92	9.29	33.56	5.50	1.31	4.78	0.57	2.99	0.54	1.60	0.20	1.37	0.19	1.20	0.92	194	175	15.7	3.4	51.9
Core T6	65	14.68	48.11	88.67	9.74	35.15	5.80	1.40	5.00	0.64	3.15	0.61	1.68	0.24	1.39	0.22	1.23	0.95	202	182	16.6	3.5	51.5
	74	12.06	45.59	80.91	9.14	33.22	5.48	1.33	4.86	0.59	3.02	0.56	1.62	0.21	1.42	0.19	1.21	0.91	188	169	15.8	3.4	48.9
	80	12.05	44.41	79.30	8.89	32.54	5.33	1,28	4.73	0.57	3.04	0.56	1.63	0.21	1.41	0.19	1.20	0.92	184	165	15.5	3.4	47.9
	86	14.38	47.80	89.38	9.81	35.71	5.76	1,39	5.13	0.61	3.16	0.57	1.66	0.22	1.44	0.20	1.20	0.95	203	183	16.6	3.5	51.9
	95	15.05	53.56	94.51	10.39	37.29	6.04	1,45	5.43	0.64	3.47	0.62	1.83	0.24	1.59	0.22	1.19	0.92	217	196	17.6	3.9	50.5
	Average	**12.92**	**45.52**	**81.52**	**9.04**	**32.77**	**5.34**	**1.29**	**4.70**	**0.58**	**2.98**	**0.55**	**1.60**	**0.21**	**1.38**	**0.20**	**1.21**	**0.93**	**188**	**169**	**15.4**	**3.4**	**49.8**
	SD	**1.33**	**4.69**	**7.78**	**0.91**	**2.94**	**0.51**	**0.12**	**0.46**	**0.05**	**0.23**	**0.04**	**0.11**	**0.02**	**0.08**	**0.01**	**0.02**	**0.03**	**17.7**	**16.1**	**1.4**	**0.2**	**2.3**
	Background	13.15	43.3	85.0	8.87	33.5	5.46	1.35	4.85	0.60	3.24	0.61	1.76	0.23	1.54	0.22	-	-	190	171	16.1	3.76	45.5
	SD	2.22	10.7	8.29	1.59	4.08	0.66	0.10	0.61	0.03	0.20	0.03	0.07	0.01	0.15	0.02	-	-	24.7	23.2	1.53	0.25	6.49

REFERENCES

Costa, P., Dórea, A., Mariano-Neto, E., Barros, F., 2015. Are there general spatial patterns of mangrove structure and composition along estuarine salinity gradients in Todos os Santos Bay? Estuarine, Coastal and Shelf Science. 166, 83–91.

Hatje, V., Barros, F., 2012. Overview of the 20th century impact of trace metal contamination in the estuaries of Todos os Santos Bay: Past, present and future scenarios. Marine Pollution Bulletin. 64 (11), 2603–2614.

Hatje, V., Masqué P., Patire, V., Dórea, A., Barros, F. Blue C stocks, accumulation rates, and associated spatial variability in Brazilian mangroves (2020). Limnology and Oceanography.

Krull, M., Abessa, D. M.S., Hatje, V., Barros, F., 2014. Integrated assessment of metal contamination in sediments from two tropical estuaries. Ecotoxicology and Environmental Safety. 106, 195–203.